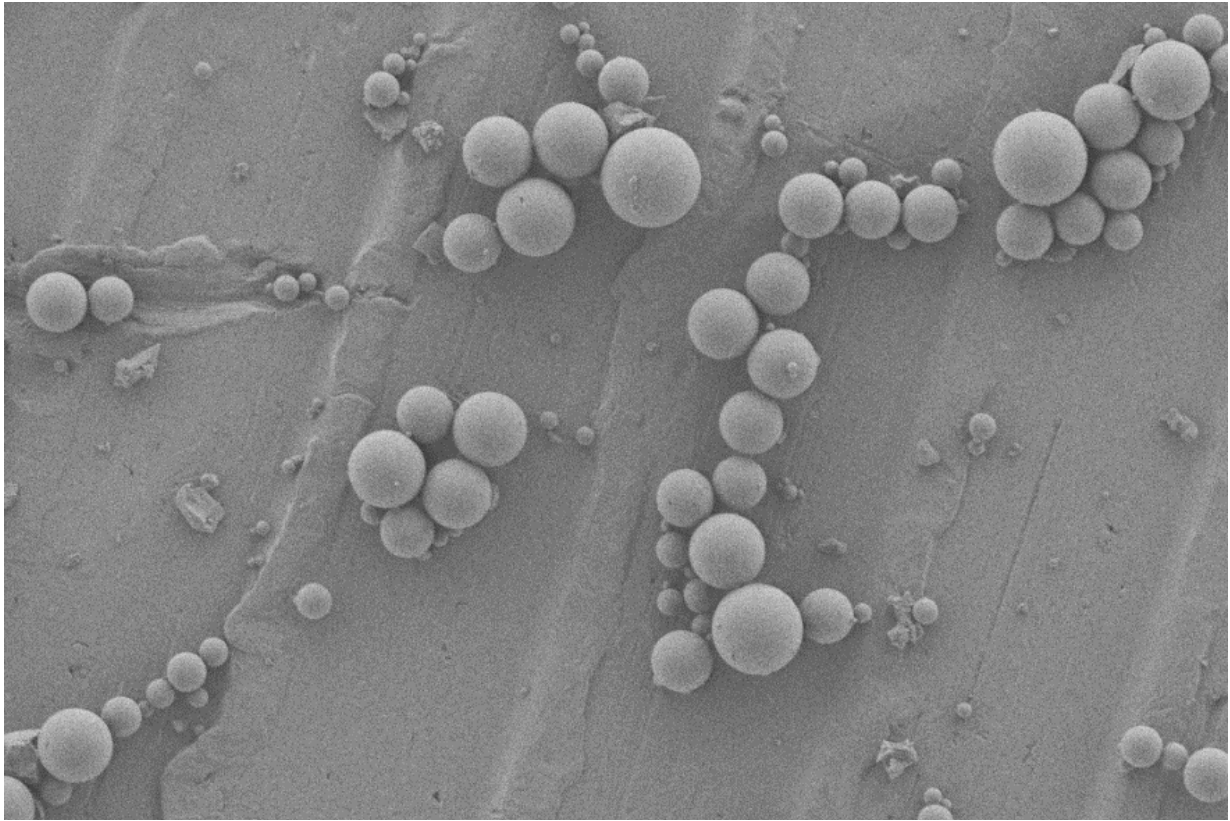




# CHALMERS

---



## **The effect of synthesis parameters on mesoporous silica particles morphology and size distribution**

Master's thesis within the *Innovative and Sustainable Chemical Engineering* programme and the *Materials Chemistry and Nanotechnology* programme

Cecilia Duong  
Cecilia Lu

---

Department of Chemical and Biological engineering  
Chalmers University of Technology  
Gothenburg, Sweden 2014

MASTER'S THESIS

# The effect of synthesis parameters on mesoporous silica particles morphology and size distribution

30 hp Master's thesis within the Innovative and Sustainable Chemical Engineering programme and the Materials Chemistry and Nanotechnology programme

CECILIA DUONG

CECILIA LU

The thesis was performed at the Division of Applied Chemistry, Department of Chemical and Biological Engineering, Chalmers University of Technology, Gothenburg, Sweden, August, 2014

Supervisor: Johan Lif (PhD Senior Scientist), sBU Bleaching Chemicals, Process RD&I

Christoffer Abrahamsson (PhD student), Applied Chemistry, Department of Chemical and Biological Engineering, Chalmers University of Technology, Gothenburg, Sweden

Examiner: Michael Persson (Adjunct Professor), Applied Chemistry, Department of Chemical and Biological Engineering, Chalmers University of Technology, Gothenburg, Sweden

# The effect of synthesis parameters on mesoporous silica particles morphology and size distribution

Master's thesis within the Innovative and Sustainable Chemical Engineering programme  
and the Materials Chemistry and Nanotechnology programme

CECILIA DUONG

CECILIA LU

The effect of synthesis parameters on mesoporous silica particles morphology and size distribution

Cecilia Duong and Cecilia Lu

©Cecilia Duong and Cecilia Lu, 2014

Chalmers University of Technology  
Department of Chemical and Biological Engineering  
Division of Applied Chemistry

SE-412 96 Gothenburg  
Sweden  
Telephone: +46 (0)31-772 1000

Cover: SEM image of spherical mesoporous silica particles synthesized from a water-in-oil emulsion system containing benzyl alcohol as continuous phase and silica sol dispersion and EHEC E230 as dispersed phase. The stirring rate was set to 450 rpm, the pressure to 160 mbar and temperature to 65 °C during gelation.

# Acknowledgment

We would like to thank everybody who has helped us during the performance of this thesis work.

First of all, thanks to Applied Surface Chemistry at Chalmers University of technology for giving us the opportunity to conduct our master thesis there.

Special thanks to our supervisor Johan Lif for all his patience, support and valuable discussions throughout the thesis. This thesis and report would not be the same without your guidance.

Thanks to our second supervisor Christoffer Abrahamsson for his support and guidance of report and instruction of SEM.

Thanks to Ulrika Andersson, Emelie Öhgren and Sanna Björkegren for the instructions and help with Coulter counter Multisizer, Malvern and the Du Noüy ring method.

# Abstract

The interest for mesoporous silica materials have increased significantly during the past decades due to the benefits these materials can provide. The characteristic for mesoporous silica materials are the high surface area to volume ratio which results in a wide range of potential applications, from catalyst to drug delivery. A lot of effort has been made to develop processes for synthesis of mesoporous silica materials since the first reports released on mesoporous materials. One property that has proved hard to obtain is monodisperse particle size distributions for micrometer sized spherical mesoporous particles. In 2006, Nina Andersson et al. reported a new method, the emulsion with solvent evaporation method, ESE-method, for synthesizing mesoporous spherical silica particles. According to them, this method has several potential advantages over classic precipitation routes.

The aim of the thesis was to investigate the ESE-method for synthesis of spherical mesoporous silica particles and to see how different reaction parameters affect the particle morphology and size distribution. The aim was also to modify the process with a Couette cell and investigate which parameters that can be used to further control the particle size distribution.

In this thesis spherical mesoporous silica particles were successfully synthesized with the ESE-method. Through variations in the synthesis conditions different particle morphologies and size distributions were obtained. Small particles with narrow size distribution were achieved by increasing the stirring rate or by increasing the viscosity of the continuous phase. The type and amount of emulsifier affected the particle size distributions. The temperature during gelation turned out to have a minor effect on the particle morphology and size distribution. The Couette cell had major effect on the particles size distribution. The significant parameters, which have impact on the final particle morphology and size distribution are stirring rate, viscosity of dispersed phase and continuous phase. The phase ratio, that is the ratio between the inorganic and organic phase, had a minor effect, while the temperature during gelation did not have significant impact. For the process modified with Couette cell the viscosity of the continuous phase and the retention time in the Couette cell did not have a significant impact on the particle size distribution, while stirring rates and viscosity of the dispersed phase had major effects. Syntheses conditions with high viscosity of the dispersed phase and high stirring rates proved to result in the narrowest particle size distributions.

# Table of Content

1. Introduction .....	1
1.1 Aim .....	1
1.2 Limitation .....	1
2. Theoretical background .....	2
2.1 Colloidal systems.....	2
2.1.1 DLVO-theory .....	3
2.1.2 Emulsions .....	5
2.1.3 Emulsion stability and destabilization mechanisms .....	6
2.1.4 Emulsifiers.....	6
2.2 Silica and colloidal silica.....	7
2.2.1 Mesoporous silica .....	8
2.3 The sol-gel process in emulsions.....	9
2.3.1 Synthesis of silica particles .....	10
2.3.2 How different reaction parameters affects the particle size .....	10
2.3.3 Process modified with Couette cell .....	10
2.4 Characterization methods .....	12
2.4.1 Optical microscopy.....	12
2.4.2 Scanning electron microscopy.....	12
2.4.3 Surface tension measurements .....	12
2.4.4 Coulter counter Multisizer.....	13
2.4.5 Malvern (Sysmex FPIA 3000).....	13
2.4.6 Particle size distribution .....	13
3. Method.....	15
3.1 Pre-experiments for the reference system .....	15
3.2 Materials .....	16
3.3 Experimental procedure.....	17
3.3.1 Procedure modified with Couette cell .....	18
3.4 Emulsion stability.....	18
3.5 Optical microscopy.....	19
3.6 Coulter counter .....	19
3.7 Malvern.....	19
3.8 SEM.....	19

3.9 Surface tension .....	19
4. Results .....	21
4.1 Process system without Couette cell .....	21
4.1.1 The effect of stirring rate .....	23
4.1.2 The effect of the viscosity in the dispersed phase .....	24
4.1.3 The effect of increasing both stirring rate and viscosity in dispersed phase .....	29
4.1.4 The effect of temperature .....	30
4.1.5 The effect of phase ratio .....	31
4.1.6 The effect of the viscosity of the continuous phase .....	33
4.1.7 The effect of different type of organic solvent .....	35
4.2 Process system modified with Couette cell .....	37
4.2.1 The effect of viscosity of the dispersed phase in Couette cell .....	39
4.2.2 The effect of stirring rates .....	41
4.2.3 The effect of the viscosity in the continuous phase .....	45
4.2.4 The effect of the retention time in the Couette cell .....	46
4.3 Investigation of emulsion stability .....	47
5. Discussion .....	49
5.1 Evaluation of reaction parameters .....	49
5.2 Evaluation of Couette cell .....	52
5.3 Characterization methods .....	53
6. Conclusion .....	55
7. Future work .....	56
8. References .....	57
9. Appendix .....	61
9.1 Surface and interfacial tension .....	61
9.2 List of organic solvents from literature .....	62
9.3 Corrosion of the Couette cell .....	64

# 1. Introduction

In the past decade well-defined porous materials have been of great interest due to their structures and properties. The presence of pores in the material increases the material surface area, enhancing the capacity of the material to interact with surrounding molecules. Porous materials can be classified in several categories depending on the pore size. International Union of Pure and Applied Chemistry (IUPAC) has defined microporous materials as materials with pore diameter  $< 2\text{nm}$ , mesoporous materials with pore diameter  $2\text{-}50\text{ nm}$  and macroporous materials with pore diameter  $> 50\text{nm}$  (1).

The synthesis of mesoporous materials has been a research field of rapid development, attracting great interest due to these materials' wide variety of potential applications. Mesoporous materials provide many interesting properties such as high surface area to volume ratio, large surface area and well defined pore size distribution. These properties are of interest in applications such as adsorption, separation, catalysis, drug delivery and purification (2, 3). Because of the increasing interests in application of mesoporous materials, parameters that control the particle morphology and size distribution are of great significance. A controlled particle size and a narrow particle size distribution are desired in many applications. In chromatography higher separation efficiency is obtained using monodispersed mesoporous silica spheres (4) and in some drug delivery techniques a better controlled drug release profile is gained when the particles size distribution is monodisperse (5).

In the early 90's mesoporous material made of amorphous silica was discovered and since then the interest has increased substantially. Silica is thermally stable, inexpensive and can be found in nature e.g. as quartz mineral and/or as sand (6). Spherical amorphous mesoporous silica particles can be synthesized by several different methods e.g. spray drying or emulsion based methods. In this thesis a method based on a water-in-oil emulsion will be used to create well-defined spherical mesoporous silica particles. The method is largely based on the emulsion with solvent evaporation method, ESE-method, developed by Nina Andersson et al. (7).

## 1.1 Aim

The aim of the thesis was to investigate how variations in the reaction parameters during the synthesis of spherical mesoporous silica particles, using the ESE-method, affect the particle morphology and size distribution. To form spherical particles the method aims to form the silica particles in the water phase of a W/O-emulsion. The process was also modified with a Couette cell to study how the Couette cell affected the particle morphology and size distribution.

## 1.2 Limitation

The thesis was limited to investigate only one synthesis method of spherical silica particles and only one silica precursor with specific particle size was used. Analysis of the mesopores of the silica particles was not included in this thesis.

## 2. Theoretical background

This chapter will provide a background to the emulsion based syntheses of the mesoporous silica particles. The reaction is performed as a gelation of silica sol particles kept in water droplets in a water-in-oil emulsion. As will be described below an intricate network of factors affect each step of the particle synthesis. These factors will decide the emulsion stability, the emulsion droplet size as well as silica precursor aggregation and gelation and in the end the mesoporous silica particle characteristics.

### 2.1 Colloidal systems

Colloidal systems are mixed phase systems consisting of solids, liquids or gases where one phase commonly is dispersed in the other. Table 2.1 exemplifies 8 different colloidal systems (8).

*Table 2.1 Examples of common types of colloidal systems (8).*

Medium/phases		Dispersed phase		
		Gas	Liquid	Solid
<b>Continuous phase</b>	Gas	<b>None</b> (all gases are mutually miscible)	<b>Liquid aerosol;</b> fog, hair spray	<b>Solid aerosol;</b> smoke, air, cloud, air particulates
	Liquid	<b>Foam;</b> shaving cream	<b>Emulsion;</b> milk, hand cream	<b>Sol;</b> pigmented ink, blood
	Solid	<b>Solid foam;</b> aerogel	<b>Gel;</b> jelly, silica gel	<b>Solid sol;</b> glass

Colloidal systems where materials are dispersed in a liquid are called colloidal dispersions, such systems are heterogeneous and consists of two distinct phases. The type of dispersion, according to Thomas Graham (1861), is defined by the size of the solute particle (solid particles), which is dispersed in the liquid, typically between 1-1000 nm. A true solution has solute particles with diameters less than 1 nm, which form a stable and homogeneous system. A suspension is a heterogeneous dispersion where the solute particles has typically diameters bigger than 1000 nm, which make them microscopic visible and they have a tendency to settle down by gravity forces. Colloidal dispersions can be categorized in many different ways, e.g. water-in-oil/oil-in-water, hydrophilic/hydrophobic, macroemulsions/microemulsions or lyophilic/lyophobic colloids (8).

In this thesis there are two colloidal systems that are more interesting and utilized; the sol and the emulsion. Sol is defined as solid particles dispersed in a continuous liquid phase and emulsion as a liquid dispersed in another liquid, see table 2.1. The silica nanoparticles form a sol in water,

which in turn is the dispersed phase in an emulsion. The two different colloidal systems will be discussed in section 2.1.2 Emulsions and 2.2 Silica and colloidal silica.

### 2.1.1 DLVO-theory

Colloidal particles have a large interfacial area to volume ratio and because of this the behavior of colloidal sols often depend on the specific surface chemistry of the particles and the properties of the dispersions media, resulting in a characteristic particle-particle interaction (8). The DLVO-theory, named after Derjaguin, Landau, Verwey and Overbeek can be used to explain this interaction between colloidal particles (9). Van der Waals forces and electrostatic forces are two opposite forces that act between colloidal particles and determine the rate of many dynamic phenomena e.g. aggregation, coagulation, coalescence, flocculation, phase separation, etc.

The DLVO-theory combines Van der Waals attractions and the electrical double layer (EDL) repulsion to describe the total energy of interaction between two particles as a function of the distance between the particles. The shape of the interaction energy profile affects the kinetics of dynamic phenomena and is determined by the physicochemical parameters such as particle size, zeta potential, electrolyte composition and the Hamaker constant. A typical interaction energy profile follows the shape shown in Figure 2.1 presenting from the left; a deep minimum (primary minimum), followed by a maximum (energy barrier) and another minimum (second minimum) as the distance increases (10).

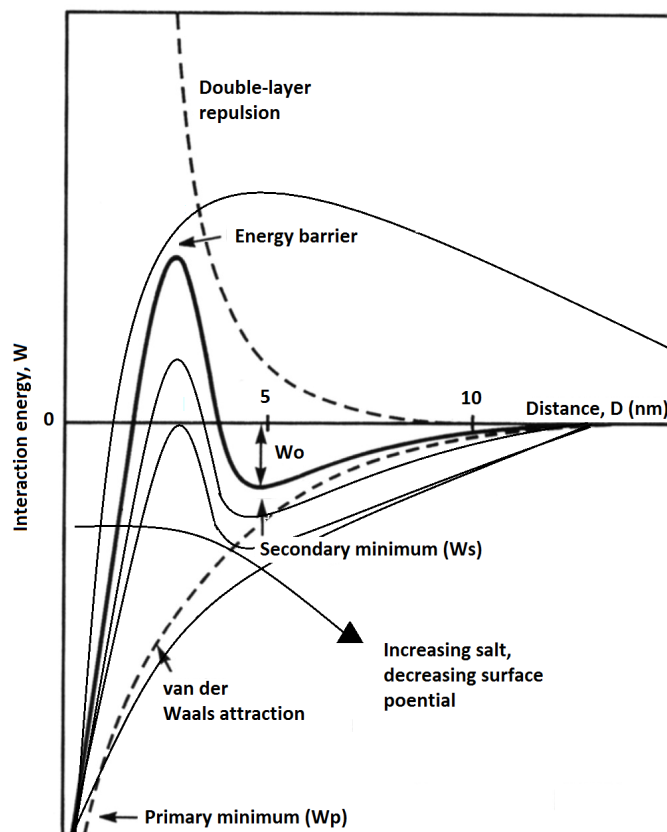


Figure 2.1 Typical interaction energy between colloidal particles at varied interparticle distances (11). Copyright 2006 by ProQuest Information and Learning Company. Adapted with permission.

The deep primary minimum in the interaction energy profile is implied from the binding energy between two particles where the binding energy has overcome the energy barrier of the repulsion from the double layer and/or electrostatic forces. The particles will be attracted by Van der Waals forces and in some cases by other types of forces causing chemical bonds between the particles, i.e. aggregation, or if the colloidal system is an emulsion the droplets will coalesce. The second minimum indicates a weak aggregation where the interaction energy is dependent of particle size, the electrostatic forces and the double layer. Bigger particles have more tendencies to adhere than smaller. In the presence of an energy barrier, the repulsion forces dominate and the colliding particles must overcome these forces to adhere, therefore aggregation is prevented. In the case of electrostatically stabilized particles the particles are kept apart due to the electrical charge which repels the particles (12).

Because of the charged silica particle surface there is an electric double layer formed close to the particle surface that have a higher concentration of ions than in the bulk, see figure 2.2. The formation of the double layer can be explained by the fact that charged surfaces attract oppositely charged counter-ions that in turn again attract ions that are oppositely charged compared to the counter-ions. The layer by layer organization of the ions becomes increasingly disordered as the distance from the surface increases. The zeta potential is the electric potential difference at a shear plan in the double layer and the higher zeta potential, the more stable particles (8).

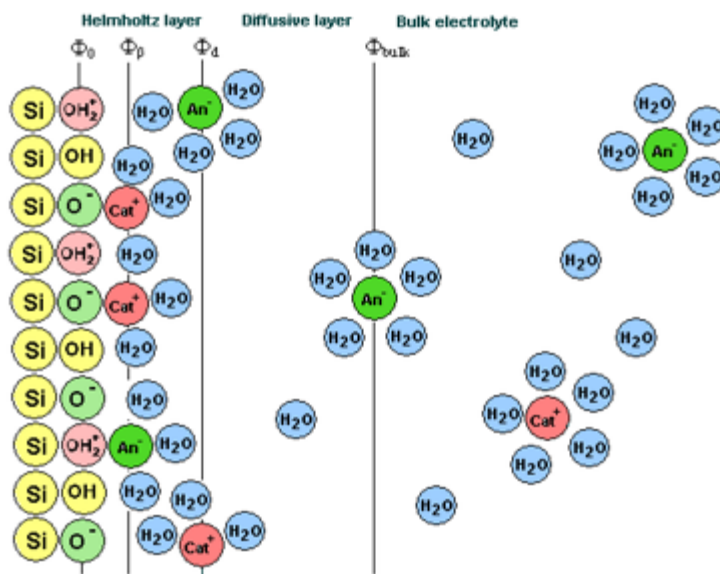


Figure 2.2 Schematic picture of the double layer close to a silica surface (13). Copyright 2014 by The bios lab-on-a-chip Group – university of Twente. Adapted with permission.

The salt concentration affects the thickness of the double layer and hence the kinetics and the rate of aggregation. The rate of aggregation as a function of salt concentration can be measured to find out the stability ratio of a colloidal dispersion. The effect of increasing salt concentration on the rate of aggregation follows an S-shape curve and the aggregation kinetics can be divided into fast and slow aggregation regimes. In the fast aggregation regime, large salt concentration is present and suppresses the double layer repulsion so that collision occurs between particles. In contrast, potential energy barrier is present in slow aggregation regime and controls the kinetics of aggregation (14).

### 2.1.2 Emulsions

An emulsion is a dispersion of one liquid in another liquid and concern liquids that are normally immiscible. The droplets in an emulsion are generally referred to as the dispersed phase and the surrounding liquid as the continuous phase. In most emulsions water is included in one phase while the other phase is an organic liquid (15).

There are two types of emulsions; macro- and microemulsion. Macroemulsions are thermodynamically unstable systems with relatively large droplets,  $>0.1 \mu\text{m}$ . There are two main types of macroemulsion, water-in oil (W/O) and oil-in-water (O/W), where the latter is by far the most common one. Examples of common emulsions in the daily life are paints, glues, margarines, hand creams, lotions etc. Microemulsions usually have droplets in the size range of 5-50 nm but should not be seen as macroemulsions with very small droplet size. Macro- and microemulsions are fundamentally different as microemulsions are thermodynamically stable and no energy is needed to create the microemulsions. Once the conditions are right, spontaneous formation occurs while formation of macroemulsion requires input of energy (15, 16).

In this thesis macroemulsions are in focus, and from now on these will be referred to as emulsions. Besides the two immiscible liquids a third component, an emulsifier, and energy are needed to create an emulsion. An emulsion can be formed fairly easy by simply shaking the mixture, usually resulting in large dispersed droplets (few micrometers) that are unstable. The challenge lays in making smaller droplets that tend to be more stable against creaming, coalescence and flocculation. Hence the essential process is not the droplet formation instead the break-up of the droplets. In order to break up a droplet high energy is required which can be explained by the Laplace pressure,  $\Delta P$ , which is the difference in pressure between inside and outside the droplet:

$$\Delta P = P_{inside} - P_{outside} = \frac{2\gamma}{R} \quad (\text{eq. 1})$$

where  $\gamma$  is the surface tension and  $R$  is the radius of the droplet. To break up the droplet into smaller ones, it is needed to apply higher energy since smaller droplets have higher Laplace pressure. As the stress is generally transmitted by the surrounding liquid, a very high energy has to be dissipated in the liquid to break up the droplets. By adding emulsifier and thereby lowering the surface tension, Laplace pressure is reduced and thus also the stress needed to break the droplets. This is one important role of the emulsifier. Another essential function of emulsifiers is stabilizing the emulsion, in other words prevent coalescence of newly formed droplets (17).

### **2.1.3 Emulsion stability and destabilization mechanisms**

As mentioned earlier, mixtures of immiscible liquids, known as emulsions, are thermodynamically unstable systems that sooner or later separate. Emulsions can be stabilized by several different methods using emulsifiers that provide stabilization usually through electrostatic- or steric stabilization or particle stabilization.

By adding emulsifiers, the emulsion can be fairly stable and it can take several years before the separation occurs. Emulsifiers are molecules that have a tendency to adsorb at the surfaces and interfaces. The tendency to assemble at interfaces is a fundamental property of an emulsifier. By adsorbing at the interfaces the emulsifier reduces the free energy of the phase boundary. Emulsifiers consist of at least two parts, a hydrophilic part and a hydrophobic part normally referred to as the head group and the tail. The tail consists normally of a hydrocarbon. Emulsifiers are often categorized in four groups according to the charge of the head group; anionic (negatively charged, e.g. acid), non-ionic (neutral, e.g. ethoxylate), cationic (positively charged, e.g. quaternary amines) and zwitterionic (both negatively and positively charged, e.g. amino acids) (15, 18)

Electrostatic stabilization is based on the use of ionic emulsifier or ions. When the droplets are covered with the charge and the emulsion droplets get close to each other they will electrostatically repel each other, keeping the droplet size of the emulsion stable.

On the other hand, there is steric stabilization that is based on the use of non-ionic emulsifiers, usually with a long polyoxyethylene chain or polymer tails. With long chain molecules protruding from the surface aggregation is inhibited due to the repulsive force from the entropy decrease when the chains from two different droplets start to entangle.

Another way to stabilize an emulsion is using solid particles. The particles accumulate and form a monolayer at the interface which stabilizes the emulsion droplets against coalescence. A requirement is that the particles must be very small compared to the emulsion droplets.

There are four common types of phenomena that occur when an emulsion destabilizes, e.g. creaming/sedimentation, flocculation, coalescence and Ostwald ripening. Creaming or sedimentation occurs when the density of the droplets is lower respectively higher than the continuous phase. Droplets can also flocculate, which means that the droplets aggregate without merging. Creaming, sedimentation and flocculation are all reversible mechanisms and the emulsion can often be regained by applying some stress e.g. by stirring the emulsion. However, if the droplets start to coalesce, that is if smaller droplets merge and form larger droplets, the emulsion will phase separate. Coalescence can be seen as an irreversible mechanism and the emulsion can only be regained by applying high stress. The last destabilization mechanism, Ostwald ripening, is a process where large droplets grow at the expense of small droplets. The process is caused by diffusion of molecules from the dispersed phase through the continuous phase and since small droplets have a large area per volume they will be more affected than large droplets (15, 18).

### **2.1.4 Emulsifiers**

Two common emulsifiers that are used in this thesis are ethyl hydroxyethyl cellulose, EHEC, and methyl hydroxyethyl cellulose, MEHEC. Hydroxyethylene celluloses are a water soluble

derivative of cellulose used as a gelling and thickening agent. Typical uses of cellulosic ethers are in paint, cement based applications, household cleaning products such as, soap and shampoos (19).

EHEC consists of ethylene oxide and ethylene groups attached to the cellulose polymer by ether linkages, while MEHEC in addition has methyl groups and less ethylene oxide groups. Figure 2.3 shows a schematic picture of these emulsifiers at molecular level (20).

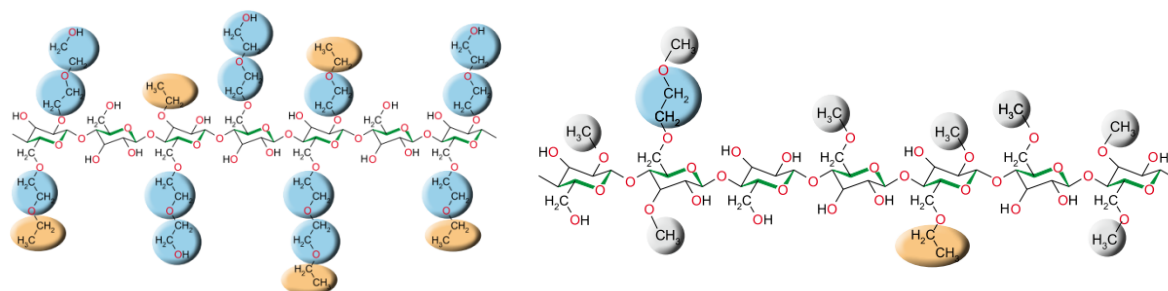


Figure 2.3 Molecular structure of EHEC (left) and MEHEC (right). EHEC contains ethylene oxide (blue) and ethylene (orange) groups, while MEHEC in addition has methyl (grey) groups (20). Copyright Akzo Nobel. Adapted with permission.

The presumed function of these emulsifiers is to adsorb at the emulsion droplet surfaces and both lower the interfacial tension and stabilize the droplets to avoid coalescence. The alcohols, ethoxy groups and ether links are more or less hydrophilic and the methyl and ethyl groups are hydrophobic. Since cellulosic ethers are highly water soluble one can also assume that some of the cellulosic ethers will be dissolved in the water droplets and potentially act as a template for the mesoporous system (20).

## 2.2 Silica and colloidal silica

Silica has the molecular formula  $\text{SiO}_2$ , and is an abundant mineral in nature where it is commonly found as quartz. Usually silica has a tetrahedral structure where the Si-atom shows tetrahedral coordination with four surrounding oxygen atoms. The tetrahedral  $[\text{SiO}_4]^{4-}$  building blocks are rigid but by binding the oxygen atoms, forming Si-O-Si bridges, it can be fairly flexible. This flexibility is what makes silica a great glass former (21).

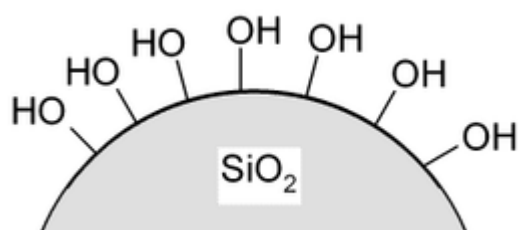


Figure 2.4 The surface of a silica particle (22).

Amorphous silica has a high thermal stability due to the absence of volume changes during phase transformation. The expansion coefficient of silica is extremely low. Silica is soluble in alkalis but has an extremely high chemical resistance against water and acids. Hydrofluoric acid and

phosphoric acid are the only two acids that dissolve silica. Beside the unique thermal and chemical properties, silica has good electrical and thermally insulating properties (23).

According to Iler (24), the term colloidal silica refers to “stable dispersions or sols of discrete particles of amorphous silica”. The silica particles are usually small, ranging approximately from 7 to 100 nm. If the silica sol dispersion has a silica concentration of more than 10-15% the particle size can be approximated visually by the turbidity. If the diameter of the particles is smaller than 7 nm the dispersion is clear. The turbidity of the dispersion increases with increasing particle size and above about 50 nm the appearance is transformed to white/milky. Particles larger than 100 nm are often not stable and settle after few days or weeks leaving a transparent upper layer. In the 1940s stable concentrated silica sols, in other words silica sols that did not gel or settle down for at least several years, were available. This was possible after it turned out that alkalis, e.g. ammonia, could stabilize the system. Over the years larger and larger silica particles have been successfully stabilized (24).

The application of colloidal silica varies and colloidal silica has many functions. It can e.g. be used in decorative coatings where the colloidal silica prevents dirt to adhere, improves the hardness, enhances the pigment dispersion and also increases the time between repaintings. Colloidal silica can also be used for shaping, smoothing and polishing different substrates, e.g. silicon, aluminum and sapphire, to obtain a low-defect and ultra-flat surface (25).

### 2.2.1 Mesoporous silica

According to IUPAC, porous materials can be classified in mainly three categories: microporous (with pore diameter  $<2$  nm), mesoporous (2-50 nm) and macroporous ( $>50$  nm). The pores of mesoporous silica can have various shapes, such as cylindrical or spherical, as exemplified in figure 2.5 (26).

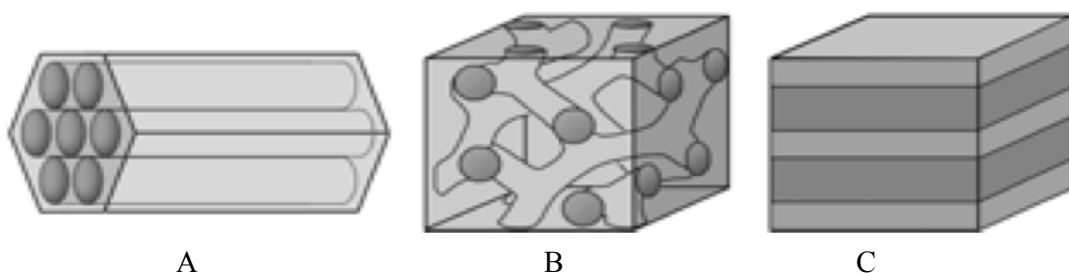


Figure 2.5 Illustration of porous structures with the following morphologies; cylindrical (A), network (B) and layered (C) (26).

The unique property of high surface area to volume ratio results in a wide range of potential applications where the properties are of high relevance. Inside mesoporous silica it is possible to accommodate various molecules, which is a property that can be used in applications such as catalysis and drug delivery. Mesoporous silica is also commonly used as the stationary phase in chromatography. In addition, mechanical strength, thermal and pH stability and stability over time are some of the properties that mesoporous silica particle can offer over their organic counterparts (27).

Mesoporous silica particles can be synthesized with different morphology characteristics such as particle shape, size distribution, pore structure and pore size distribution (2). Mesoporous silica can also be synthesized in the form of thin films or monolithic materials (28, 29). In this thesis, the synthesis of mesoporous spherical silica particles will be in focus. Mesoporous spherical silica particles are often synthesized in the presence of an emulsifier as template. The method to prepare the mesoporous silica particles is further explained in section 2.3.1 Synthesis of silica particles.

## 2.3 The sol-gel process in emulsions

The sol-gel process is a synthesis method used to make organic, inorganic and organic-inorganic porous materials. There are three main sol-gel methods for synthesizing solid silica and metal oxide particles in a liquid; gelation of a solution of colloidal particles, hydrolysis and polycondensation of alkoxide or nitrate precursors followed by hypercritical drying of gels and hydrolysis and polycondensation of alkoxide precursors followed by aging and drying. In this thesis the first mentioned sol-gel method has been used, where silica gel has been formed from discrete colloidal silica particles (30).

A colloidal gel is defined as a colloidal system where colloidal solid particles form an aggregated solid network that binds the liquid present in the pores of the network. During the gelation the colloidal silica particles forms a three-dimensional network by aggregation of the particles that close to gelation causes a sharp rise in viscosity. For colloidal silica particles the three most common parameters to tune the gelation time is pH, salt and particle concentration. The aggregation rate, see figure 2.6, of the silica particles increases with increasing particle concentration. At high pH (7-10.5) silica becomes negatively charged and aggregation of the colloidal particles is therefore prevented due to the charges which creates repulsion. However, the presence of salt reduces the repelling forces and aggregation occurs. At low pH (1.5-3) colloidal silica particles are temporary stable even if the particles have little ionic charge, but this is not sufficient to prevent aggregation and gelation long-term (24, 30).

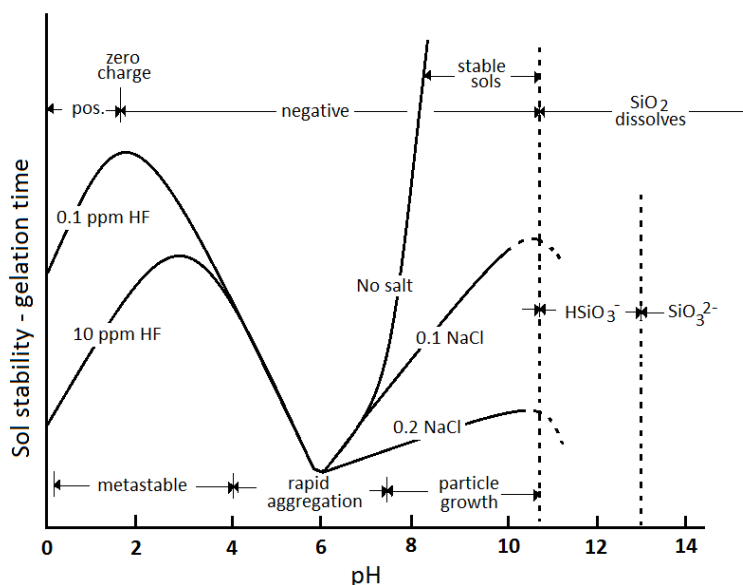


Figure 2.6 Schematic illustration of the rate of silica sol gelation at different conditions (24). Copyright by John Wiley & Sons. Adapted with permission.

One advantage with the sol-gel processes, among others, is the low processing temperature related with sol-gel method compared to other traditional glass melting or ceramic powder methods. Also, the sol-gel process can be used to produce and easily shaped materials into complex geometries in a gel state and to produce high purity products (30).

### **2.3.1 Synthesis of silica particles**

The first successful synthesis of spherical silica particles with controlled particle size was the Stöber method, in which sol-gel reaction of silicon alkoxides in a homogenous aqueous ammonia/alcohol solution was utilized. The Stöber method was further combined with templating methods to synthesize mesoporous materials.

Another synthesis method is aerosol based, where the evaporation-induced self-assembly method is utilized and the silica precursor solution is atomized and heat-treated to evaporate the liquid medium and collect particles without filtration or centrifugation (3). A development of the evaporation-induced self-assembly method is the ESE-method, i.e. W/O-emulsion with solvent evaporation, where silica precursor and emulsifier solution is dispersed in the organic phase (31, 32). In the ESE-method water is evaporated from the emulsion droplets containing silica sol, causing irreversibly gelation of the silica precursor particles that form an aggregated network structure within each emulsion droplet. The gelation of the silica particles is caused by both an increase in salt and particle concentration as a result of the water evaporation from the emulsion droplets (33). The particles are collected with filtration or centrifugation and calcined to expel any organic substituents and obtain the mesoporous silica particles. The ESE-method is the method used in this thesis.

### **2.3.2 How different reaction parameters affects the particle size**

Andersson et al. (2006) reported that the mesoporous silica particle size distribution is determined by the droplet size distribution of the emulsion. The emulsion droplets are affected by several critical parameters, such as shear forces e.g. stirring rate, temperature, composition in terms of both continuous phase and emulsifier and the viscosities of both the continuous phase and the dispersed phase (7).

Kosuge et al. (2004) have synthesized spherical mesoporous silica particles and noticed that the particle size distribution became narrower with decreasing particle size and that the stirring rate affected the particle size distribution, which Huo et al. also confirmed (34, 35). Kosuge claimed that monodisperse spheres were obtained in the range of 500-700 rpm and Huo noticed that low stirring speed (<200 rpm), medium stirring speed (200-400 rpm) and high stirring speed (>450 rpm) resulted in what was defined respectively as “soft” gel particles, spheres and fine powders. In an article, Nooney et al. reported how the particles size could be controlled over a range of diameters only by varying the initial silicate/emulsifier concentration. They observed that the particle size increased with increasing concentration of silicate and emulsifier (36).

### **2.3.3 Process modified with Couette cell**

Preparation of emulsions using stirring or shaking is a common emulsification method in use today. However, the conditions are hard to control precisely and that contribute to highly polydisperse emulsion droplets distributions. There are many methods claiming to produce

monodisperse emulsions which include depletion flocculation fractionation (37), controlled shear rupturing (38), controlled coalescence (39) and membrane emulsification (40, 41).

Another method is the Couette cell method that utilizes shear stress by a so called Couette cell to obtain narrower particles size distributions (32, 38). The Couette cell creates well-defined shear stresses on the liquid that fractures the droplets and in that way the droplet sizes of the emulsion is changed. The exact mechanism behind the monodispers emulsions that can be created by this method is not fully understood. Numerous experiments have been done by Mason and Bibette (32, 38) and they found two important conditions that must be fulfilled to get a monodisperse droplet distribution. First, the premixed emulsion needs to be viscoelastic and second a uniform shear stress needs to be applied to the premix emulsion in the Couette cell; preferably by using a narrow gap between the outer and inner cylinder, see figure 2.7.

The Couette cell contains two cylinders; the outer cylinder is fixed and the inner cylinder is connected to a motor that rotates at a selected angular velocity. In our setup, the diameter of the outer cylinder was 40 mm. The inner cylinder was divided into two parts giving a gap of 0.1 and 0.05 mm respectively. The height and the diameter of the lower part differed from the height and the diameter of the upper part, see figure 2.7 for the dimensions of the Couette cell. The premixed emulsion was pumped in at bottom of the cell and out at the top, allowing for continuous production of emulsion. The emulsion was pumped by a predetermined velocity thereby controlling the retention time, i.e. the time the premixed emulsion stays inside the Couette cell.

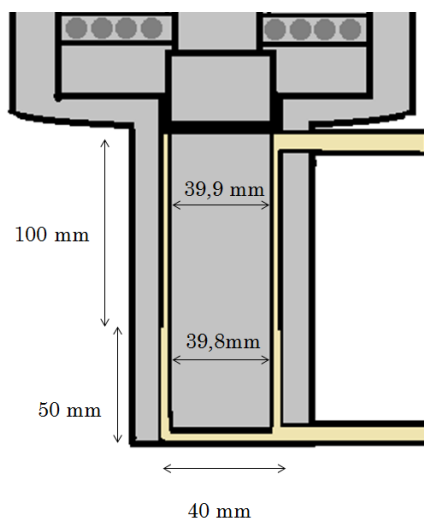


*Figure 2.7 Schematic cross section of the Couette cell.*

The rheological properties of the premixed emulsion can be controlled by modifying the continuous phase and also the volume fraction of the dispersed phase. Firstly, the concentration of emulsifier does play an important role to the rheology of the continuous phase. In small amounts it will stabilize the water-oil border and lower the interfacial tension between the two immiscible liquids, but in excess it will change the rheology of the continuous phase by creating micelles. Micelles can be seen as aggregates of the emulsifier. The emulsion rheology can also be modified by adding thickeners in the continuous and/or the dispersed phase. An increase in thickener concentration increases the viscosity but not coalescence of the droplets in the emulsion (32). Secondly, by increasing the volume fraction of the dispersed phase, the emulsion will turn from a

viscous to an elastic liquid. When the emulsion is sheared, energy is transferred into the droplets' interfaces and deforms the droplets to create more droplets. Higher droplet packaging and closer contact between the droplets and their deformation is the reason to elastic behavior of the emulsion (41).

## 2.4 Characterization methods

Different characterization methods have been used to analyze and determine the particle size of the spherical mesoporous silica particles produced. These methods are briefly described below.

### 2.4.1 Optical microscopy

Optical microscopy uses visible light to observe the image of small objects after enlarging the image through a system of lenses. Typically the setup includes a light source, a condenser, an objective and an ocular/eyepiece. The condenser is a lens with the purpose to focus the light from the light source onto the sample. Some condensers might also contain other features, such as filter or diaphragm, to obtain the quality and intensity of the lightning. The objectives are probably the most complex component in a microscope that provides magnified images of the sample. The magnification can range from 2x to 200x. The resolution limit of a standard optical microscope is around ~200 nm. Usually the objective is a cylinder housing containing multi-element compound lens. The eyepiece also has magnification that together with the objective contributes to the overall system magnification. The eyepiece consists of a field lens and an eye lens and the purpose is to bring the image into focus for the eye (42).

### 2.4.2 Scanning electron microscopy

Scanning Electron Microscopy (SEM) is an analysis method that uses a focused beam of high-energy electrons to study the surface of solid materials. The electron source releases electrons which interact and reflect of the solid material before hitting a detector that provide a 2-dimensional image. The images provide information about the surface morphology, such as structure and orientation of down to nanometer scale features. SEM can detect much smaller particles than the optical microscope due to the small wavelength of the electrons, i.e. a resolution in the area of ~5-10 nm (43, 52).

### 2.4.3 Surface tension measurements

The Du Noüy ring method is one of the most widely used methods for measuring the surface tension and interfacial tension ( $\gamma$ ) of liquids, probably because it is a relatively simple and quick method. In the instrument a solid ring with well-defined geometry is attached to a balance. This ring is immersed into the liquid to be analyzed. It is then slowly withdrawn from the liquid while the balance continuously record the force applied on the ring when it pulls through the liquid-liquid or air-liquid interface. The maximum force is the force required to detach the ring from the interface and from such measurements the interfacial tension can be calculated using the following equation:

$$\gamma = \frac{F_{max}}{4\pi R f_{corr}} \quad (\text{eq. 2})$$

where R is the radius of the ring and  $f_{\text{corr}}$  is the correction factor which depends on geometry of the ring and the density of the liquid.

#### 2.4.4 Coulter counter Multisizer

Coulter Counter is an instrument developed for counting and sizing particles suspended in electrolyte solution. Coulter Counter technology uses a tube with two electrodes, one placed inside and one outside of the tube, in which an electric field is applied between the electrodes. Before analysis the particles are dispersed in a special type of salt solution. Since the electrolyte is conducting the impedance between the electrodes will decrease when a particles passes through them and the changes are measured as voltage or current pulse. The pulse heights are proportional to the solid volume of the particles, which enables counting and sizing of the particles. The Coulter Counter assumes that all particles are spherical as it measures the volume and number of particles. If a particle is porous the Coulter Counter will interpret the particle to be smaller than its actual size as the porous system is conductive. Particles of sizes from 0.4  $\mu\text{m}$  up to 1600  $\mu\text{m}$  can be measured and the technology is suitable for drugs, pigments, fillers, toners, foods, minerals, metals, coating and filter materials, etc. (44).

#### 2.4.5 Malvern (Sysmex FPIA 3000)

The Sysmex FPIA 3000 instrument is an image analyzer that can measure the shape and size of particles in suspension. Particles properties that can be characterized are circle equivalent diameter, circularity and convexity. The instrument measures particles from 0.8  $\mu\text{m}$  to 300  $\mu\text{m}$  and up to 300,000 particles can be analyzed. A sample is taken from a dilute suspension of particles which is then passed through a measurement cell, called the Sheath-Flow cell. The cell forces the particle suspension into a flat capillary that ensures that all particles are in the plane of focus and that all particles are aligning with their largest area facing the camera. The images of the particles are then captured by using stroboscopic illumination and a camera (45, 46).

Circularity is defined as the circumference of the circle of equivalent area divided by the real circumference of the particle.

$$\text{Circularity} = \frac{2\sqrt{\pi A_p}}{P_p} \quad (\text{eq. 3})$$

where,  $A_p$  is the area of the particle and  $P_p$  is the circumference of the particle. The closer the circularity is to 1, the more spherical the particle is. The circularity decreases with more elongated or rough-edged particles (45). The circularity distribution,  $d_{90}/d_{10}$ , indicates how spherical the particles are, the closer to 1 the more uniform spherical particles.

#### 2.4.6 Particle size distribution

The particle size, e.g. the results from Coulter counter, Malvern or any other particle counter/sizer, are displayed as a particle size distribution curve with the differential- and cumulative volume in percent as a function of particle diameter in  $\mu\text{m}$ . The differential volume curve shows the relative amount of particles at each size. The highest peak indicates the biggest relative amount of particles at the specific size, e.g. in figure 2.8 it is shown that the most particles have diameter of approximately 16  $\mu\text{m}$ . The corresponding continuous cumulative volume curve shows the relative amount of particles at or below a specific size. The diameter at the 50<sup>th</sup>

percentile,  $d_{50}$ , is 16.79  $\mu\text{m}$  in figure 2.8, therefore 50% of the particles have particle diameter of  $\leq 16.79 \mu\text{m}$ . The narrowness can be measured by percentile ratio,  $d_{90}/d_{10}$  and the distribution is narrowest as the ratio approaches 1 (47). The narrowness value is relative due to the dependence of the particle size, i.e. a  $d_{90}/d_{10}=1.5$  with a  $d_{50}=1 \mu\text{m}$  is much more narrow than a  $d_{90}/d_{10}=1.5$  with a  $d_{50}=10 \mu\text{m}$ . The particle size distribution could be measured as number, volume or mass. These particle size distributions are as they sound correlated to the size and the density of the particles. However, in this thesis only volume particle size distributions are used.

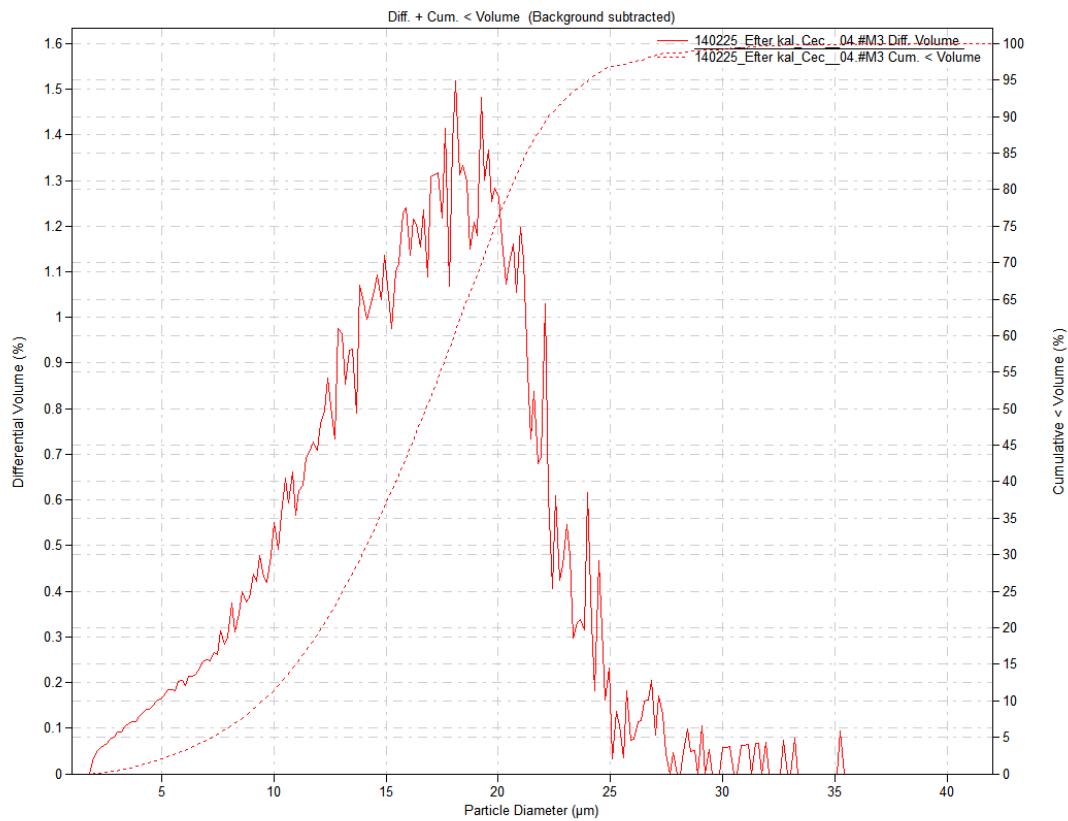


Figure 2.8 Particle size distributions from Coulter counter for the reference system.

## 3. Method

In this thesis, mesoporous spherical silica particles were synthesized with the ESE-method. The reaction method consisted of the following steps; the inorganic phase was prepared by mixing water and stabilizer/emulsifier. The inorganic phase was added to the organic phase under stirring to create an emulsion. The silica sol dispersion was thereafter supplied to the emulsion under stirring, giving water droplets with silica sol inside. The emulsion was then heated to evaporate the water. During evaporation the droplets became smaller leading to an increase in both silica and salt concentration, resulting in particle aggregation and ultimately gelation within the dispersed phase. By using a vacuum pump, the pressure was reduced, lowering the evaporation temperature of the water droplets. After gelation, the mesoporous particles were separated from the continuous phase through filtration followed by calcination to remove the emulsifier to create the mesoporous particles.

In the emulsion with solvent evaporation method, ESE-method, the dispersed inorganic phase must be slightly soluble in the continuous organic phase as the inorganic phase must be able to diffuse through the continuous phase during solvent evaporation. Still, the two phases cannot be totally miscible as this would prohibit emulsion formation. In this thesis, pre-experiments were made to find an emulsion system that gave mesoporous silica particles with a spherical morphology with a reasonable narrow particle size distribution. A literature study was conducted to find organic solvent candidates to be used as the continuous phase. Organic molecules that have suitable water solubility are typically alcohols, esters, ketones etc. table 9.2 in appendix 9.2, shows that some alcohols have a suitable solubility in water while at the same time having a significantly higher boiling point than water. The high boiling point is beneficial both for safety reasons but also prevents boiling in the continuous phase, which could disturb the emulsion and mesoporous particle formation. Furthermore, alcohols are not hazardous.

The reaction parameters that were varied were gelation temperature, stirring rate, concentration of chemicals and additives etc. The particle morphology and size distribution were compared to the results from a reference system with a defined composition and set of reaction parameters. The specifics of the reference system are described later in following section, 3.1 Pre-experiments for the reference system.

A Couette cell was used in this thesis with the aim to achieve a narrower particle size.

### 3.1 Pre-experiments for the reference system

Some pre-experiments were conducted to find a reference system to compare with. Benzyl alcohol was chosen as the organic phase since it seemed to be the most promising candidate given its water solubility and boiling point. The emulsifier was preselected to be EHEC E230 since cellulosic ethers have shown interesting emulsion stability behaviors (48). The reaction temperature was set to 65 °C (30). To evaporate the water the pressure in the reactor was set to 160 mbar. The boiling point of water is 55 °C at 160 mbar. The stirring rate was set to 450 rpm since Hou (35) indicated that this was the limit for fine particles. See table 3.1 for the chosen parameters for the reference system.

Table 3.1 Parameters for the reference system.

Temperature during gelation	Stirring rate	Pressure	Amount of emulsifier	Organic solvent
65 °C	450 rpm	160 mbar	1 wt% EHEC E230	Benzyl alcohol

## 3.2 Materials

The organic solvents selected to be used in the experiments were; benzyl alcohol (Univar AB, Malmö, Sweden), 2-metyl-1-butanol (98%, VWR), 3-pentanol (98%, Sigma-Aldrich), 1-hexanol (98%, Sigma-Aldrich), cyclohexanol (>99.5%, Fluka Chemie AG) and 3-metyl-3-pentanol (>99%, Sigma-Aldrich).

The 14 wt% silica sol used was ammonium stabilized and contained particles that were 7-8 nm in diameter with a 400 m<sup>2</sup> particle surface area/g silica (Akzo Nobel Pulp and Performance Chemical).

Some different emulsifiers were selected and used; EHEC E230, EHEC E351, EHEC E511 and MEHEC EMB5500 (Akzo Nobel Performance Additives). These different cellulosic ethers have different thickening potential, i.e. E230 being the least thickening and EMB5500 the most. Thickeners for the organic phases were poly(isobutyl methacrylate) and isobutyl methacrylate copolymer (Akzo Nobel Surface Chemistry). See table 3.1-3.2 for more details for the different type of emulsifier and organic solvents respectively.

Table 3.1 Molar substitution, degree of substitution and viscosity of different types of EHEC and MEHEC emulsifiers.

Type	MS <sub>EO</sub>	DS <sub>ethyl</sub>	DS <sub>methyl</sub>	Viscosity (cP)	
				1% conc	2% conc
E230	1.9	0.9	-	-	300
E351	1.9	0.9	-	-	5000
E511	1.9	0.9	-	7000	-
EBM5500	2.4	0.4	0.5	5500	-

Table 3.2 Viscosity and water solubility of the different organic solvents.

Organic solvent	Water solubility (mg/kg)	Viscosity (cP)	Boiling point at 1 bar (°C)
1-hexanol	5875	4.596 at 25 °C	157.4
2-methyl-1-butanol	30000	4.16 at 25 °C	128
3-methyl-3-pentanol	33476	0.61 at 25 °C	120.91
Benzyl alcohol	35000	6.54 at 25 °C	205
Cyclohexanol	42000	41.07 at 30 °C	161.1
3-pentanol	52000	4.15 at 25 °C	115.3

### 3.3 Experimental procedure

Unless otherwise stated, all experiments were conducted as follows: 0.5 g emulsifier was dissolved in 50 g distilled water (1wt% emulsifier). The solution of 1 wt% emulsifier was stirred until the emulsifier was fully dissolved, approximately 10-15 min. For higher viscosity or amount of emulsifier the respective solutions was stirred for up to 30-40 min. The solution of 1 wt% emulsifier was then mixed with 615 g organic solvent in a reactor (1L double-walled reactors with belonged lid with 4 openings) under stirring at ~450 rpm (Eurostar digital from IKA Werke, Staufen, Germany) to create a water-in-oil (W/O) emulsion. The emulsion was stirred for 20 min at 20 °C before the stirring rate was decreased to ~350 rpm and 117.07 g silica sol dispersion was added. The stirring was continued for 60 min and then the stirring rate was decreased to ~275 rpm. The reactor was heated to 65 °C using a refrigerated and heating circulator (Julabo F25-ME, Allentown, USA) and the pressure was reduced to 160 mbar using a vacuum pump (Büchi B-178, Flawil, Switzerland). The evaporation temperature was kept at this temperature until the water was fully evaporated (~2 hours) and the temperature was further increased to 80 °C (~30 minutes) to secure that all water was removed. After the evaporation the particles were separated from the organic solvent by filtration (Pyrex 4, England and Werner glas P4) and dried in an oven (Raypa, Barcelona, Spain) connected to a vacuum pump (Büchi V-710, Flawil, Switzerland) in 100 °C for one day. Finally, the particles were calcined in an oven (Nabertherm, Bremen, Germany) using a temperature program with constant increase in temperature from room temperature to the final temperature during 8 h, constant temperature at 650 °C for 4 h and thereafter cooling to room temperature, to remove the organic emulsifier. See figure 3.1 for the experimental setup.



*Figure 3.1 Experimental setup for the ESE-process containing refrigerated and heating circulator (1), double-walled reactor (2) and condenser system (3).*

### 3.3.1 Procedure modified with Couette cell

In the reactions modified with a Couette cell, a pre-emulsion is mixed with a rotor (Eurostar digital IKA Werke, Staufen, Germany) in a 3L-beaker, called reactor 1, the mixture is pumped (Watson, Marlow 400, SciQ, Stockholm, Sweden) through the Couette cell to reactor 2 where the gelation process is taking place (1L enclosed double-walled reactor with belonged lid with 4 openings). The Couette cell was custom made in-house by stainless steel. During gelation, the emulsion was stirred (RW20 DZM from IKA Labortechnik, Staufen, Germany) to obtain homogeneity. The Couette cell was set to a specific stirring rate (motor: CAT R100SD, Germany) to achieve the desired shear stress. The temperature was set to 65 °C with a refrigerated and heating circulator (Julabo F25-ME, Allentown, USA) and the pressure was reduced to 160 mbar by a vacuum pump (Büchi V-800, Flawil, Switzerland). The evaporation temperature was kept at this temperature until the water was fully evaporated (~2 hours) and the temperature was further increased to 80 °C (~30 minutes). The water vapor was cooled in the double-walled condenser with attached flask. See figure 3.2 for the experimental setup.

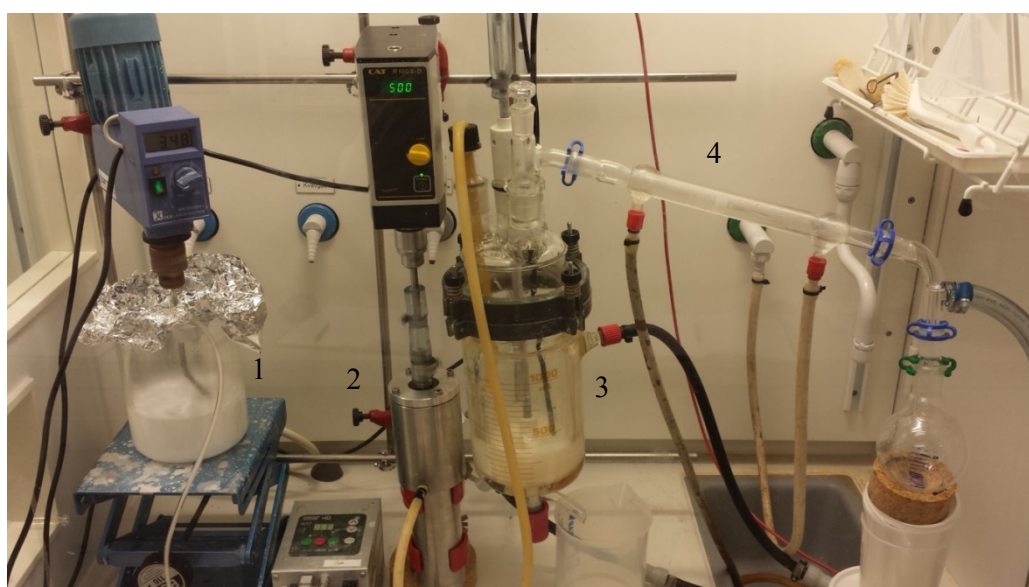


*Figure 3.2 Experimental setup of the process tighter with the Couette cell containing emulsion reactor (1), Couette cell (2), double-walled gelation reactor (3) and condenser system (4).*

### 3.4 Emulsion stability

The emulsions are often unstable and phase separate to an upper and lower phase over time. The stability of emulsions plays an important role for the synthesis of mesoporous silica particles and therefore a method was developed to study the rate of phase separation visually. To do this, transparent plastic jars of 50 mL (diameter 40 mm and height 45 mm, Nunc, Denmark) with lid were filled with a number the emulsions used for particle synthesis experiments. The jars were filled with 37.7 g and then shaken by hand for 1 minute. A camera (Panasonic DMC-TZ10, Osaka, Japan) was used to image the kinetics of the phases. The state when the emulsion has two distinct phases and does not appear to further separate for 2 hours is defined as complete phase separation.

### **3.5 Optical microscopy**

2 mL of emulsion from the reactor was taken with a glass pipette (HE Assistant, Germany) to a 4mL-vial with lid before gelation. 1-2 drops of the sample was placed on a microscope slide (26x76 mm, Kinder GmbH, Germany) and analyzed with magnification lens (Nikon LU Plan Flour 50x/0.80) in optical microscope (Nikon Eclipse Ci-L, Beijing, China) which is connected to a camera (Nikon DS-Fi1, Tokyo, Japan).

### **3.6 Coulter counter**

Approximately 50-60 mg silica particles were added to a beaker which was filled with 40 mL isotone (Beckman Coulter Inc. 250 S. Kraemer Blvd Brea, USA) The sample preparation was stirred and then treated with the ultrasonic bath (Bandelin Sonorex RK 52, Berlin, Germany) in 3 minutes. After the ultrasonic bath, the sample preparation was stirred again. Some of the sample preparation was added to the beaker inside the Coulter counter instrument (Multisizer 3 Beckman Coulter, Bromma, Sweden) with a plastic pipette until it reached a concentration of 2.5-3.5 % particles. The beaker inside the Coulter counter was prefilled with pure isotone before the sample preparation was added. The sample preparation was analyzed within 5 minutes after ultrasonication.

### **3.7 Malvern**

15-20 mg of silica particles were added to a 30 mL-vial and 2 drops of Igepal CA-630 (5%, Sigma-Aldrich Company Ltd, Gillingham, United Kingdom) was added to wet the silica particles. Thereafter 20 mL of distilled water was added to the vial before ultrasonication for 60 seconds. With a plastic pipette 2 mL of the sample preparation was added to the beaker in the Malvern instrument (Sysmex FPIA 3000, United Kingdom). The analyses were limited to 4000 particles per analysis.

### **3.8 SEM**

2-3 mg of silica particles and 500  $\mu$ L of distilled water were vortexed for a few seconds in a 1.5 ml Eppendorf tube. 4 drops of the dispersions were placed on a SEM sample holder and allowed to air dry. The sample was sputtered with a 10 nm thick layer of gold (JEOL JFC-1100E ion sputtering device, Japanese Electron Optics Laboratory Co. Ltd., Tokyo, Japan). The samples were then imaged with SEM (LEO Ultra 55 FEG SEM from Leo Electron Microscopy Ltd, Cambridge, England at an acceleration voltage of 3 kV).

### **3.9 Surface tension**

A Sigma 70 tensiometer (KSV Instruments, Helsinki, Finland) was used for surface tension measurements with the du Noüy ring method. The temperature was set to 25 °C by a cryostat (Neslab RTE-200, Thermo Electron Corporation, Newington, USA). 10-15 mL organic solvent was added to the tensiometer crystallization beakers. 10-15 mL of silica sol dispersion/EHEC

E230/water was carefully added above the organic solvent in the beaker so that they did not mix with each other.

## 4. Results

In this chapter the results are presented from the investigation of how the particle size distribution is affected by variations in the reaction parameters during the synthesis using ESE-method, and the Couette cell.

### 4.1 Process system without Couette cell

A reference synthesis was performed using benzyl alcohol as organic solvent and the emulsifier EHEC E230. The particle size distribution measured by Coulter counter that was obtained under these synthesis conditions are shown in figure 4.1. The reference system will from here on be recognized as a red curve in the figures.

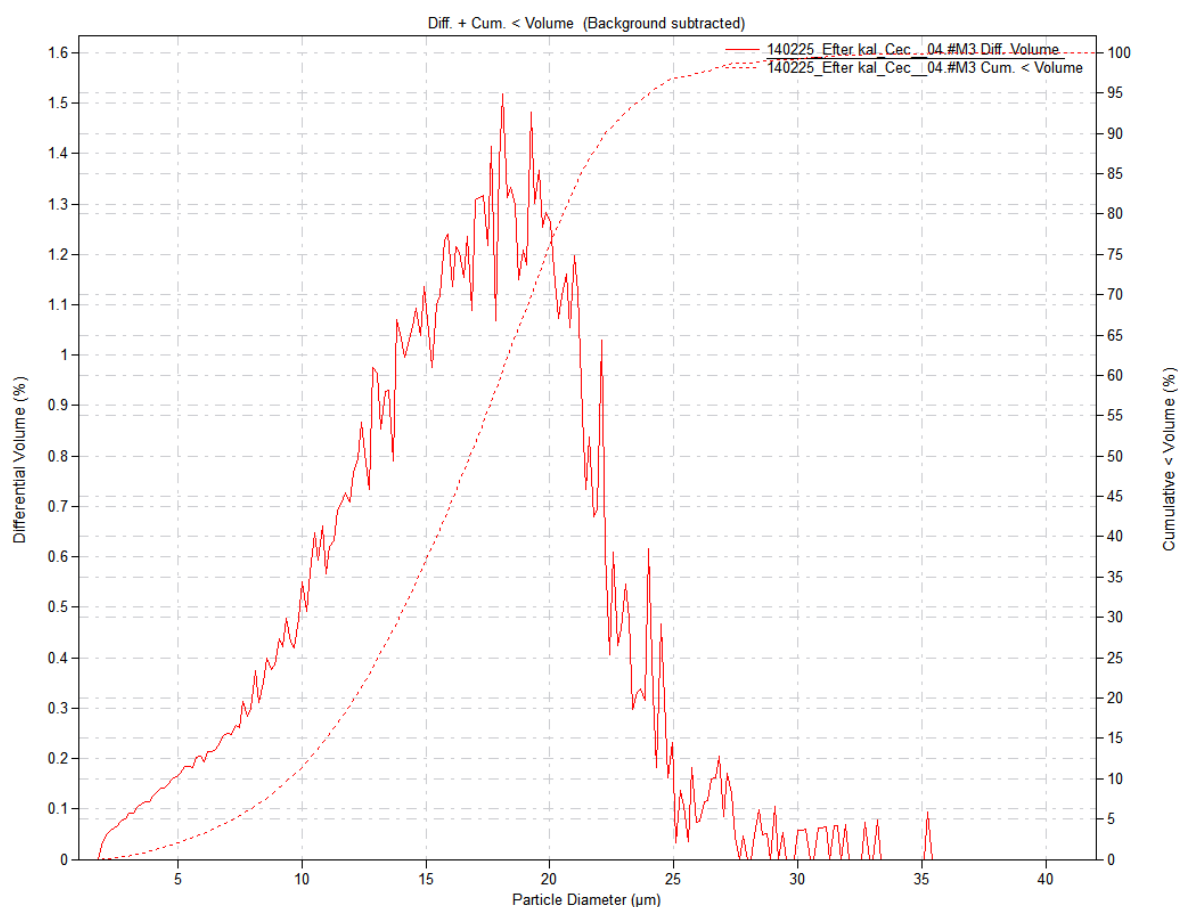


*Figure 4.1 Particle size distribution from Coulter counter measured for the reference system.*

From the Coulter counter curve the particle median size,  $d_{50}$ , is 16.79  $\mu\text{m}$  and the range of particle size,  $d_{90}/d_{10}$ , is 2.34. Figure 4.2 displays the reference system analyzed with Malvern. The figure to the left shows the particle size distribution and the figure to the right the circularity. In the particle size distribution from Malvern  $d_{50}$  is 19.29  $\mu\text{m}$  and  $d_{90}/d_{10}$  is 2.75. The circularity distribution  $d_{90}/d_{10}$  is 1.79. The particle median size and range of particle size are summarized in table 4.1 and from here on to table 4.10 the reference values are printed in bold.

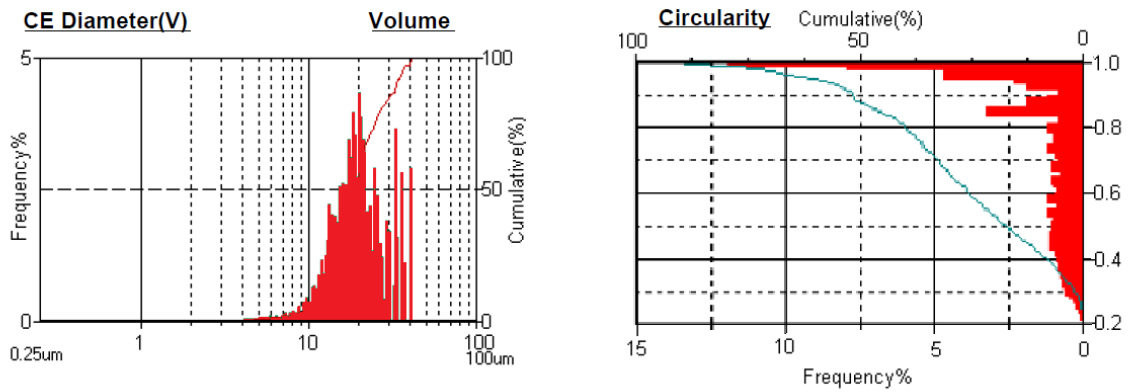


Figure 4.2 Particle size distribution and circularity curve for the reference system analyzed with Malvern.

Table 4.1 List of median size and range of particle size from the reference system.

Reference system		
Coulter counter	d <sub>50</sub> (μm)	16.79
	d <sub>90</sub> /d <sub>10</sub>	2.34
Malvern	d <sub>50</sub> (μm)	19.29
	d <sub>90</sub> /d <sub>10</sub>	2.75

Image of the spherical silica particles obtained from the reference system is taken with SEM and illustrated in figure 4.3.

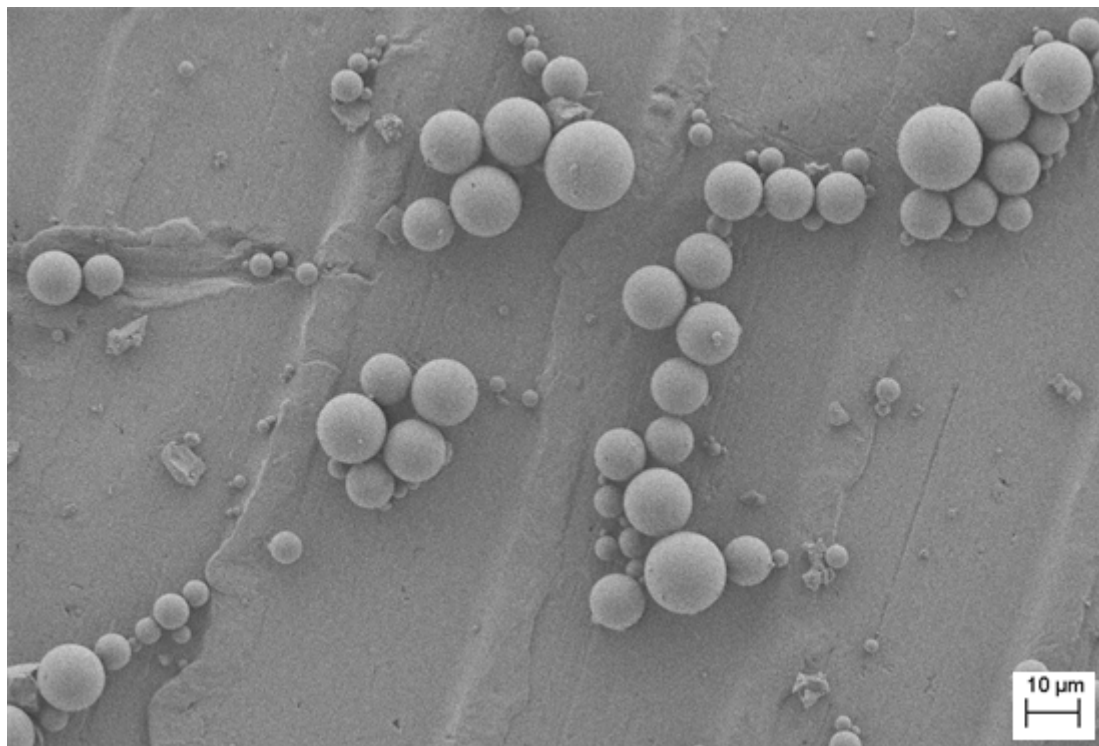


Figure 4.3 SEM image of spherical silica particles.

#### 4.1.1 The effect of stirring rate

The effect of stirring rate was investigated by varying the stirring rate during the emulsification step. The stirring rate in the reference system was 450 rpm. The green and the blue curve represent in figure 4.4 the synthesis where the stirring rate was increased to 550 rpm and decreased to 350 rpm respectively.

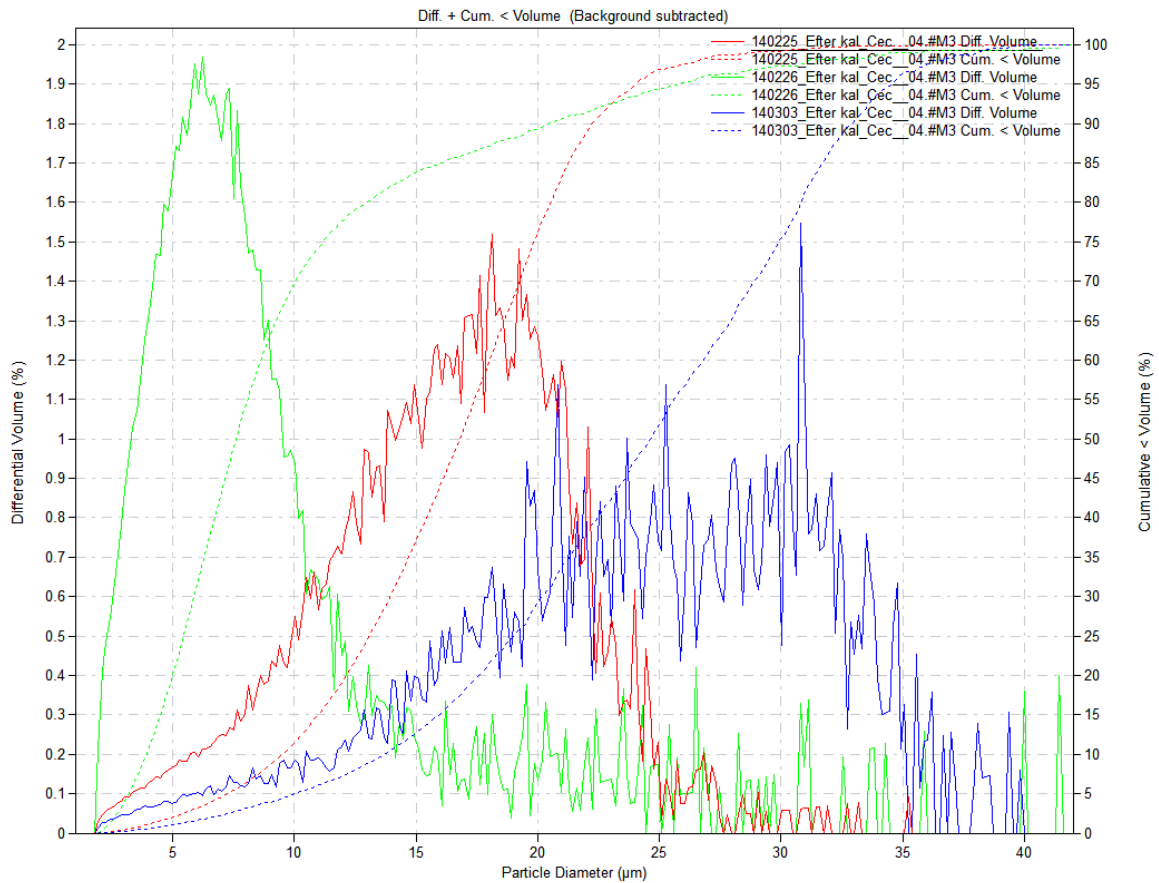


Figure 4.4 Particle size distributions from Coulter counter with different stirring rates. The green and the blue curve represent 550 rpm and 350 rpm respectively.

As can be seen in the figure 4.4 the particle size distributions differ greatly due to the stirring rate. The particle size distribution becomes narrower at higher stirring rate. The particle median size and range of particle size from both Coulter counter and Malvern is displayed in table 4.2.

Table 4.2 List of median size and range of particle size for different stirring rates.

		350 rpm	450 rpm	550 rpm
Coulter counter	$d_{50}$ ( $\mu\text{m}$ )	24.64	<b>16.79</b>	7.60
	$d_{90}/d_{10}$	2.40	<b>2.34</b>	5.22
Malvern	$d_{50}$ ( $\mu\text{m}$ )	26.58	<b>19.29</b>	7.75
	$d_{90}/d_{10}$	2.37	<b>2.75</b>	3.87

### 4.1.2 The effect of the viscosity in the dispersed phase

The viscosity of the dispersed phase was varied by adding different amounts and types of emulsifiers. The used emulsifiers are tabulated in table 3.1.

The amount of emulsifier of EHEC E230 in the reference system was 0.066 wt%. The green curve, see figure 4.5, represents the synthesis where the amount of emulsifier was decreased to 0.033 wt%. The blue and the black curves display the results from runs with 0.13 wt% and 0.26 wt% emulsifier respectively. Figure 4.5 shows that an increasing amount of emulsifier makes the average particle size smaller and the distribution narrower. However, the figure illustrates that this effect reaches a plateau at an emulsifier concentration above 0.13 wt% as the blue and black curves representing 0.13 wt% and 0.26 wt% emulsifier fully overlap. This result is not consistent with the result from the Malvern measurements, see table 4.3, where 0.26 wt% has a median particle size  $d_{50}$  which is smaller than 0.13 wt%.

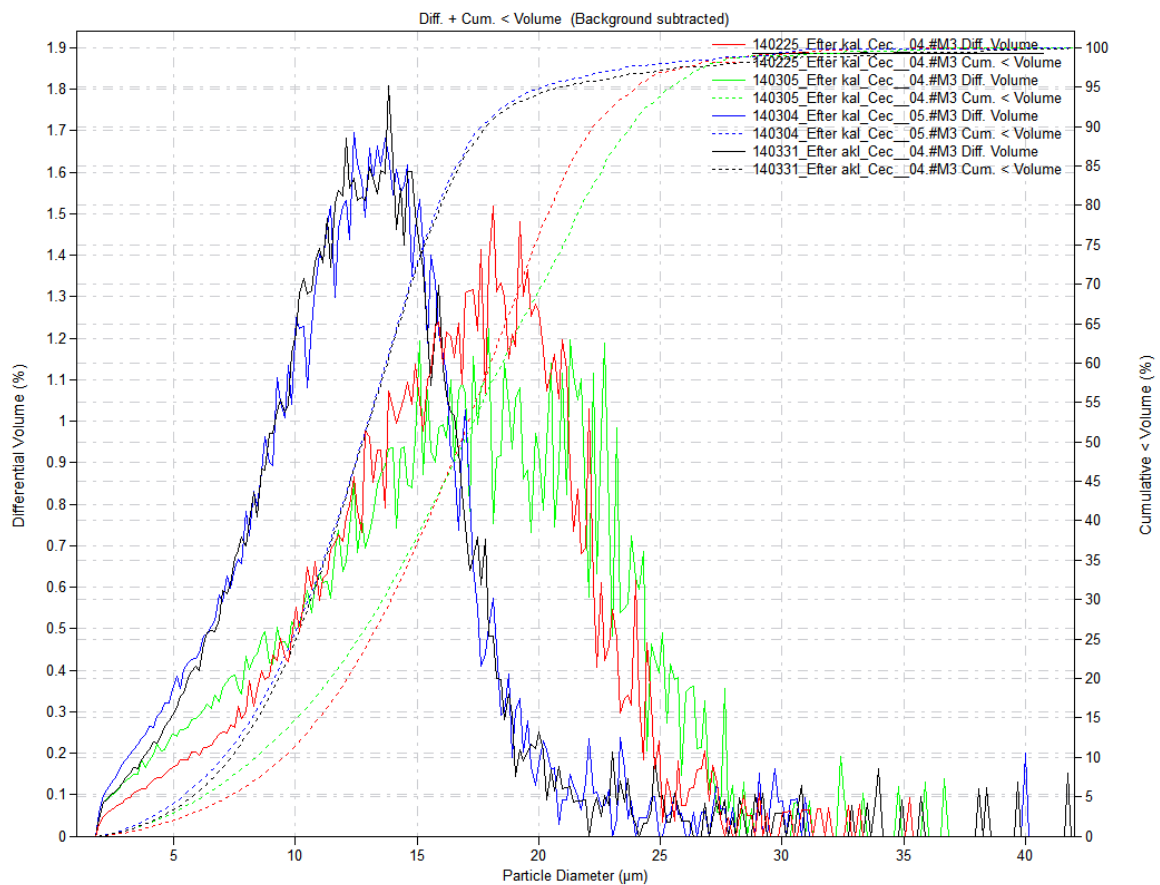
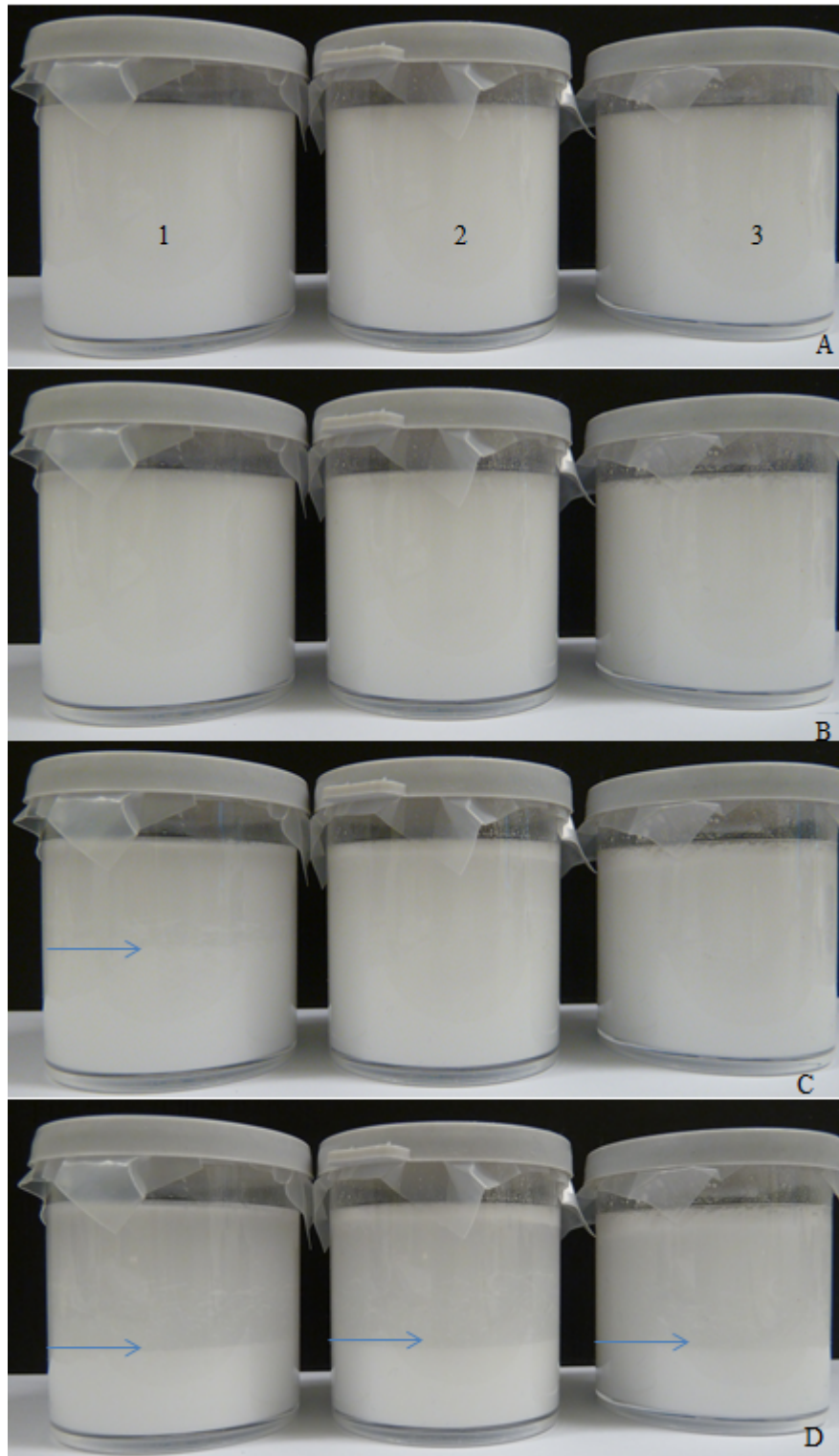


Figure 4.5 Particle size distributions from Coulter counter for different viscosity in the dispersed phase. The green, blue, red and black curve represents 0.033 wt%, 0.066 wt%, 0.13 wt% and 0.26 wt% emulsifier, respectively, of EHEC E230.

*Table 4.3 List of median size and range of particle size for different amount of emulsifier EHEC E230.*

		0.033 wt%	0.066 wt%	0.13 wt%	0.26 wt%
<b>Coulter counter</b>	d <sub>50</sub> (µm)	16.92	<b>16.79</b>	12.74	12.77
	d <sub>90</sub> /d <sub>10</sub>	2.84	<b>2.34</b>	2.51	2.42
<b>Malvern</b>	d <sub>50</sub> (µm)	24.74	<b>19.29</b>	18.13	13.18
	d <sub>90</sub> /d <sub>10</sub>	2.45	<b>2.75</b>	2.77	2.21

The amount of emulsifier affects the emulsion system and a visual stability test showed that 0.13 and 0.26 wt% emulsifier were more stable than reference system with 0.066 wt% emulsifier, see figure 4.6.



*Figure 4.6 Emulsion phase separation observation for benzyl alcohol and emulsifier of EHEC E230 at 0.066 wt%(1), 0.13 (2) and 0.026 wt% (3). Image (A) was taken right after the emulsion was mixed and the three following images were taken 4 (B), 30 (C) and 120 (D) minutes after mixing, respectively. The small arrows indicate the upper limit of the lower phase of the phase separated emulsion.*

The particle size distributions when using different types of emulsifier are displayed in figure 4.7. The amount of emulsifier was 0.066 wt% for all samples. In the reference system EHEC E230 was used as the emulsifier. The green, black and blue curve represents the respective synthesis were EHEC E351, EHEC E511 and MEHEC EBM5500 were used. The results show that with increasing viscosity in the inorganic phase the particles gets larger and the particle size distribution gets broader. The largest particles and broadest distribution is obtained when a methylated emulsifier is used, i.e. MEHEC EBM5500. Table 4.3 tabulates the median size and range of particle size for different types of emulsifier.

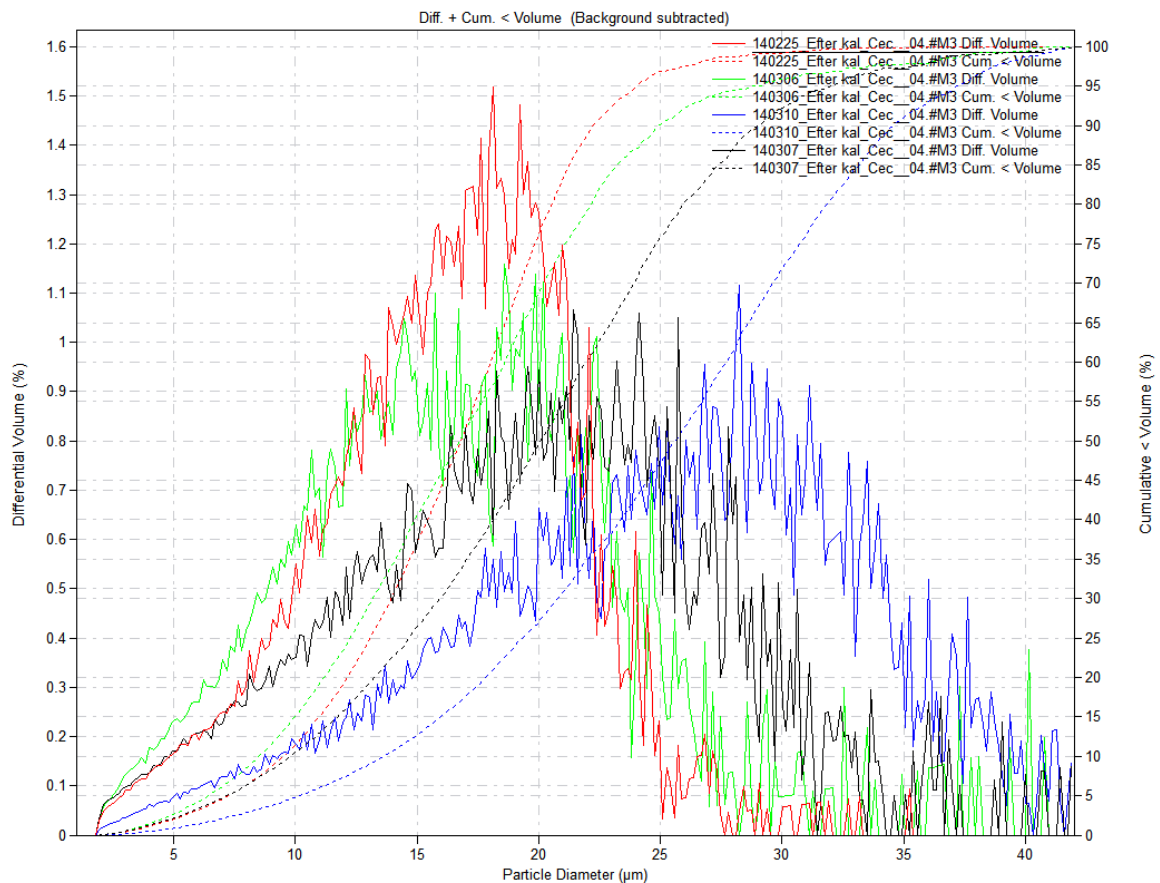


Figure 4.7 Particle size distribution curve from Coulter counter of the different type of emulsifier. EHEC E351 is represented in green, EHEC E511 in blue and MEHEC EBM5500 in black.

Table 4.4 List of median size and range of particle size for different types of emulsifier; EHEC E230, EHEC E351, EHEC E511 and MEHEC EBM5500.

		EHEC E230	EHEC E351	EHEC E511	MEHEC EBM5500
<b>Coulter counter</b>	$d_{50}$ ( $\mu\text{m}$ )	<b>16.79</b>	16.75	20.08	25.60
	$d_{90}/d_{10}$	<b>2.34</b>	2.93	2.96	2.53
<b>Malvern</b>	$d_{50}$ ( $\mu\text{m}$ )	<b>19.29</b>	17.15	28.80	28.91
	$d_{90}/d_{10}$	<b>2.75</b>	2.83	2.81	2.33

The particles obtained from the emulsion system containing 0.066 wt% emulsifier MEHEC EBM5500 were larger which can be useful in some applications. A test was performed where the amount of emulsifier was increased to 0.11 wt%, see the green curve in figure 4.8. As can be seen in the figure 4.8, the particle size became much smaller with increasing amount of emulsifier and the distribution much narrower when the amount of emulsifier was enhanced. Table 4.5 lists the median size and range of particle size for different amount of emulsifier MEHEC EBM5500.

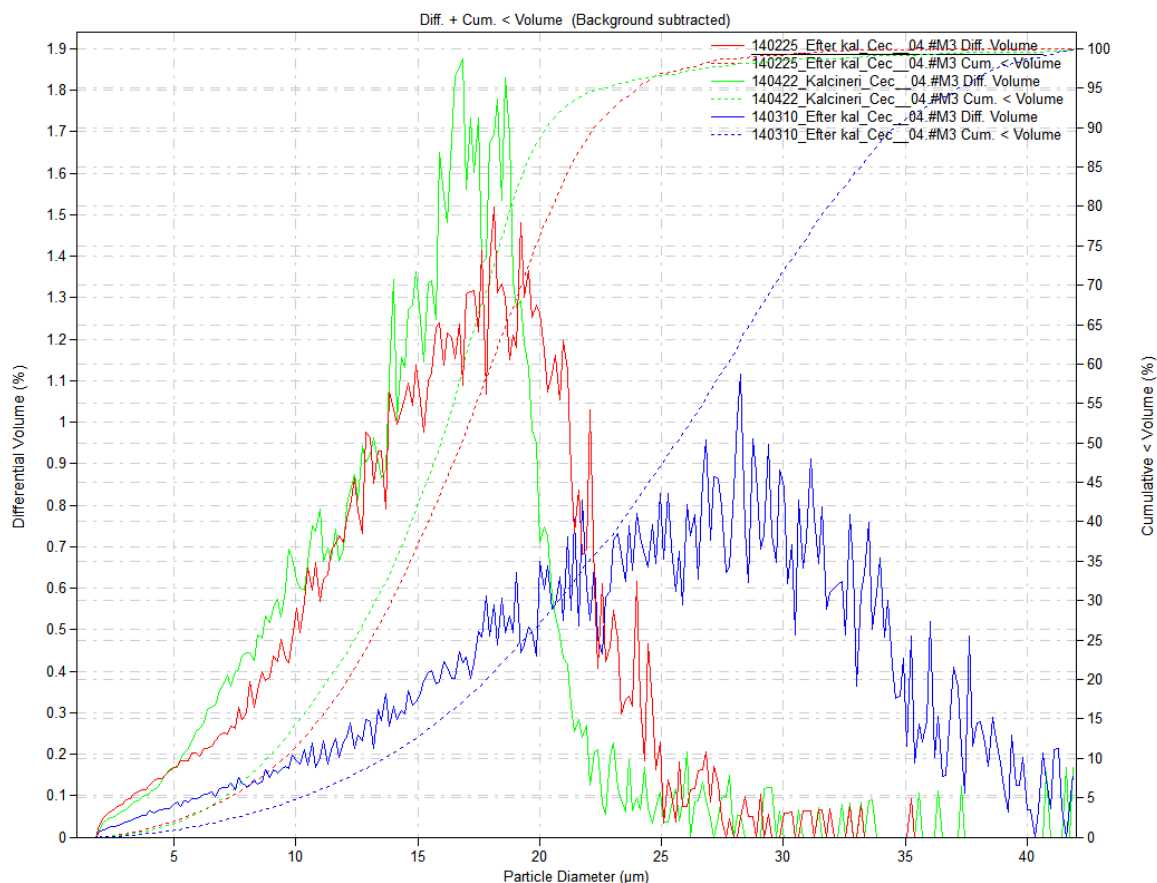


Figure 4.8 Particle size distributions from Coulter counter for the syntheses with varied amount of emulsifier MEHEC EBM5500. The red curve is the reference with EHEC E230, the blue curve represents 0.066 wt% MEHEC EBM5500 and the green curve demonstrates when the amount of emulsifier was increased to 0.11 wt% MEHEC EBM5500.

Table 4.5 List of median size and range of particle size for different amount of emulsifier MEHEC EBM5500 and 0.066 wt% EHEC E230.

		0.066 wt% EHEC E230	0.066 wt% MEHEC EBM5500	0.11 wt% MEHEC EBM5500
Coulter counter	d <sub>50</sub> (μm)	<b>16.79</b>	25.60	15.95
	d <sub>90</sub> /d <sub>10</sub>	<b>2.34</b>	2.53	2.29
Malvern	d <sub>50</sub> (μm)	<b>19.29</b>	28.91	19.36
	d <sub>90</sub> /d <sub>10</sub>	<b>2.75</b>	2.33	2.75

### 4.1.3 The effect of increasing both stirring rate and viscosity in dispersed phase

As previously shown variations in the stirring rate and the amount of emulsifier gave large effects on the particle size, see figures 4.4-4.5. Figure 4.9 illustrates the effect of increasing both these factors compared to the reference system. The blue curve represents the synthesis with increased amount of emulsifier and the green curve shows the synthesis where the stirring rate was increased. The black curve represents the size distribution obtained when both parameters were combined. The green continuous cumulative volume curve for particle size up to 9  $\mu\text{m}$  is steeper than the black curve. However, the particles in the green curve suffer from a low amount of “oversized” particles up to 35  $\mu\text{m}$ . When comparing the continuous cumulative volume curves, the black line has the steepest slope which means that it has the narrowest distribution. Table 4.6 lists the median size and range of particle size for the reference system, increased stirring rate and viscosity in dispersed phase separately and combined parameters of both increased stirring rate and viscosity in dispersed phase.

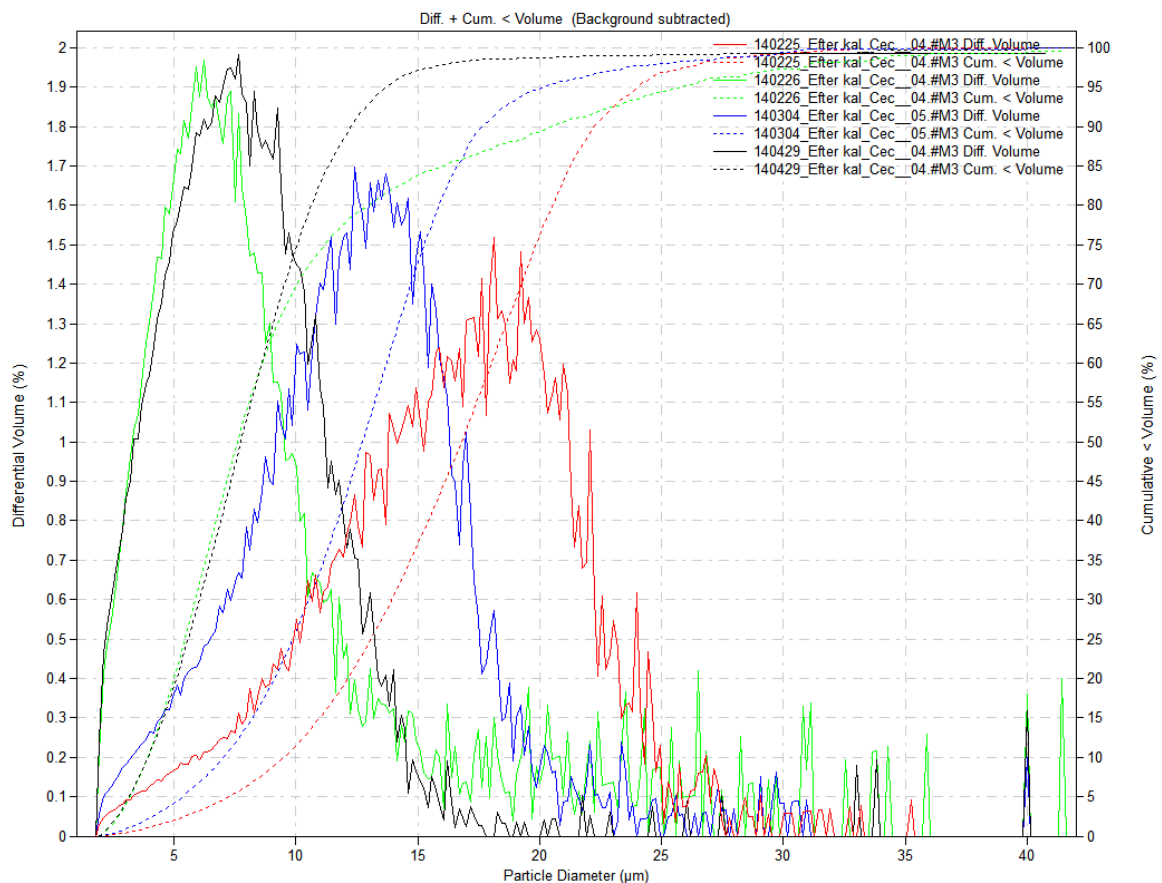


Figure 4.9 Particle size distributions from Coulter counter for 0.13wt% emulsifier (blue) and 550 rpm in stirring rate (green). The black curve is the synthesis where both parameters were increased to 0.13wt% emulsifier and 550 rpm.

Table 4.6 List of median size and range of particle size for the reference system, increased stirring rate and viscosity in dispersed phase separately and combined parameters of both increased stirring rate and viscosity in dispersed phase.

		450 rpm, 0.066 wt% EHEC E230	550 rpm, 0.066 wt% EHEC E230	450 rpm, 0.13 wt% EHEC E230	550 rpm, 0.13 wt% EHEC E230
Coulter counter	d <sub>50</sub> (μm)	<b>16.79</b>	7.60	12.74	7.74
	d <sub>90</sub> /d <sub>10</sub>	<b>2.34</b>	5.22	2.51	3.12
Malvern	d <sub>50</sub> (μm)	<b>19.29</b>	7.75	18.13	9.77
	d <sub>90</sub> /d <sub>10</sub>	<b>2.75</b>	3.87	2.77	4.10

#### 4.1.4 The effect of temperature

The effect of using different temperatures during the evaporation of the solvent is shown in figure 4.10. Five different syntheses were performed at temperatures between 55-75 °C. The particle size distributions did not appear to change when the temperature was varied as all curves overlap. Table 4.7 lists the median size and range of particle size for different temperatures during gelation.

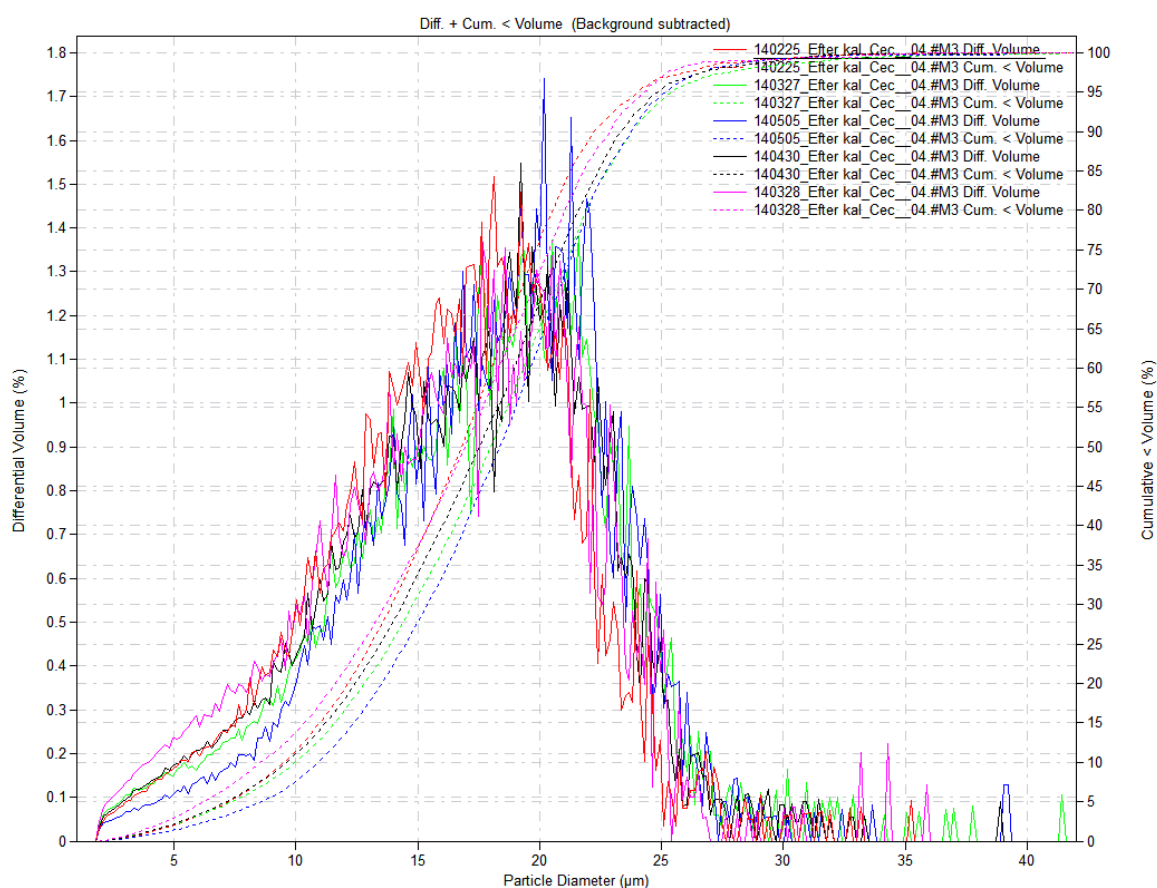


Figure 4.10 Particle size distribution curves from Coulter counter for the synthesis at 55-75 °C with an interval of 5 °C. Green represent the size distribution obtained after water evaporation at 55 °C, blue 60 °C, red 65 °C, black 70 °C and purple 75 °C.

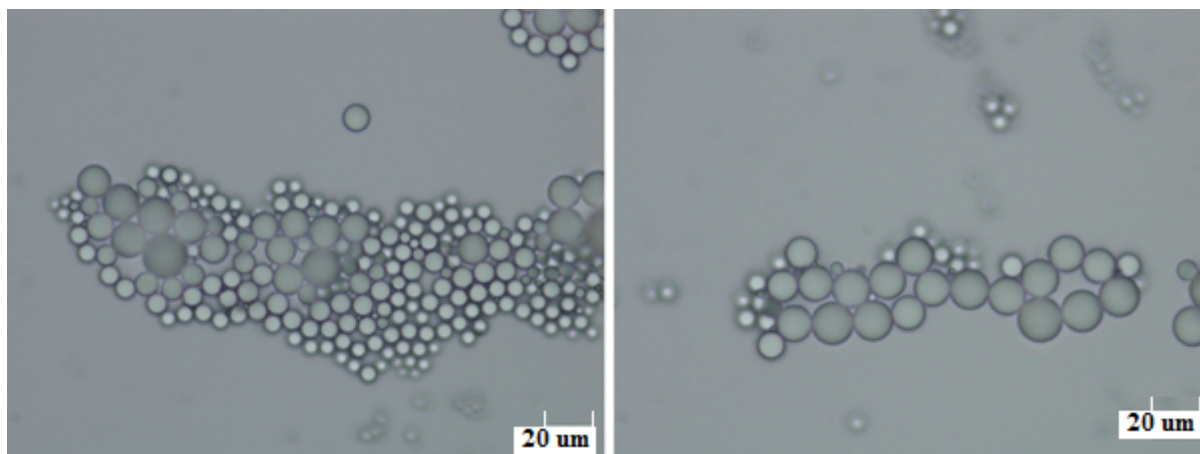


Figure 4.10a Optical microscopy image of mesoporous silica particles synthesized at 55 °C (left) and 75 °C (right).

Table 4.7 List of median size and range of particle size for different temperature during gelation.

		55 °C	60 °C	65 °C	70 °C	75 °C
<b>Coulter counter</b>	d <sub>50</sub> (μm)	17.99	18.37	<b>16.79</b>	17.53	16.94
	d <sub>90</sub> /d <sub>10</sub>	2.23	2.18	<b>2.34</b>	2.43	2.67
<b>Malvern</b>	d <sub>50</sub> (μm)	20.95	20.03	<b>19.29</b>	19.04	18.38
	d <sub>90</sub> /d <sub>10</sub>	2.38	2.54	<b>2.75</b>	3.25	2.54

#### 4.1.5 The effect of phase ratio

Nina Andersson et al. (2006) had a phase ratio 1:3 between the inorganic and organic phase. The green curve in figure 4.11 represents the synthesis where the organic phase was decreased from 1:3.64 to reach the same phase fraction as Nina Andersson et al. The difference between the green- and the red curve is 109.9 g of organic solvent (approx. 18% increase of the organic solvent). As can be seen in the figure below, less organic phase resulted in slightly larger particles and slightly broader size distribution.

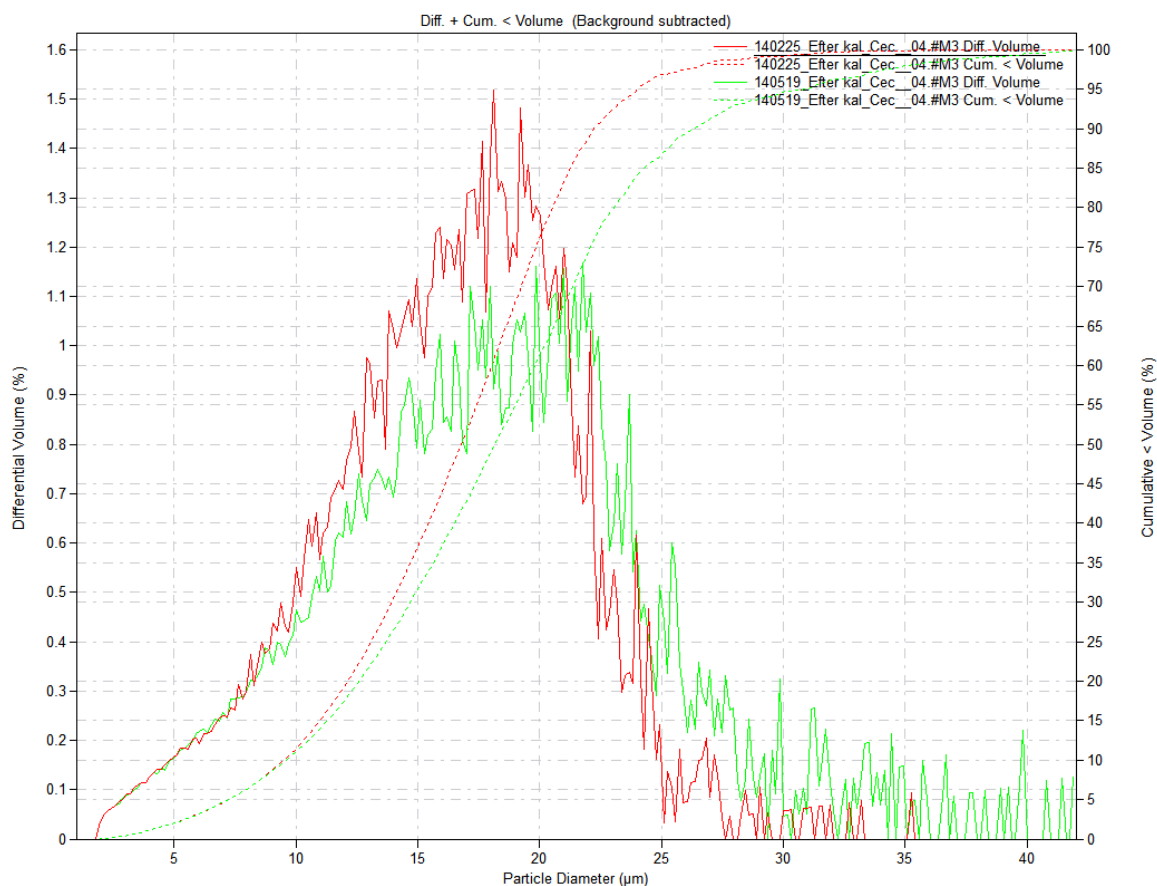


Figure 4.11 Particle size distributions from Coulter counter for the syntheses where the organic solvent was decreased compared to the reference system. The difference between the green- and the red curve is 109.9 g of organic solvent.

Two different syntheses were made to see if the amount of silica sol dispersion and the total amount of water had any effect on the particle size and size distribution, see figure 4.12. The green curve represents the synthesis when a double amount of silica sol dispersion was added compare to the reference system and the blue curve represent when 100 g extra distilled water was supplied. When increasing the amount of silica sol dispersion and adding 100 g of distilled water the resulting phase ratio was approximately 1:2.22. As shown in figure 4.11 the effect of the particle size distribution was negligible. All three curves are overlapping quite well, which means that the amount of silica sol dispersion and the amount of water do not have any major effect on the particle size and size distribution. Table 4.8 lists the median size and range of particle size for different phase ratios.

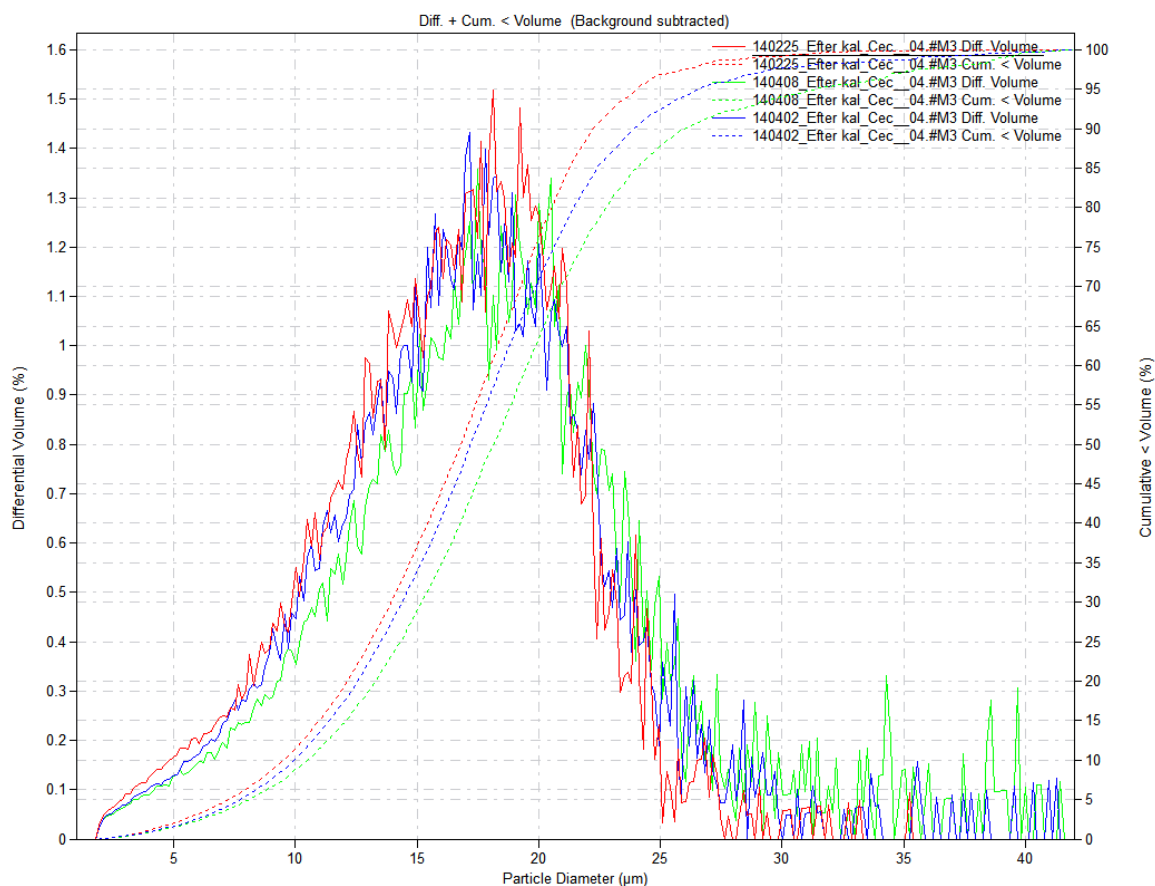


Figure 4.12 Particle size distribution from Coulter counter for double amount of silica sol dispersion as green curve and the reference system as the red curve. The blue curve represents the particle size distribution for the synthesis when 100 g extra distilled water was supplied.

Table 4.8 List of median size and range of particle size for different phase ratios.

		1:3.64	1:3	1:2.22
Coulter counter	d <sub>50</sub> (μm)	16.79	18.15	~17.68
	d <sub>90</sub> /d <sub>10</sub>	2.34	2.74	~2.45
Malvern	d <sub>50</sub> (μm)	19.29	25.96	~20.61
	d <sub>90</sub> /d <sub>10</sub>	2.75	3.14	~2.64

#### 4.1.6 The effect of the viscosity of the continuous phase

Two different thickeners for the organic continuous phase were used to see how they affect the particle size distribution. In figure 4.13 the red curve represents the reference system with no thickening of the benzyl alcohol. The green curve shows the effect of dissolving 5 wt% of poly(isobutyl methacrylate) in the benzyl alcohol and the blue curve shows when 5 wt% of isobutyl methacrylate copolymer was dissolved. In Figure 4.14 the viscosities for the different organic phases were visually compared and it appears as if the solution with 5 wt% of isobutyl methacrylate copolymer had the highest viscosity. Table 4.9 lists the median size and range of particle size for different viscosities of the continuous phase.

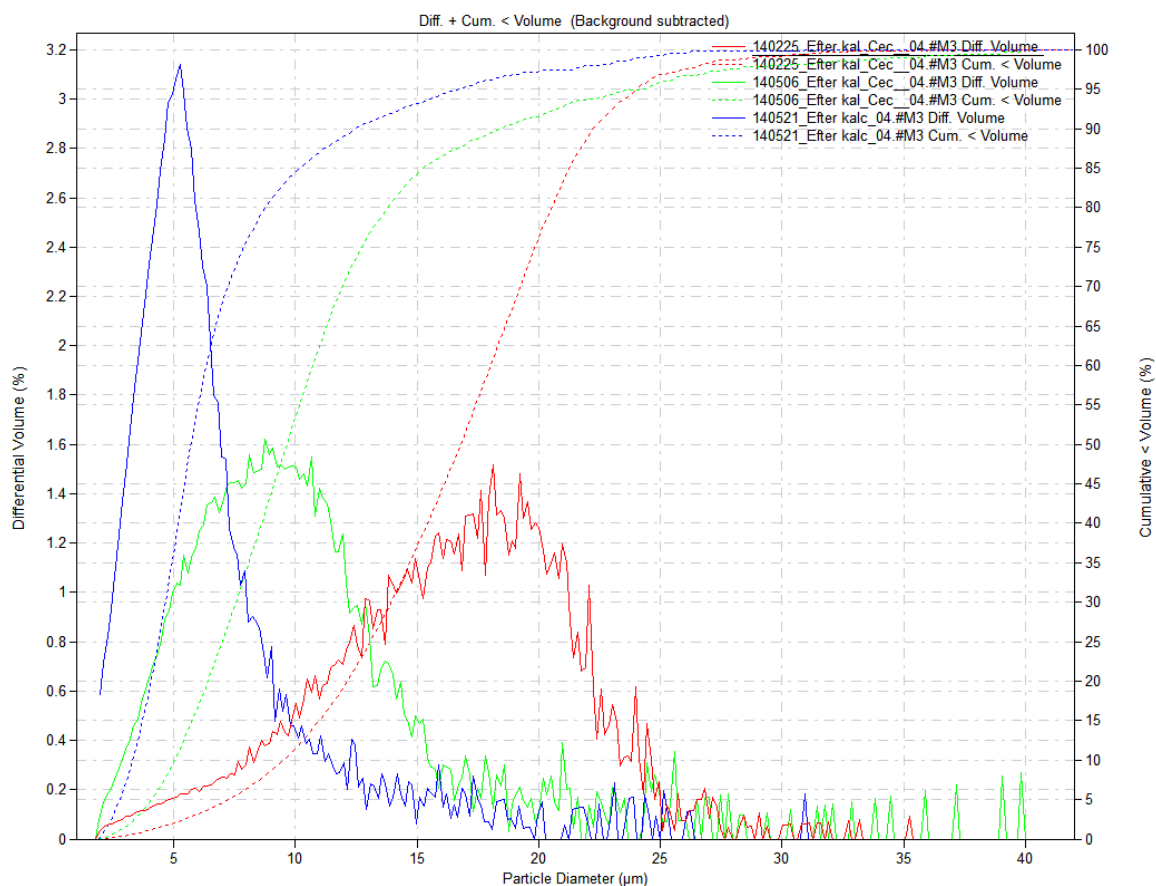


Figure 4.13 Particle size distribution from Coulter counter where the red curve represents the reference system when no thickener was used and the green curve when 5 wt% of poly(isobutyl methacrylate) was dissolved in the organic phase and the blue curve shows when 5 wt% of isobutyl methacrylate copolymer was used.

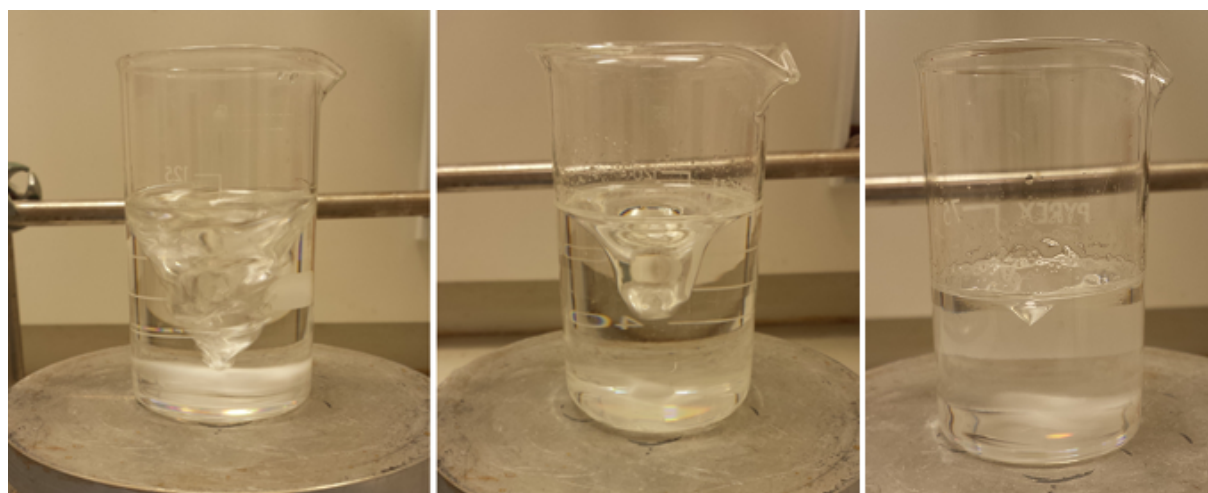


Figure 4.14 Comparison of viscosities of organic phase of reference system (left), 5wt% of thickener poly(isobutyl methacrylate) (middle) and 5wt% of thickener isobutyl methacrylate copolymer (right).

Table 4.9 List of median size and range of particle size for different viscosities of the continuous phase.

		No thickener	5wt% of thickener poly(isobutyl methacrylate)	5wt% of thickener isobutyl methacrylate copolymer
Coulter counter	d <sub>50</sub> (μm)	16.79	9.65	5.72
	d <sub>90</sub> /d <sub>10</sub>	2.34	3.65	3.76
Malvern	d <sub>50</sub> (μm)	19.29	10.36	5.15
	d <sub>90</sub> /d <sub>10</sub>	2.75	4.42	4.50

#### 4.1.7 The effect of different type of organic solvent

The various organic solvents that were tested were 2-methyl-1-butanol, cyclohexanol, 3-methyl-3-pentanol, 3-pentanol and 1-hexanol. Syntheses of spherical silica particles with different organic solvents gave some interesting results. The majority of the different organic solvents gave defect silica particles. The particles were not spherical, instead they looked as collapsed spheres that were oval and large, see figure 4.15-4.16.

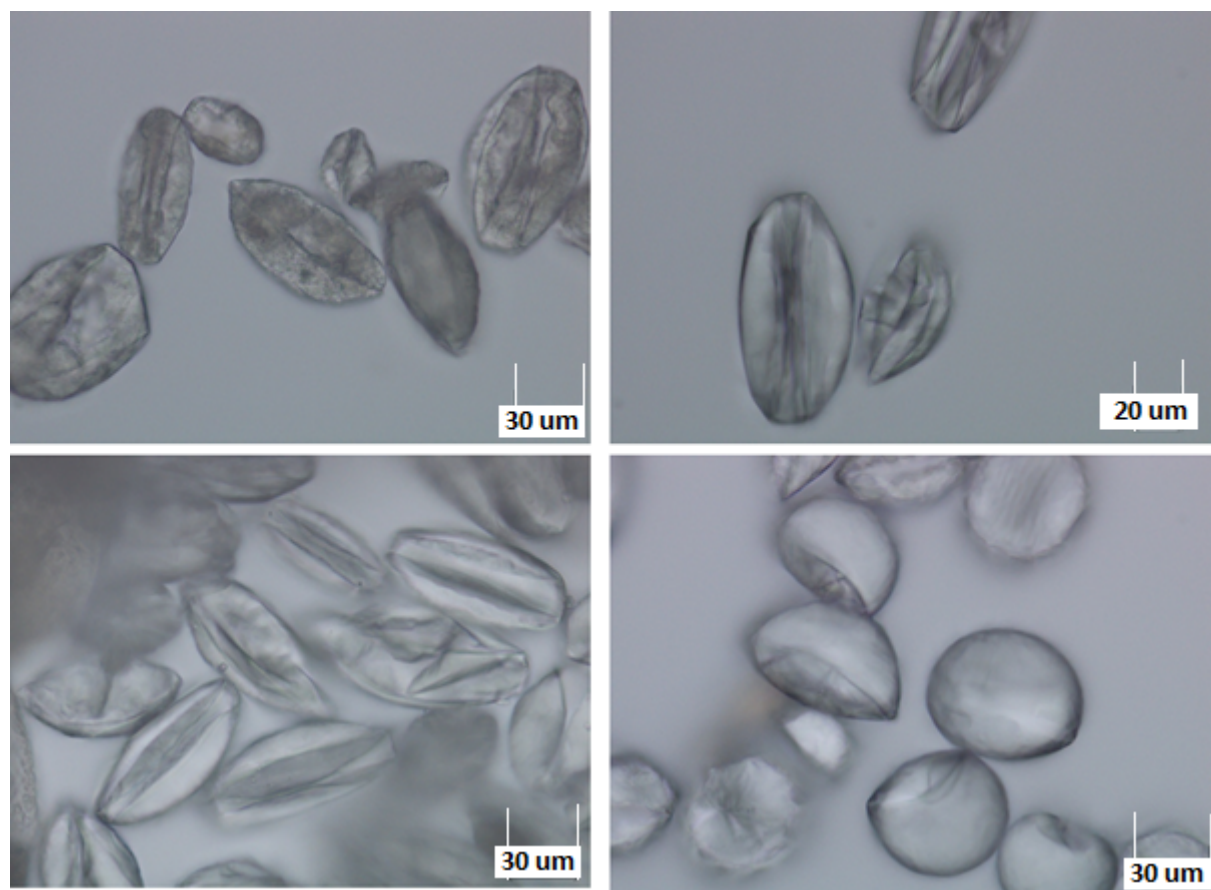
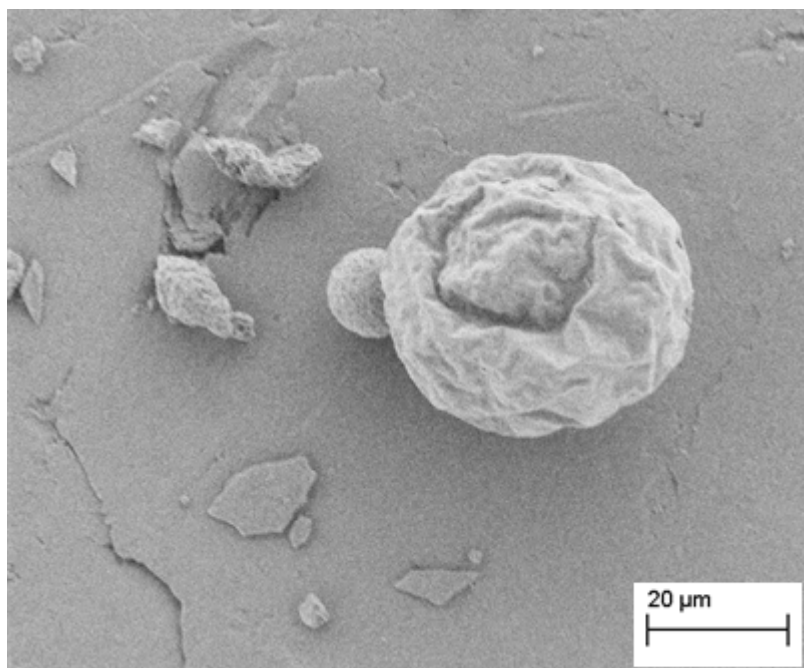
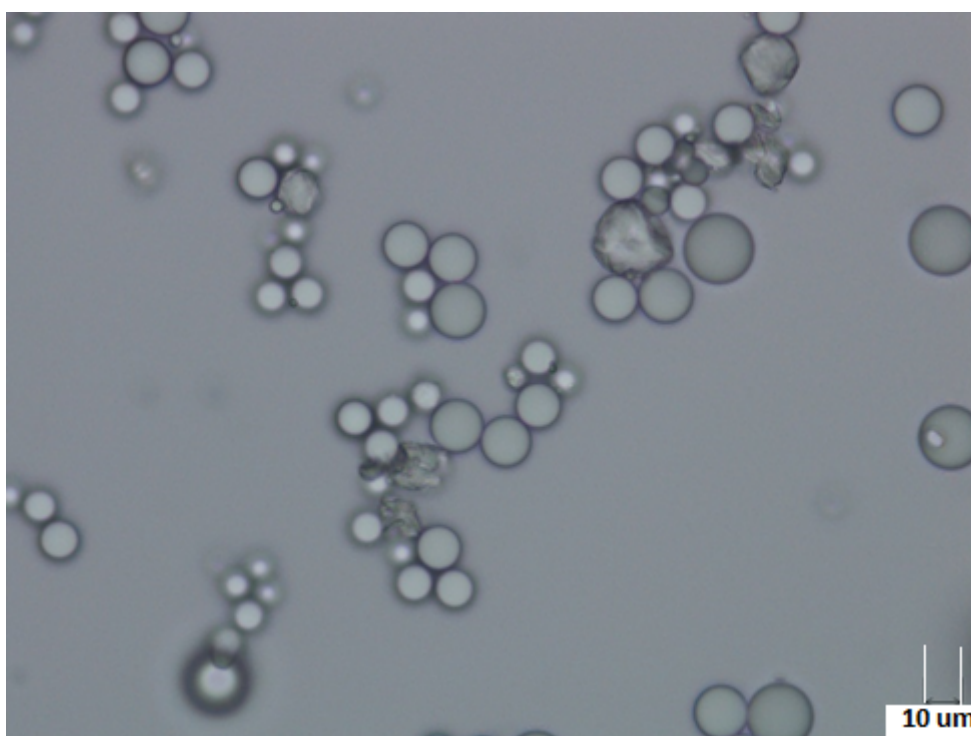


Figure 4.15 Optical microscopy images of oval and defected silica particles synthesized with 2-methyl-1-butanol (upper, left), 3-methyl-3-pentanol (upper, right), 3-pentanol (lower, left) and 1-hexanol (lower, right) as organic phase.



*Figure 4.16 SEM image of defect silica particles synthesized with 1-hexanol as continuous phase.*

Defect particles were obtained by using 2-methyl-1-butanol, 3-methyl-3-pentanol, 3-pentanol and 1-hexanol as the organic phase. The use of cyclohexanol as the organic solvent gave a better result, see figure 4.17-4.18. The majority of the particles were spherical but there were still some particles that had defects.



*Figure 4.17 Optical microscopic image of silica particles synthesized with cyclohexanol as organic phase.*

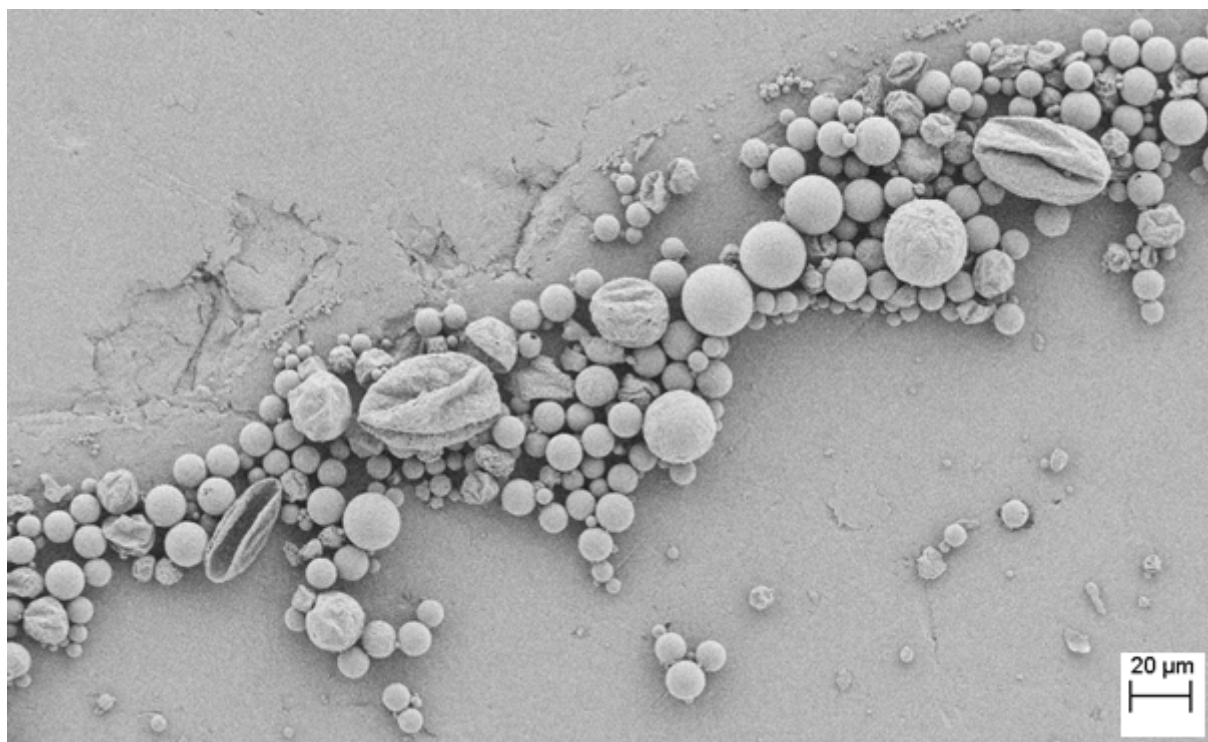


Figure 4.18 SEM images of defected silica particles synthesized with cyclohexanol as continuous phase.

In table 4.10 the particle size and the circularity of the particles from the different organic solvents are presented, measured by Malvern as the particles were too large to be measured with Coulter counter (with the aperture available).

Table 4.10 Particle size and circularity of the particles obtain from syntheses with organic solvents.

		Organic solvent					
Malvern		1-hexanol	2-methyl-1-buthanol	3-methyl-3-penthanol	Benzyl alcohol	Cyclohexanol	3-penthanol
Particle diameter (μm)	$d_{50}(\mu\text{m})$	57.13	71.59	53.42	19.29	31.46	62.98
	$d_{90}/d_{10}$	2.26	2.74	2.85	2.75	3.04	2.22
Circularity	$d_{90}/d_{10}$	4.32	6.27	7.47	1.79	2.23	6.00

## 4.2 Process system modified with Couette cell

The Couette cell was tested by comparing the reference synthesis with the reference system modified with Couette cell at a stirring rate of 500 rpm and a retention time of 9 seconds, which corresponds to a shear rate of  $20,000 \text{ s}^{-1}$ . In figure 4.19 the green curve represents the size distribution for particles synthesized in the process system modified with Couette cell, while the red curve represents the reference system. Table 4.11 lists the median size and range of particle size for syntheses without and with Couette cell.

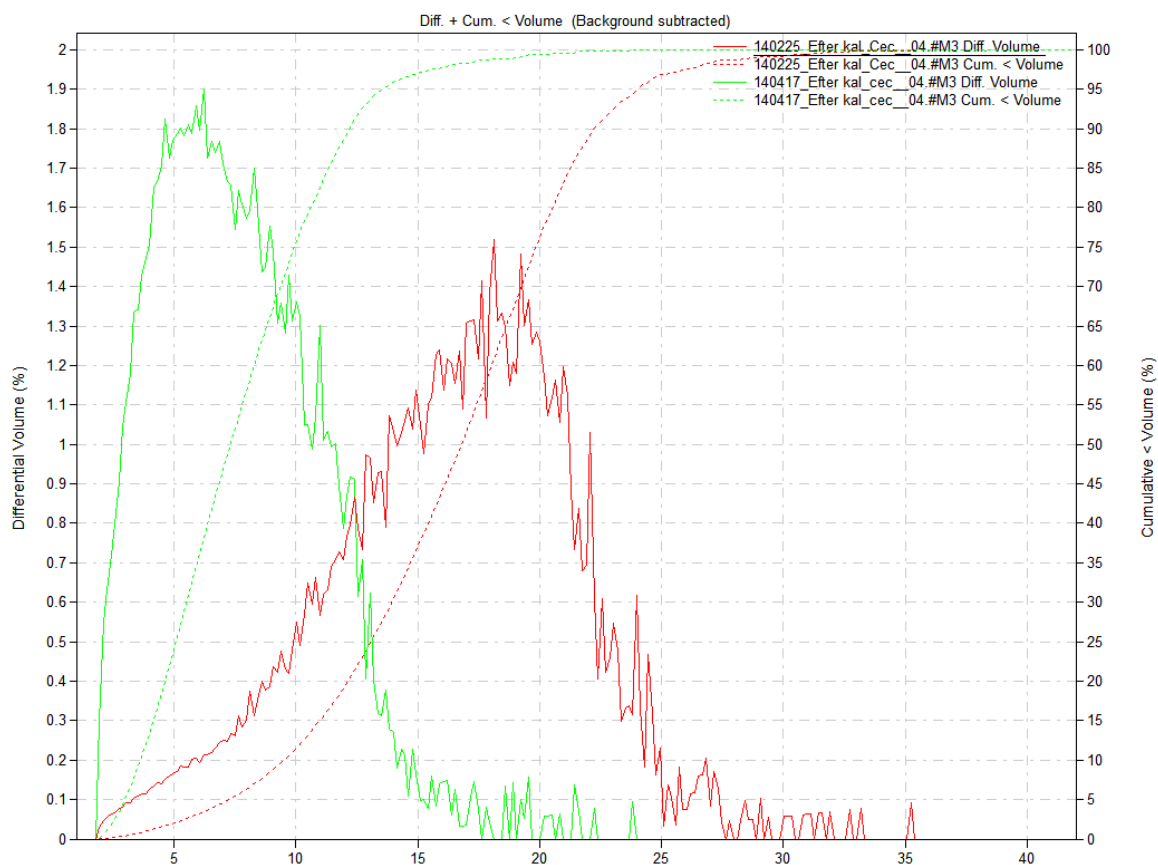


Figure 4.19 Particle size distributions from Coulter counter of the syntheses with and without Couette cell. The red curve represents the processes without the Couette cell and the green curve with the Couette cell.

Table 4.11 List of median size and range of particle size for syntheses without and with Couette cell.

		Reference system	Treatment with Couette cell
Coulter counter	$d_{50}$ ( $\mu\text{m}$ )	<b>16.79</b>	7.31
	$d_{90}/d_{10}$	<b>2.34</b>	3.36
Malvern	$d_{50}$ ( $\mu\text{m}$ )	<b>19.29</b>	6.83
	$d_{90}/d_{10}$	<b>2.75</b>	3.92

The emulsion droplets were analyzed in the optical microscopy showing that the treatment of the Couette cell gave much smaller droplets compared to the droplets from the reference system, see figure 4.20.

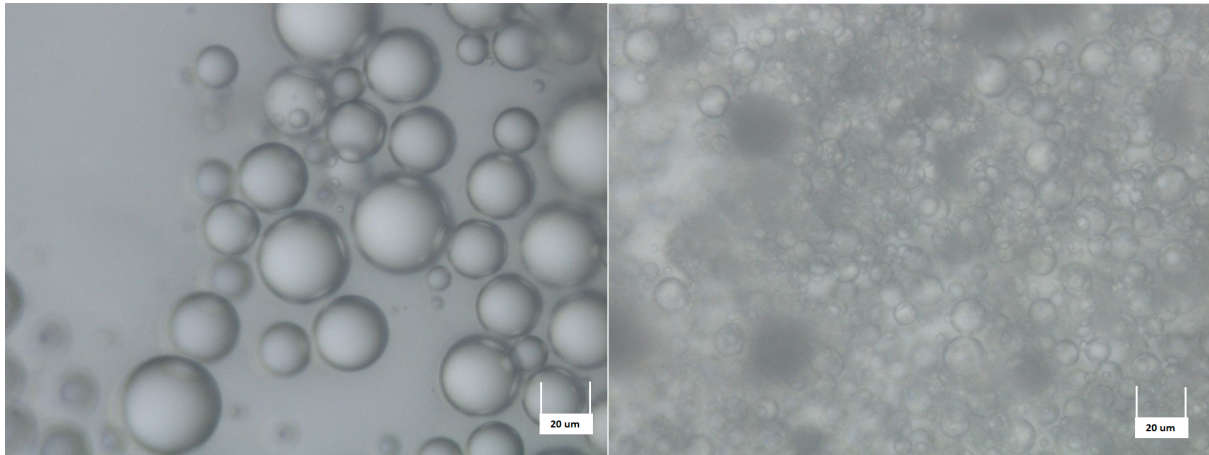


Figure 4.20 Optical microscopic images of emulsion droplet size before (left) and after (right) treatment of the Couette cell.

#### 4.2.1 The effect of viscosity of the dispersed phase in Couette cell

Figure 4.21 shows that the higher viscosity of dispersed phase when using 0.13 wt% of emulsifier EHEC E230 (green curve), resulted in a narrower size distribution compared to the reference with 0.066 wt% (red curve). The particle size distribution from the synthesis with 0.13 wt% emulsifier modified with the Couette cell (blue curve) became even narrower. Table 4.12 lists the median size and range of particle size for syntheses with 0.13 wt% emulsifier EHEC E230 without and with Couette cell compared to the reference system with 0.066 wt%.

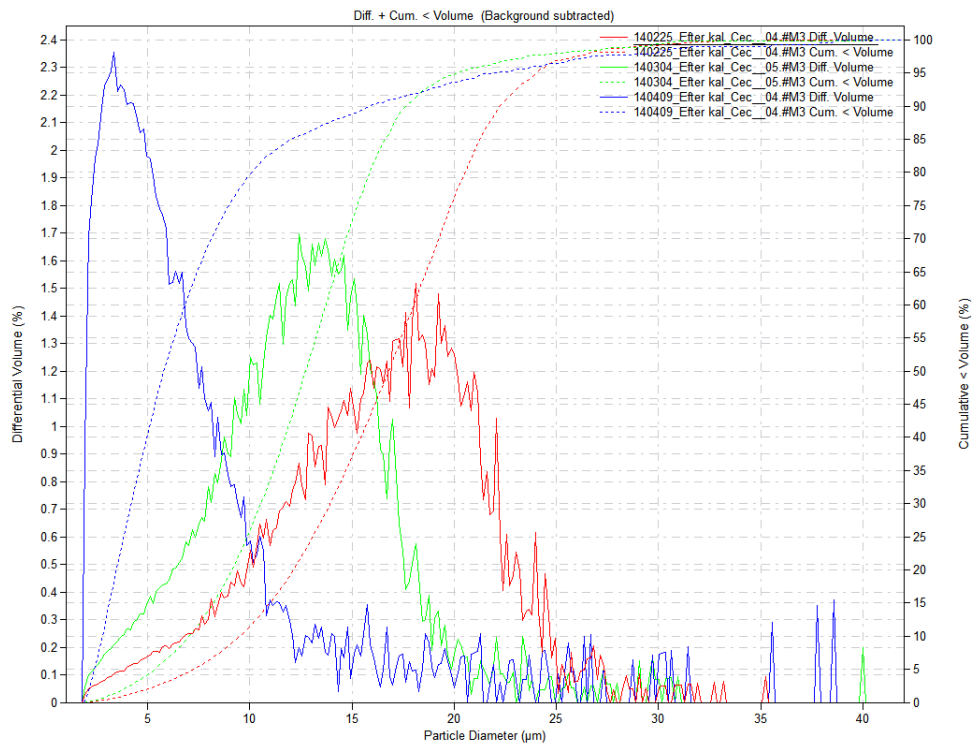


Figure 4.21 Particle size distribution from Coulter counter for the reference system with 0.06 wt% emulsifier and without the Couette cell (red curve) and with increased amounts of emulsifier to 0.13 wt% with and without Couette cell as blue and green curve, respectively.

A clear difference in particle size can be seen in the SEM images in figure 4.22 SEM for the particles synthesized with 0.13 wt% emulsifier EHEC E230 without and with Couette cell, see figure 4.22.

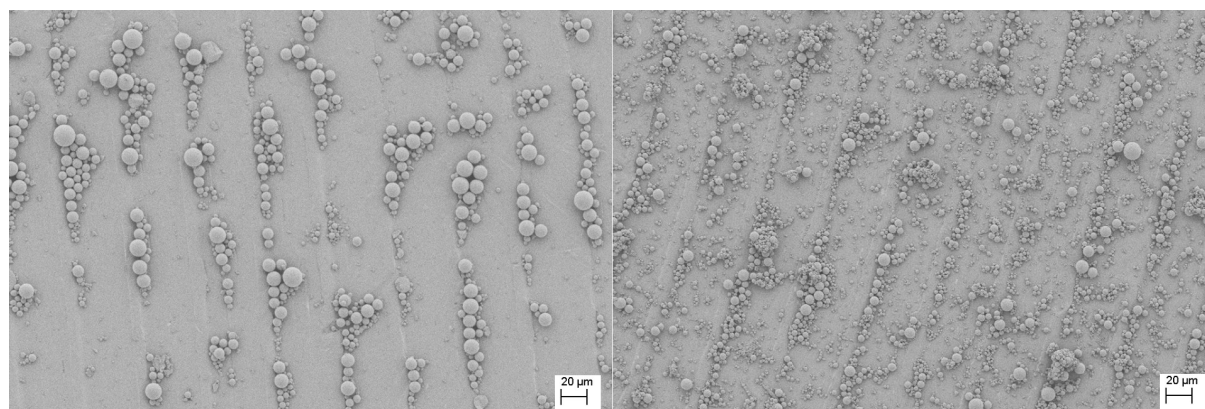


Figure 4.22 SEM images of particles synthesized without (left) and with (right) the Couette cell.

Table 4.12 List of median size and range of particle size for syntheses with 0.13 wt% emulsifier EHEC E230 without and with Couette cell compared to the reference system with 0.066 wt%.

		0.066 wt% EHEC E230 without Couette cell	0.13 wt% EHEC E230 without Couette cell	0.13 wt% EHEC E230 with Couette cell
<b>Coulter counter</b>	$d_{50}$ ( $\mu\text{m}$ )	<b>16.79</b>	12.74	5.81
	$d_{90}/d_{10}$	<b>2.34</b>	2.51	5.69
<b>Malvern</b>	$d_{50}$ ( $\mu\text{m}$ )	<b>19.29</b>	18.13	4.94
	$d_{90}/d_{10}$	<b>2.75</b>	2.77	3.60

From here on the red curve in the figures and the bolded values in the tables will represent a new reference system which is the reference system modified with the Couette cell. The previous reference system will not appear anymore. The red curve in Figure 4.23 displays the synthesis with 0.066 wt% emulsifier, the blue curve 0.13 wt% and the green curve 0.25 wt%. As can be seen in the figure, there is no clear trend in the size distribution when the emulsifier concentration is varied in the Couette cell. Table 4.13 lists the median size and range of particle size for syntheses with 0.066, 0.13 and 0.25 wt% emulsifier EHEC E230 with Couette cell.

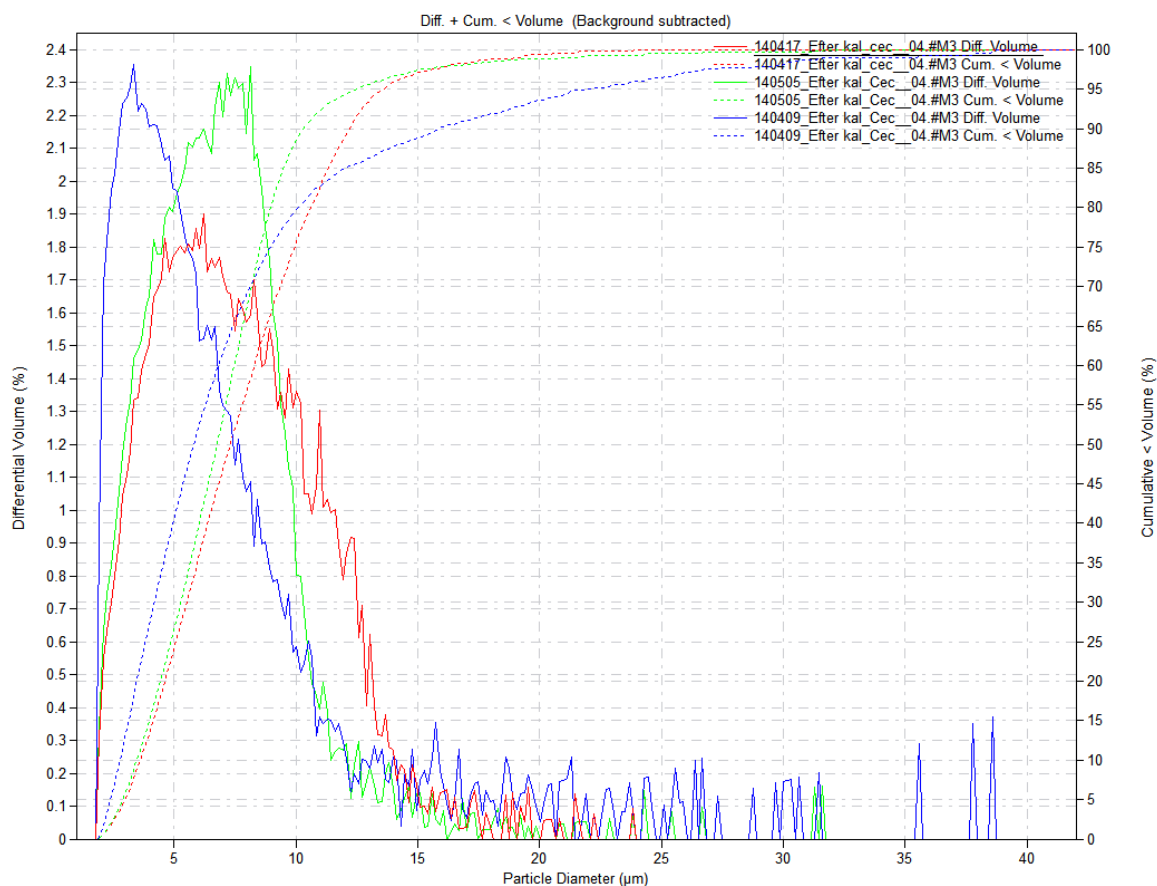


Figure 4.23 Particle size distributions from Coulter counter for the reference system with 0.066 wt% emulsifier as red curve and the blue and the green curves show an increase in emulsifier with 0.13 wt% and 0.25 wt% respectively.

Table 4.13 List of median size and range of particle size for syntheses with 0.066, 0.13 and 0.25 wt% emulsifier EHEC E230 with Couette cell.

		0.066 wt% EHEC E230	0.13 wt% EHEC E230	0.25 wt% EHEC E230
Coulter counter	d <sub>50</sub> (μm)	7.31	5.81	6.78
	d <sub>90</sub> /d <sub>10</sub>	3.36	5.69	2.95
Malvern	d <sub>50</sub> (μm)	6.83	4.94	8.50
	d <sub>90</sub> /d <sub>10</sub>	3.92	3.60	5.53

#### 4.2.2 The effect of stirring rates

The size of the emulsion droplets entering the Couette cell had an effect on final particle size. Figure 4.24 shows the synthesis with different stirring rates in the emulsion reactor, reactor 1. The blue curve represents the synthesis at 550 rpm in the emulsion reactor and the red and the green curves display 450 and 350 rpm respectively. With increasing stirring rate the average particle size became smaller. The size distribution looks broader for the reference system than for the synthesis exposed to 550 rpm and 350 rpm. The continuous cumulative curves have approximately the same slopes, which mean that the size distribution becomes narrower with

increasing stirring rate in the emulsion reactor. Table 4.14 lists the median size and range of particle size for syntheses with different stirring rates in the emulsion reactor.

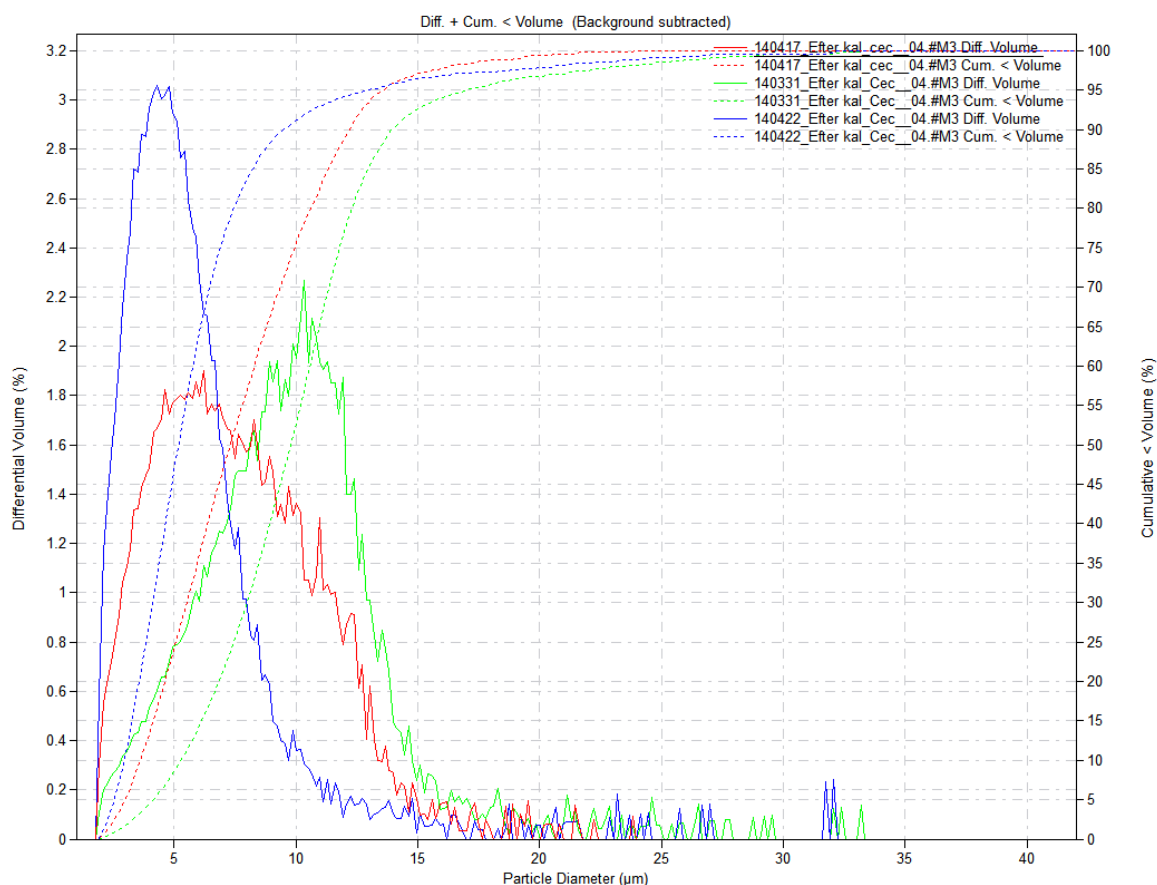


Figure 4.24 Particle size distribution from Coulter counter for the references system treated with the Couette cell (red curve). The droplet size in the emulsion is created by varying the stirring rate at 550 rpm and 350 rpm respectively. The blue distribution curve represents a stirring rate at 550 rpm the green 350 rpm.

Table 4.14 List of median size and range of particle size for syntheses with different stirring rates in the emulsion reactor.

		350 rpm	450 rpm	550 rpm
Coulter counter	d <sub>50</sub> (μm)	9.80	7.31	5.18
	d <sub>90</sub> /d <sub>10</sub>	2.64	3.36	3.22
Malvern	d <sub>50</sub> (μm)	10.61	6.83	4.53
	d <sub>90</sub> /d <sub>10</sub>	2.61	3.92	2.52

In figure 4.25 the stirring rate in the Couette cell itself was varied. The green, red and blue curves represent 700, 500 and 300 rpm, respectively. Higher stirring rate resulted in smaller particles with narrower size distribution. Table 4.15 lists the median size and range of particle size for syntheses with different stirring rates in the Couette cell.

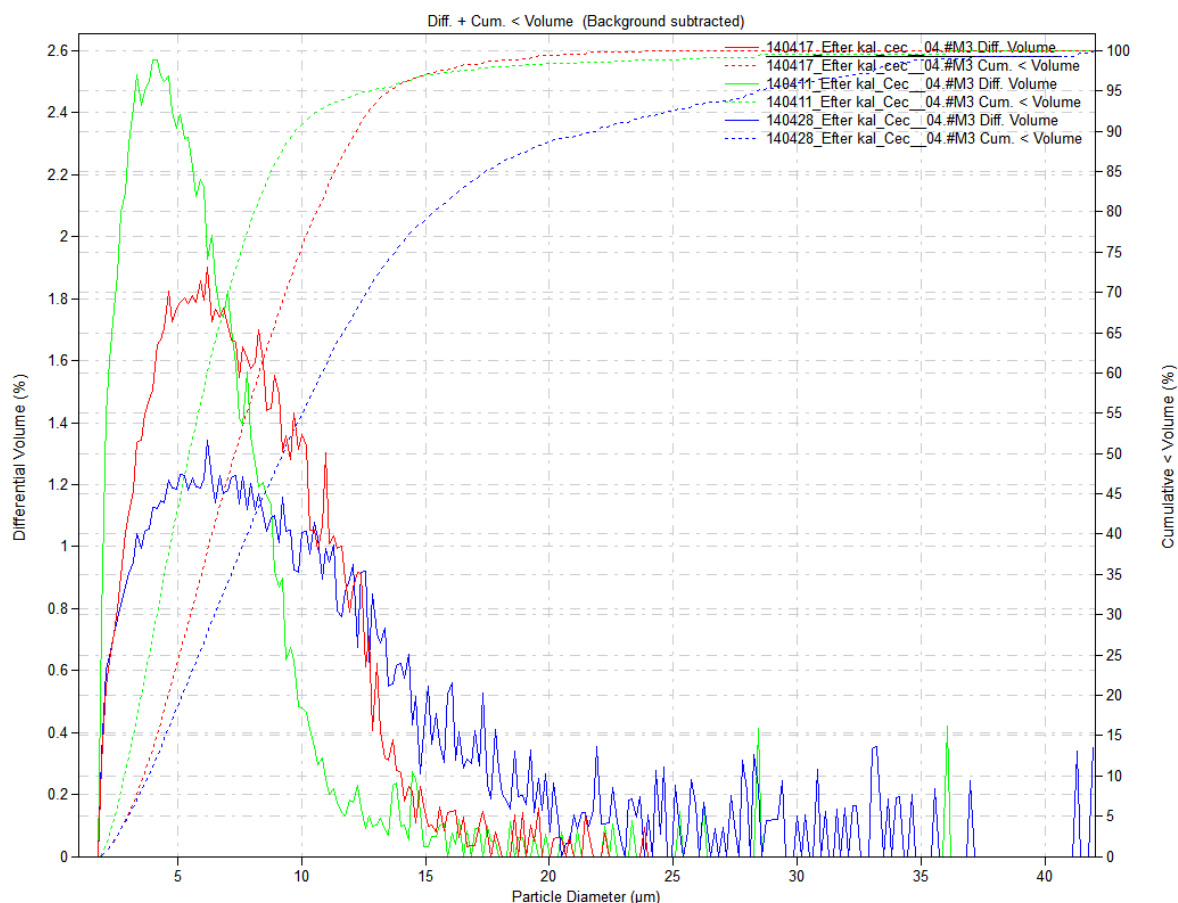


Figure 4.25 Particle size distribution from Coulter counter of syntheses with different stirring rates in the Couette cell. The green, red and blue curves represent 700 rpm, 500 rpm and 300 rpm.

Table 4.15 List of median size and range of particle size for syntheses with different stirring rates in the emulsion reactor.

		300 rpm	500 rpm	700 rpm
Coulter counter	$d_{50}$ ( $\mu\text{m}$ )	9.25	<b>7.31</b>	5.47
	$d_{90}/d_{10}$	5.71	<b>3.36</b>	5.40
Malvern	$d_{50}$ ( $\mu\text{m}$ )	8.20	<b>6.83</b>	5.81
	$d_{90}/d_{10}$	4.32	<b>3.92</b>	3.78

In the syntheses modified with Couette cell a slightly narrower distribution has been achieved when the stirring rate in the emulsion reactor was increased. A narrow distribution was also obtained when the shear rate in the Couette cell was increased. Further trails were made to see if the distribution could be narrowed by combining these two parameters. The black curve represents the synthesis with both parameters combined. Moreover, the blue and green curves represent the syntheses with increased stirring rate in the emulsion reactor and in the Couette cell, respectively, see figure 4.26. Table 4.16 lists the median size and range of particle size for syntheses seen in figure 4.26.

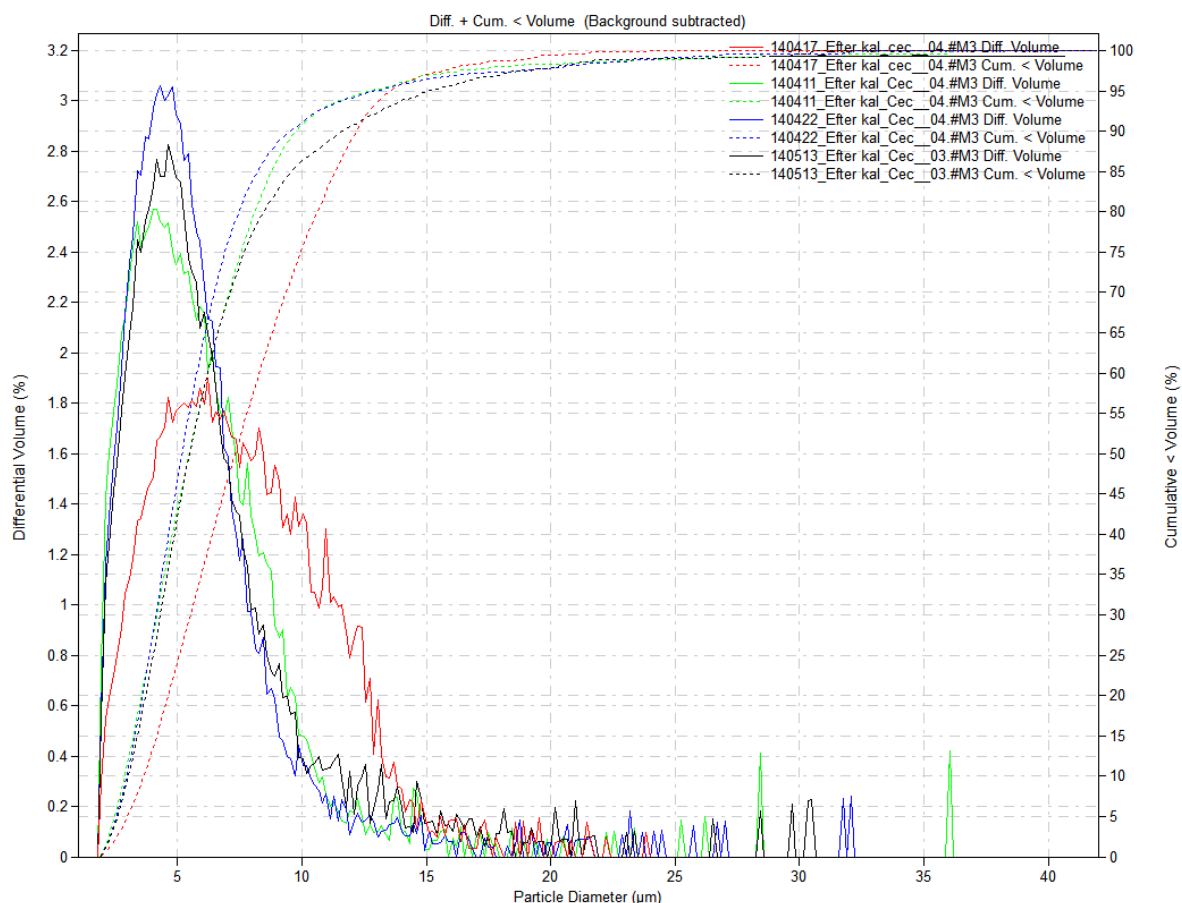


Figure 4.26 Particle size distribution from Coulter counter for the syntheses with both increased stirring rates in emulsion reactor and Couette cell (black curve) and the synthesis with increased stirring rate in just the emulsion reactor (blue curve) or the Couette cell (green curve).

Table 4.16 List of median size and range of particle size for syntheses with increased stirring rates in the emulsion reactor, in the Couette cell and a combination of them both.

		Reference system	550 rpm in the emulsion reactor	700 rpm in the Couette cell	Combined parameters
Coulter counter	$d_{50}$ ( $\mu\text{m}$ )	<b>7.31</b>	5.18	5.47	5.49
	$d_{90}/d_{10}$	<b>3.36</b>	3.22	5.40	3.85
Malvern	$d_{50}$ ( $\mu\text{m}$ )	<b>6.83</b>	4.53	5.81	4.56
	$d_{90}/d_{10}$	<b>3.92</b>	2.52	3.78	2.96

The effect of stirring rate during gelation in reactor 2 was investigated, where the emulsion which is already treated with Couette cell is kept. In figure 4.27 the green, red and blue curves represents the size distributions when the stirring rates during the solvent evaporation were set to 175, 275 and 375 rpm, respectively. It appears as if an increased stirring rate at this step of the synthesis made the particles smaller, but the effect is minor. Table 4.17 lists the median size and range of particle size for syntheses with increased stirring rates during the solvent evaporation.

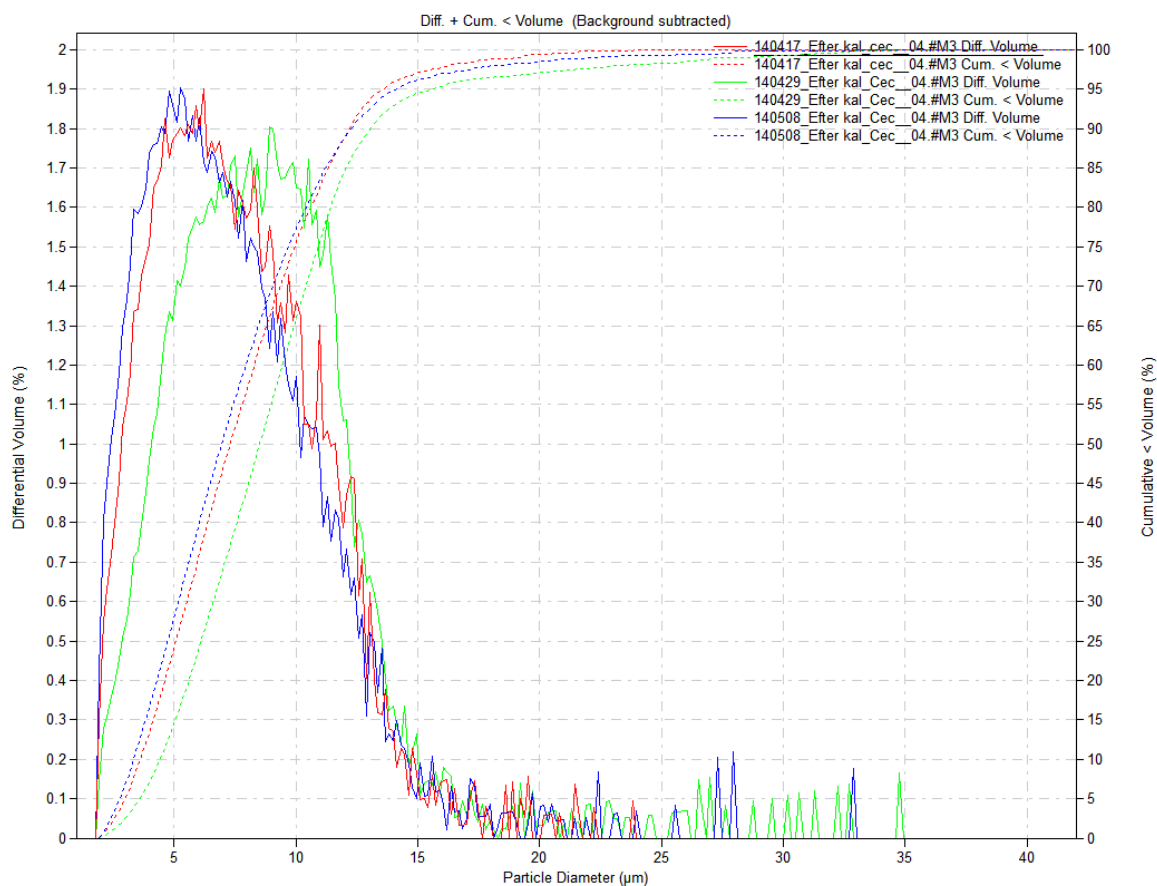


Figure 4.27 Particle size distribution from Coulter counter for the syntheses with varied stirring rate during the solvent evaporation. Green curve represents when the stirring where set to 175 rpm, red curve 275 rpm and blue curve 375 rpm.

Table 4.17 List of median size and range of particle size for syntheses with different stirring rates during gelation.

		175 rpm	275 rpm	375 rpm
Coulter counter	d <sub>50</sub> (μm)	8.52	<b>7.31</b>	6.96
	d <sub>90</sub> /d <sub>10</sub>	2.95	<b>3.36</b>	3.66
Malvern	d <sub>50</sub> (μm)	7.48	<b>6.83</b>	7.28
	d <sub>90</sub> /d <sub>10</sub>	2.84	<b>3.92</b>	4.38

### 4.2.3 The effect of the viscosity in the continuous phase

The particle size distribution from the synthesis without the Couette cell became narrower when the viscosity of the organic phase was increased, see figure 4.13. The red curve represents the reference system without thickener and the green curve shows the synthesis with 5 wt% addition of poly(isobutyl methacrylate) as thickener, see figure 4.28. For the synthesis with increased viscosity of the organic phase and the use of the Couette cell, the size distribution did not become narrower than the reference system. The continuous cumulative volume curve for the reference system is steeper which means that the absence of thickener resulted in a narrower particle size distribution. Table 4.18 lists the median size and range of particle size for the syntheses with and without thickener.



Figure 4.28 Particle size distributions from Coulter counter for syntheses with and without thickener of the organic phase, while at the same time using the Couette cell. The green curve represents 5 wt% addition of poly(isobutyl methacrylate) and the red curve is the reference system with no thickener.

Table 4.18 List of median size and range of particle size for syntheses with and without thickener.

		No thickener	5wt% of thickener poly(isobutyl methacrylate)
Coulter counter	d <sub>50</sub> (μm)	7.31	7.92
	d <sub>90</sub> /d <sub>10</sub>	3.36	5.37
Malvern	d <sub>50</sub> (μm)	6.83	7.44
	d <sub>90</sub> /d <sub>10</sub>	3.92	6.51

#### 4.2.4 The effect of the retention time in the Couette cell

The retention time in the Couette cell was varied by the pump speed to see if the particle morphology and size distribution was affected. Half way through our experiments the Couette cell was submitted for repair, where the cell walls had to be polished. After this, the particle size distribution of the reference system slightly differed from the particle size distribution before the repair. The bearing in the Couette cell was contaminated with organic solvent and started to corrode, see figure 9.1-9.2 in Appendix 9.3. The corrosion was removed by polishing. In figure 4.29 both the blue and the green curve are almost identical with the respective red curve, which is the reference system before (left) and after (right) repair. The synthesis with a retention time of 18

seconds, display in figure to the left as blue curve, was done before the repair and the synthesis with a retention time of 6 seconds, shown in the right figure as the green curve, was done after the reparation. The particle size and size distribution did not differ when varying the retention time from 6 to 18 seconds. Table 4.19 lists the median size and range of particle size for syntheses with different retention time in the Couette cell.

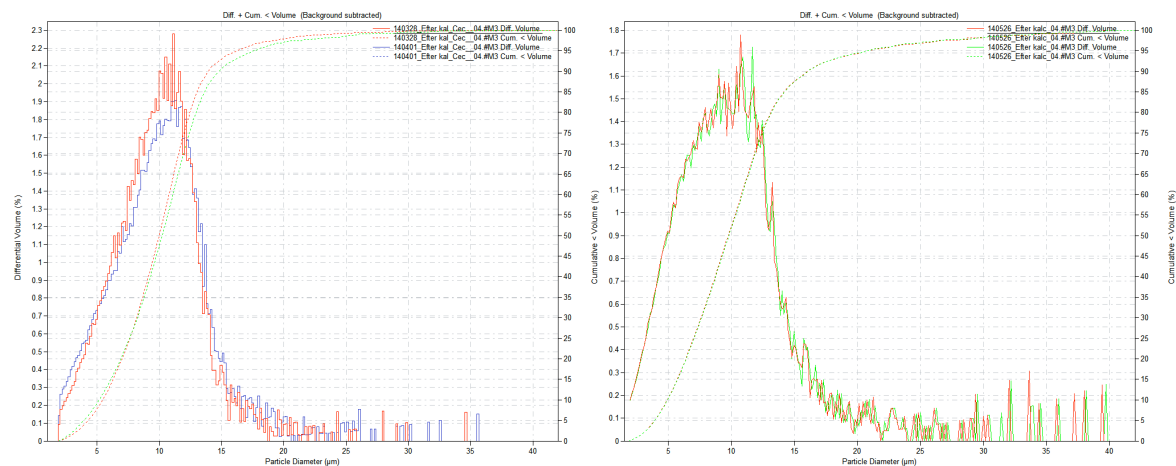


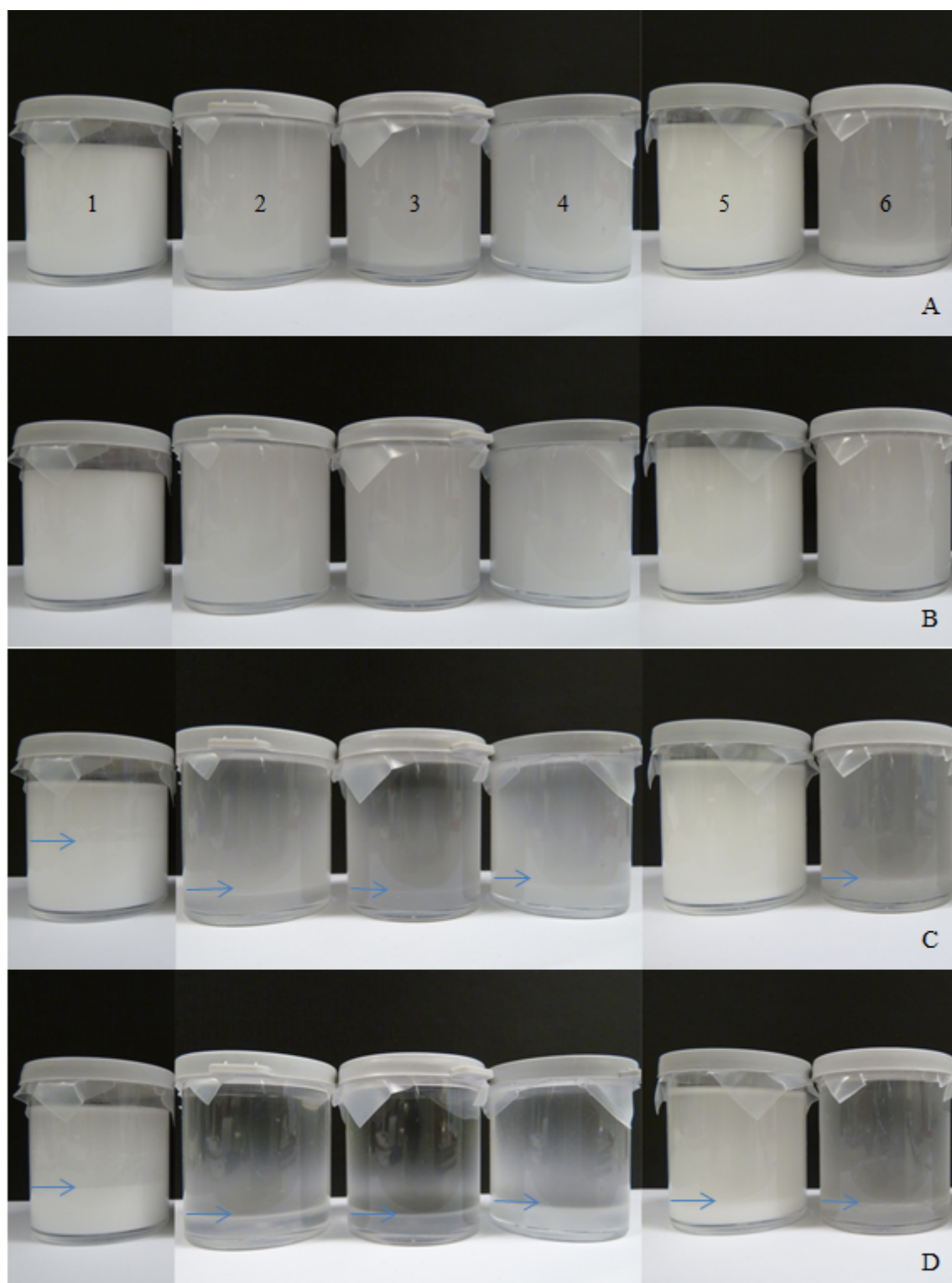
Figure 4.29 Particle size distributions from Coulter counter for the reference system before (left) and after (right) the repair of Couette cell had retention time of 9 seconds which are shown as red curves. The blue and green curve shows the size distribution for a retention time of 18 (left) and 6 seconds (right).

Table 4.19 List of median size and range of particle size for syntheses with different retention time in the Couette cell.

		6 s (after polishing)	9 s (after polishing)	9 s (before polishing)	18 s (before polishing)
Coulter counter	$d_{50}$ ( $\mu\text{m}$ )	9.76	<b>9.81</b>	<b>9.80</b>	10.22
	$d_{90}/d_{10}$	3.25	<b>3.25</b>	<b>2.64</b>	2.87
Malvern	$d_{50}$ ( $\mu\text{m}$ )	7.67	<b>9.37</b>	<b>10.61</b>	9.93
	$d_{90}/d_{10}$	3.12	<b>2.77</b>	<b>2.61</b>	2.89

### 4.3 Investigation of emulsion stability

The emulsion stability of the different emulsion systems was compared by visual observation. Benzyl alcohol and cyclohexanol were the two organic solvents that showed to have the most stable emulsions. However, for the other emulsions using the organic solvents 2-methyl-1-butanol (2), 3-pentanol (3), 1-hexanol (4), and 3-methyl-3-pentanol (6) the phase separation occurred much faster. For the fast phase separating samples phase separation were observed after approximately 30 minutes and complete phase separation after 2 hours.



*Figure 4.30 Emulsion phase separation observation for benzyl alcohol (1), 2-methyl-1-buthanol (2), 3-penthanol (3), 1-hexanol (4), cyclohexanol (5) and 3-methyl-3-penthanol (6). Image (A) was taken right after the emulsion was mixed and the three following images were taken 4 (B), 30 (C) and 120 (D) minutes after mixing, respectively. The small blue arrows indicate where border between the upper and lower phase was when phase separation could be observed by eye.*

## 5. Discussion

In this chapter, the development of the reference system and how the different parameters affect the final particle size and size distribution with and without the Couette cell will be discussed. The different analytical methods will also be discussed.

### 5.1 Evaluation of reaction parameters

The aim of this thesis was to investigate how variations in the reaction parameters during the synthesis of spherical mesoporous silica particles affect the particle morphology and size distribution. The modified versions of the ESE method, developed by Nina Andersson et al. (7), were chosen as the method for producing the spherical silica particles. Andersson used hexadecane as continuous phase, ethanol as dispersed phase and a polymeric PEG-30 dipoly(hydroxystearate), Arlacel P135, as emulsifier. They used a solvent evaporation temperature of 30 °C under a reduced pressure of 3 mbar for 30 minutes and separated the particles by centrifugation, followed by calcination in air at 500 °C for 5 hours (7). Water as the evaporating solvent in Andersson's system was not appropriate because the solubility of water in hexadecane is very low. The ESE method works by removing the solvent from the dispersed phase i.e. the emulsion droplets. To achieve solvent transport through the continuous phase the dispersed phase need to have a certain level of solubility in the continuous phase. As the solvent is removed the silica and salt concentration in the emulsion droplets becomes large enough for gelation to take place in the emulsion droplets.

This thesis work started with a literature study to identify suitable organic phases for the experimental part. The criteria in the literature search was that the organic phase should have a boiling point higher than water, a melting point below room temperature and that it has an acceptable (high) solubility of water. Data of water solubility in the organic phase are not commonly tabulated, however the solubility of the organic phase in water are most commonly listed and was used for the purpose of finding a suitable organic phase, with the assumption that if a substance have a high solubility in water it will most probably also have the possibility to solve large amounts of water, i.e. the solubility in water was used as guidance for the water solubility in organic phase. Substances suitable as organic phase are alcohols, ether, esters, amines and acids, see table 9.2 in Appendix 9.2. However, many of them are toxic and carcinogenic except for alcohols, which were chosen as organic phase candidates. Hence, the following six alcohols, with increasing water solubility, were chosen to be tested as organic phase; 1-hexanol, 2-methyl-1-butanol, 3-methyl-3-pentanol, benzyl alcohol, cyclohexanol and 3-pentanol, see Table 3.2.

The chosen alcohols were tested as organic phase in a gelation experiment without fully optimized reaction parameters. The chosen reaction parameters for this reaction were: an emulsifier, EHEC E230, too stabilize the droplets, a temperature of 65 °C at 160 mbar (the boiling point of water is 55 °C at 160 mbar). The emulsifier in the reference system was arbitrarily preselected to be EHEC E230. A stability test of different amounts of emulsifier indicated that 0.066 wt% was sufficient to stabilize the emulsion, see figure 4.6. As none of the emulsions with 0.066, 0.13 and 0.26 wt% emulsifier began to separate before 1 hour and the concentration of the emulsifier must be low enough so that dissolution of emulsifier into the inorganic phase is avoided, the amount of emulsifier in the reference system was set to 0.066 wt% EHEC E230. Kosuge et al. (2004) have

varied the stirring rate from 400-1000 rpm to see how the particle size distribution affects and found out that monodisperse spherical silica particles are obtained in the range of 500-700 rpm (34). However, they had another kind of stirrer. As no specific stirring rate was found in literature, the stirring rate was arbitrarily set to 450 rpm.

Given the goal of the thesis, the syntheses of mesoporous spherical silica particles resulted in both success and failure. Most systems produced particles with defects, see figure 9.12-9.13. Particles produced with 1-hexanol, 2-methyl-1-butanol, 3-methyl-3-pentanol and 3-pentanol had defect such as oval shape and collapsed morphology. Cyclohexanol produced mostly spherical particles, but some still had defects. Benzyl alcohol on the other hand produced a high yield of spherical particles under most process conditions. The surface and interfacial tension between the organic solvents and silica sol dispersion/EHEC E230/water systems was measured but no data was obtained from the system with benzyl alcohol and cyclohexanol, see Table 9.1. The interfacial tensions between benzyl alcohol and cyclohexanol as the organic phase, and the silica sol dispersion/EHEC E230/water as dispersed phase were too low to be measured with the used tensiometer. The lowest interfacial tension, that could be measured, was 2.3 mN/m for 2-methyl-1-butanol and silica sol dispersion/EHEC E230/water. This coincidentally indicates that a low surface and interfacial tension is advantageous as benzyl alcohol and cyclohexanol were the only organic solvents that produced a high yield of spherical particles. These two solvents have very similar molecular structures which could explain why both of them yielded fairly good results.

The emulsion stability tests in figure 4.15 indicates that the emulsions are more stable with lower interfacial tension, as it took longer time for benzyl alcohol and cyclohexanol to separate compared to the other organic solvents. An emulsion stability test can probably be used as a quick first test to find out if the emulsion system has potential to produce spherical particles.

The reaction parameters that were investigated when using benzyl alcohol as the continuous phase were; stirring rate, temperature, emulsifier, phase ratio, thickener of organic phase and combinations thereof.

Common stirring rates found in literature vary between 200-600 rpm. When increasing the stirring rate the particles became smaller and the size distribution narrower which can be explained by the higher energy input in to the emulsion when the stirring rate is high. Larger emulsion droplets tend to break up as they have lower Laplace pressures (17). See figure 4.4 for the size distribution for the different stirring rates. The amount of energy input to the emulsion affects and breaks the droplets into a specific size.

The amount of emulsifier had major effects on the particle size distributions, see figure 4.5. By increasing the amount of emulsifier the mean particle size became smaller and the size distribution narrower. An explanation might be that there was not enough emulsifier to stabilize the emulsion droplets against aggregation and coalescence in the two systems with 0.033 and 0.066 wt%, resulting in broader size distributions. The system with 0.13 wt% emulsifier on the other hand seems to be saturated with the emulsifier as further addition did not change the emulsion droplet size and particle size distribution. The amount of dissolved emulsifier in the dispersed phase was not measured. The experiments prove that an increasing amount of emulsifier resulted in smaller particles and that is in agreement with Ibrahim and colleagues who observed smaller particles with increasing amount of emulsifier (49).

It is of interest to be able to synthesize narrow particle distribution of desired particle size and not just small particles. As the viscosity of the dispersed phase has a major effect on the droplet fracturing according to Tadros (2003) the viscosity was varied by using different emulsifiers and different amounts of emulsifiers (18). The emulsifiers EHEC E230, E351 and E511 are of the same kind of emulsifier but with increasing viscosity. MEHEC EBM5500 is similar to EHEC, but consists of both ethyl and methyl groups. MEHEC EBM5500 has slightly higher viscosity than EHEC E351. The results in this thesis show that the mean particle size becomes larger with increasing viscosity in the dispersed phase, see figure 4.7. An increasing viscosity increases the Laplace pressure, so that more energy is required to break up the emulsion droplets (18), which explain why the particle size becomes larger with increasing viscosity. The distribution, though, becomes broader with increasing viscosity and since higher amount of EHEC E230 resulted in narrower particle size distribution, the amount of emulsifier MEHEC EBM5500 was increased from 0.066 to 0.11 wt%. Also in this case an increased amount of emulsifier gave a narrower size distribution. However, at the same time the mean particles size became smaller. Whether the presence of methyl groups in MEHEC EBM5500 has impact on the morphology and the size distribution was not further investigated in this thesis.

Figure 4.10 illustrates that variations in temperature between 55-75°C did not affect the particle size distribution, but if comparing the results from the Malvern the particle median size decreases slightly with increasing temperature. Andersson et al. saw that the temperature affected the formation of particles and that a lower temperature during solvent evaporation improved the morphology of the particles (7). Figure 4.10a shows that the morphology of the particles synthesized at different evaporation temperatures were not affected by temperature.

The phase ratio between inorganic and organic phase in the reference system is 1:3.64. During one synthesis the organic phase was reduced to the phase ratio of 1:3 by adding less organic solvent and in another synthesis the organic phase was further reduced to the phase ratio of 1:2.22 by adding 100 g distilled water to the emulsion system. When the organic phase was reduced, the median particle size was not significantly affected according to the results from Coulter counter, but it was significantly affected according to the Malvern results, see table 4.8. The results from the emulsion system with decreasing organic phase do not follow any trend for any of the characterization methods. The median particle size increases with decreasing organic phase, but not linearly since synthesis with phase ratio of 1:3 has largest median particle size. An emulsion system with high dispersed phase ratio will be more likely to aggregate due to tighter packed droplets compared to lower disperse phase ratio (50). Ibrahim and colleagues saw that a higher dispersed phase ratio gave larger emulsion droplets in presence of more emulsifier to cover up the droplet surface (49). In the synthesis where 100 g distilled water was added to the emulsion system the emulsion droplets became larger even though the amount of emulsifier was not further increased. The particle size distribution from that synthesis did not differ from the particle size distribution obtained from the reference system, see Figure 4.12. It is possible that the addition of water would create more droplets instead of larger droplets. In such a scenario each emulsion droplet would be smaller and hence also the final particle size. However, as the particle size distribution was the same as for the reference system it is more likely the emulsion droplets became larger in size instead of larger in numbers when extra water was added.

Among the different organic solvent tested, four alcohols are within the “similar” range of water solubility (30.000-52.000 mg/kg) but they differ in viscosity. In order of increasing viscosity the

following alcohols was tested; 3-methyl-3-pentanol, 2-methyl-1-butanol, benzyl alcohol and cyclohexanol, see Table 3.2. Only benzyl alcohol and to some extent cyclohexanol produced spherical particles. The viscosity of the emulsions was not measured, but a qualitative test of the relative viscosity was made for the two different organic phase thickeners. The thickeners used were poly(isobutyl methacrylate) and isobutyl methacrylate copolymer. Figure 4.14 shows that 5 wt% of poly(isobutyl methacrylate) did not increase the viscosity of the continuous phase as well as 5 wt% of isobutyl methacrylate copolymer, as the vortex in the beaker was smaller for the latter mentioned thickener. Higher viscosity in the continuous phase contributed to smaller particles and narrower size distribution. Ramisetty et al observed that increased viscosity of the continuous phase reduced the mobility of the emulsion droplets and in that way prevented them from coalescing (51). One plausible explanation could be that the increasing viscosity acts like a stabilizer in the continuous phase and stabilizes the emulsion droplets, hence the synthesized mesoporous silica particles obtain a narrower particle size distribution. An emulsifier concentration of 0.066 wt% EHEC E230 was not enough to stabilize the emulsion, but 0.13 wt% was enough as it gave a narrower size distribution.

## 5.2 Evaluation of Couette cell

When preparing emulsion through stirring or shaking it is hard to precisely control the synthesis conditions, which often yields in polydisperse emulsion droplets distributions. Mason and Bibette (32) found two important factors to make monodisperse emulsion droplet distributions with a Couette cell. Firstly the premixed emulsion needs to be viscoelasticity and secondly the gap in between the cylinder walls where the emulsion is sheared need to be small.

The gap in the Couette cell used in the thesis was preselected to 50  $\mu\text{m}$  but the small distance prevented the inner cylinder to rotate smoothly, therefore the gap in the lower part of the inner cylinder was increased to 100  $\mu\text{m}$ , which is still within the desired dimension. Whether the emulsion system containing benzyl alcohol and water with EHEC E230 as emulsifier is viscoelastic or non-viscoelastic was not investigated.

Figure 4.24-4.25 and 4.27 illustrate that a smaller particle size and narrower size distribution was always the results when the stirring rate was increased: in the emulsion reactor, Couette cell or in the reactor during solvent evaporation. Higher energy input to the system deforms and breaks larger droplets easier compared to smaller droplets (14). Furthermore, if an emulsion droplet size is fractured into two droplets of equal size, then the radius difference between the initial and final droplet size becomes smaller with smaller initial droplet size, i.e. the difference between 10 and 5  $\mu\text{m}$  is larger than the difference between 5 and 2.5  $\mu\text{m}$ . The smaller the initial droplet size, the less the polydispersity, which also results in narrower distribution curves (38). As higher stirring rates in the emulsion system and Couette cell itself have resulted in narrower size distribution, a synthesis with higher stirring rates in both emulsion system and Couette cell was performed. The synthesis with the combination of these parameters resulted in same particle size distribution, see figure 4.26.

In the process without the Couette cell the particle size distribution became narrower when the amount of emulsifier EHEC E230 was increased from 0.066 wt % to 0.13 wt%. It was therefore interesting to do a synthesis with 0.13 wt% EHEC E230 together with the use of the Couette cell

to see if there would be any synergistic effects. Figure 4.21 indeed indicates that the combination resulted in even smaller and more monodisperse particles.

As the Couette cell produces smaller particles with an increased surface area more emulsifier is needed to stabilize the interfaces. 0.13 wt% EHEC E230 that was enough to stabilize the emulsion in the process without Couette cell might not be enough stabilize the emulsion after Couette cell treatment. This is why a synthesis was made with 0.26 wt% EHEC E230. The synthesis resulted in the same size distribution but with a larger median particle size. Andersson et al found that at high emulsifier concentration more of the emulsifier can be dissolved inside the emulsion droplets (7). This could increase the viscosity of the dispersed phase, which could explain why larger particles were obtained with 0.26 wt% EHEC E230 (18).

Increase in viscosity of the continuous phase in the process system without Couette cell has major effect on the particle size distribution. Figure 4.28 show the particle size distribution from the synthesis with the addition of 5 wt% thickener of poly(isobutyl methacrylate) and the use of the Couette cell. The size distribution for the reference system appears broader than the synthesis with 5 wt% thickener. Nonetheless, when comparing the continuous cumulative curve, the red curve representing the reference system is steeper than the green curve. This indicates that the size distribution for the reference system is narrower than the synthesis with 5 wt% thickener. The addition of thickener in the process modified with Couette cell does not make the size distribution narrower as it did in the process without Couette cell.

The retention time in the Couette cell affects the amount of shear stress that can be applied to the pre-mixed emulsion. As previously discussed the shear stress applied in the Couette cell has major effects on the particle size distribution. In the reference system, the retention time is set to 9 seconds which correspond to a shear stress of  $20.000 \text{ s}^{-1}$  in the Couette cell with gap distance of 0.1 mm and 0.05 mm in the lower and upper part respectively and stirring rate at 500 rpm. To investigate the effect of retention time on 6, 9 (reference) and 18 seconds was tested. The retention time did not affect the mesoporous silica particles significantly and the particle size distribution for the syntheses at different retention time overlapped well with its corresponding reference system.

### 5.3 Characterization methods

Two different characterization methods have been used to study the particle size and size distribution; Coulter counter and Malvern. All particles have been analyzed with the methods with a few exceptions. Defected particles obtained from the different organic solvents could not be analyzed with the Coulter counter instrument. Since all characterization methods have weaknesses it was hard to say which method that gave the most reliable results, but what could be noticed was that for larger particles with median size around  $16 \mu\text{m}$  Malvern has mostly resulted in larger median particle size than Coulter counter. The images of the analyzed particles from Malvern have also shown that larger particles have more tendencies to aggregate than smaller particles, which resulted in that two particles are measured as one with larger diameter. For smaller particles, e.g. the particles obtained from the process modified with the Couette cell, results from both Malvern and Couette cell match each other more or less.

In addition, ImageJ was used as a tool to analyze two SEM-images; 0.13wt % emulsifier EHEC E230 without and with Couette cell, see Figure 4.22. The diameters of 500 particles of each image have been measured. The median particle size for 0.13 wt% EHEC E230 without Couette is 6.02  $\mu\text{m}$  (Coulter counter: 12.74  $\mu\text{m}$ , Malvern: 18.13  $\mu\text{m}$ ) and the median particle size with Couette cell is 3.68  $\mu\text{m}$  (Coulter counter: 5.81  $\mu\text{m}$ , Malvern: 4.94)  $\mu\text{m}$ . Due to that only 500 particles were analyzed with ImageJ, the results from ImageJ were not as much statistically reliable as Coulter counter and Malvern were, which analyzed approximately 75,000 and 4,000 particles respectively.

## 6. Conclusion

Spherical mesoporous silica particles have been successfully synthesized with the ESE-method using EHEC E230 as an emulsifier, water as inorganic phase and benzyl alcohol as organic phase. This system was chosen as the reference system where reaction parameters were varied. In the process without Couette cell, the reaction parameters that have significant impact on the final particle size distribution are stirring rate, the viscosity of dispersed phase as well as the continuous phase. When increasing the stirring rate and the viscosity in the continuous phase, the particle size distribution became narrower. The way in which the viscosity of the dispersed phase was increased had significance for the particle size distribution obtained. An increase in the amount of emulsifier resulted in a smaller particle size and narrower distribution. The type of emulsifier also affected the end result as emulsifiers with high viscosity gave larger particle size and broader size distributions. Variations in the phase ratio between the inorganic and organic phase had minor impact on the final particle size distribution and a decrease in the organic phase resulted in slightly larger particle size. Temperature variations during solvent evaporation did not have significant impact on the particle size or size distribution.

The Couette cell was successfully used to produce smaller particles and narrower size distributions. Emulsion viscoelasticity and the small gap distance between the Couette cell cylinder walls have previously been reported to yield narrower size distributions. In this study viscoelasticity was not measured but the gap distance was in the range recommended in literature. The reaction parameters in the process modified with the Couette cell that had major effect on the particle size distribution were stirring rate and the viscosity of the dispersed phase. Smaller particles and a narrower size distribution was always the result when increasing the stirring rate in the emulsion reactor, the Couette cell or the solvent evaporation reactor. An increase in the viscosity of the dispersed phase had a similar effect. The reaction parameter that has minor impact on the particle size distribution is the viscosity of the continuous phase: increasing the viscosity of the continuous phase resulted in slightly broader distribution. The retention time in the Couette cell did not have any impact on the particle size distribution.

## 7. Future work

A study of the mesopores was excluded in this thesis but it would be interesting to see how the different parameters affect the pore size and pore volume of the spherical mesoporous silica particles, as the pores add important properties to the particles.

More experiments with different organic solvents and different types of emulsifiers would also have been interesting. Perhaps other types of emulsifiers than EHEC could have improved the stability of the emulsions in the systems that did produce a satisfactory yield of spherical particles.

Synthesis with other types of silica sols, with primary particles of different shape and size might also have been interesting. In order to improve and obtain more reliable results more than one synthesis per parameter change would be ideal.

An examination of the emulsion rheological properties in different emulsions would be good to understand the significance of viscoelastic for the particle size distribution.

## 8. References

1. W. Li and D. Zhao, "An overview of synthesis of ordered mesoporous materials", *ChemCommun*, vol. 49, 943-946, 2013.
2. A. Nandiyanto, et al, "Synthesis of spherical mesoporous silica nanoparticles with nanometer-size controllable pores and outer diameters", *Microporous and Mesoporous Materials*, vol. 120, no. 3, 447-453, 2009.
3. K. Shiba, N. Shimura, and M. Ogawa, "Mesoporous silica spherical particles", *Journal of Nanoscience and Nanotechnology*, vol. 13, no. 4, 2483-2494, 2013.
4. Y. Li, et al, "Large-pore monodispersed mesoporous silica spheres: synthesis and application in HPLC", *Chem. Commun*, no. 9, 1085-1087, 2009.
5. I.I. Slowing, et al, "Mesoporous Silica Nanoparticles for Drug Delivery and Biosensing Applications", *Advanced Functional Materials*, vol. 17, no. 8, 1225-1236, 2007.
6. Z. Sun, "Novel Sol-Gel Nanoporous Materials, Nanocomposites and Their Applications in Bioscience", Philadelphia : Philadelphia: Drexel University, 2005.
7. N. Andersson, et al, "Combined Emulsion and Solvent Evaporation (ESE) Synthesis Route to Well-Ordered Mesoporous Materials", *Langmuir*, vol. 23, no. 3, 1459-1464, 2006.
8. Colloids Applications. [Online] Horiba Scientific. Available: <http://www.horiba.com/scientific/products/particle-characterization/applications/colloids/>. [Cited: 2014.05.30]
9. Z. Adamczyk and P. Weronki, "Application of the DLVO theory for particle deposition problems", *Advances in Colloid and Interface Science*, vol. 83, no. 1-3, 137-226, 1999.
10. H. Haohao, "Interactions in Colloidal Systems", Buffalo : ProQuest Information and Learning Company, 2006.
11. Universiti Sains Malaysia [Online] Available: <http://imk209.wikispaces.com/Not+just+Food+-+presentation>. [Cited: 2014.05.14]
12. M. Elimelech, et al, *Particle Deposition & Aggregation: Measurement, Modelling and Simulation*, United states of America : Butterworth-Heinemann, 1995.
13. G. Raymond, Biomolecules in nanochannels and separation devices, *MESA+ institute for nanotechnology*, [Online] Available: <http://www.utwente.nl/ewi/bios/research/micronanofluidics/oldmicronanofluidicsprojects/biomoleculesinnanochannels/> [Cited: 2014.06.21]
14. C.O. Metin, et al, "Aggregation kinetics and shear rheology of aqueous silica suspensions", *Applied Nanoscience*, vol. 4, no. 2, 169-178, 2012.
15. K. Holmberg, *Surfactants and polymers in aqueous solution*. Chichester, England : John Wiley & Sons, 2003.

16. Microemulsions. *University of Bristol*. [Online] Available: [http://www.chm.bris.ac.uk/eastoe/Surf\\_Chem/3%20Microemulsions.pdf](http://www.chm.bris.ac.uk/eastoe/Surf_Chem/3%20Microemulsions.pdf). [Cited: 2014.04.12]
17. P. Walstra, "Principles of emulsion formation", *Chemical Engineering Science*, vol. 48, no. 2, 333–349, 1993.
18. T.F.Tadros, *Emulsion formation and stability*. Somerset, NJ, USA : Wiley, 2003.
19. *Compendium of Food Additive Specifications. Addendum 5*. Rome : FAO, 1997.
20. Bermocoll in construction industry. [Online] Available: [https://www.akzonobel.com/cs/system/images/AkzoNobel\\_building\\_eng\\_tcm54-18192.pdf](https://www.akzonobel.com/cs/system/images/AkzoNobel_building_eng_tcm54-18192.pdf). [Cited: 2014.03.11]
21. L. Cademartiri and G.A Ozin, *Concept of Nanotechnology*. Weinheim: WILEY-VCH Verlag GmbH & Co, 2009.
22. [Online] Available: [http://commons.wikimedia.org/wiki/File:Silica\\_gel\\_endcapping.png](http://commons.wikimedia.org/wiki/File:Silica_gel_endcapping.png).
23. H.A Schaeffer, *Silica*, Friedrich Alexander Universität, Erlangen, Germany.
24. R.K. Iler, *The chemistry of silica: Solubility, polymerization, colloid and surface properties and biochemistry*, John Wiley & Sons, 1979.
25. Akzo Nobel Colloidal Silica. [Online] Available: <https://www.akzonobel.com/colloidalsilica/application/> [Cited: 2014.06.29]
26. E.M Johansson, "*Controlling the Pore Size and Morphology of Mesoporous Silica*", Linköping : Linköping Studies in Science and Technology, 2010.
27. L. F. Giraldo, et al, "Mesoporous Silica Applications", *Macromolecular Symposia*, vol. 258, no. 1, 258, 129–141, 2007.
28. M. Ogawa, H. Ishikawa and T. Kikuchi, "Preparation of transparent mesoporous silica films by rapid solvent evaporation method", *Journal of Materials Chemistry*, vol. 8, 1783-1786, 1998.
29. A. Nakahira, T. Hamada and Y. Yamauchi, "Synthesis and properties of dense bulks for mesoporous silica SBA-15 by a modified hydrothermal method", *Materials Letters*, vol. 64, no. 19, 2053–2055, 2010.
30. L.L. Hench and J.K. West, "The Sol-Gel Process", *Chemical Reviews*, vol. 90, 33–72, 1990.
31. A. Nazir, K. Schroen and R. Boom, "Premix emulsification: A review", *Journal of Membrane Science*, vol. 362, no. 1-2, 1–11, 2010.
32. C. Mabile, et al, "Rheological and Shearing Conditions for the Preparation of Monodisperse Emulsions", *Langmuir*, vol. 16, no. 2, 422–429, 2000.
33. R. Darby, "Handbook of sol-gel science and technology : processing, characterization, and applications", *ProQuest Central*, 1851, 2005.

34. K. Kosuge, N. Kikukawa and M. Takemori, "One-Step Preparation of Porous Silica Spheres from Sodium Silicate Using Triblock Copolymer Templating", *Chemistry of Materials*, vol. 16, no. 21, 4181–4186, 2004.
35. Q. Huo, et al, "Preparation of Hard Mesoporous Silica Spheres", *Chemistry of Materials*, vol. 9, 14-17, 1997.
36. R.I. Nooney, et al, "Synthesis of Nanoscale Mesoporous Silica Spheres with Controlled Particle Size", *Chemistry of Materials*, vol. 14, no. 11, 4721-4728, 2002.
37. J. Bibette, D. Roux and F. Nallet, "Depletion interactions and fluid–solid equilibrium in emulsions", *Physical Review Letters*, vol. 65, no. 19, 1990.
38. T.G. Mason and J. Bibette, "Shear rupturing of droplets in complex fluids", *Langmuir*, vol. 13, no. 17, 4600-4613, 1997.
39. B. Deminiere, et al, "Cell growth in a three dimensional cellular system undergoing coalescence", *Physical Review Letters*, vol. 82, 1999.
40. S. Omi, "Preparation of monodisperse microspheres using the Shirasu porous glass emulsification technique", *Colloids and Surfaces A: Physicochemical and Engineering Aspects*, vol. 109, 97–107, 1996.
41. T.G. Mason, "New fundamental concepts in emulsion rheology", *Current Opinion in Colloid & Interface Science*, vol. 4, no. 3, 231–238, 1999.
42. M.J. Herzberger, Optical microscope, Access Science [Online] Available: <http://www.accessscience.com.proxy.lib.chalmers.se/content/optical-microscope/472600#472600s015> [Cited: 2014.03.02]
43. M. T. Postek and A.E. Vladár, "Does your SEM really tell the truth? How would you know? Part 1", *Scanning*, vol. 35, 355-361, 2013.
44. Beckman Coulter Counter. *The Coulter Principle*. [Online] Available: [https://www.beckmancoulter.com/wsrportal/wsrportal.portal.jsessionid=yJtrTbQdLV12XQQCG5hQPh2n46s2wfmS77QvwZW2L9fkTDkV7Mpc!-835113841!-1439949193?\\_nfpb=true&\\_windowLabel=UCM\\_RENDERER&\\_urlType=render&wlpUCM\\_RENDERER\\_path=%2Fwsr%2FIndustrial%2Fparticle-techn](https://www.beckmancoulter.com/wsrportal/wsrportal.portal.jsessionid=yJtrTbQdLV12XQQCG5hQPh2n46s2wfmS77QvwZW2L9fkTDkV7Mpc!-835113841!-1439949193?_nfpb=true&_windowLabel=UCM_RENDERER&_urlType=render&wlpUCM_RENDERER_path=%2Fwsr%2FIndustrial%2Fparticle-techn). [Cited: 2014.03.21]
45. Atomika Teknik. *Sysmex FPIA 3000, flow particle image analysis of size and shape*. [Online] Available: <http://www.atomikateknik.com/pdf/Sysmex%20FPIA%203000.pdf>. [Cited: 2014.04.05]
46. Malvern. *Sysmex FPIA3000, Rapid particle size and shape analysis of suspensions*. [Online] Available: <http://www.malvern.com/en/products/product-range/sysmex-fpia-3000/default.aspx>. [Cited: 2014.04.05]
47. B.B. Weiner, Brookhaven Instruments. 2. [Online] Available: <http://www.brookhaveninstruments.com/pdf/What%20is%20a%20Continuous%20Particle%20Size%20Distribution.pdf>. [Cited: 2014.06.27]

48. M. Karlberga, K. Thuresson and B. Lindman, "Hydrophobically modified ethyl(hydroxyethyl)cellulose as stabilizer and emulsifying agent in macroemulsions", *Colloids and Surfaces A: Physicochemical and Engineering Aspects*, vol. 262, no. 1-3, 158–167, 2005.
49. N. Ibrahim and N. Yusof, "Properties and Stability of Catfish Oil-in-water Emulsions as Affected by Oil and Emulsifier Concentrations", vol. 33, 2012.
50. A. Anisa, and A. Nour, "Affect of Viscosity and Droplet Diameter on water-in-oil (w/o) Emulsions: An Experimental Study", *World Academy of Science, Engineering and Technology*, vol. 4, 2010.
51. K.A. Ramisetty and R. Shyamsunder, "Effect of Ultrasonication on Stability of Oil in Water Emulsions", *International Journal of Drug Delivery*, vol. 3, 133-142, 2011.
52. Background information - What is scanning electron microscopy?, ammrf [Online] Available: <http://www.ammrf.org.au/myscope/sem/background/> [Cited: 2014.10.03]

## 9. Appendix

### 9.1 Surface and interfacial tension

The surface tension and interfacial surface tension towards water was measure for the most interesting organic solvents. As could be seen, benzyl alcohol has the highest surface tension and an interfacial tension comparable with the others.

*Table 9.1 List of surface and interfacial tension.*

Organic solvent	Surface tension (mN/m)	Interfacial tension towards water (mN/m)	Interfacial tension towards silica dispersion and emulsifier EHEC 230 (mN/m)
1-hexanol	26.0	6.1	4.7
2-methyl-1-buthanol	24.5	5.1	2.3
3-methyl-3-penthanol	23.5	4.2	2.7
Benzyl alcohol	39.6	4.1	-
Cyclohexanol	32.8	3.2	-
3-penthanol	24.2	4.3	2.5

## 9.2 List of organic solvents from literature

Table 9.2 List of alcohols found in literature that has a boiling point > 100 °C. The bolded values are the selected alcohols. Asterisk means that the numbers are from Wikipedia.

Substance	Boiling point, C	Freezing point, C	Density, g/ml	Surface tension, mN/m	Viscosity, cP	Water solubility, mg/kg	Price, SEK/l
Isophorone	210,5	-8	0,92 at 25 C	32,3	2,632 at 20 C	12000	274,27
Etylene glycol monobutyl ether acetate	192	-64	0,94 at 20 C	27,4	1,7 at 25 C	17000	344,66
Dietyl malonate	200	-49	1,049 at 20 C		1,94 at 25 C	23000	752,82
Etylacetoacetate	180,8	-45	1,021 at 20 C		1,51 at 25 C	28600	428,81
Diethylene glycol monobutyl ether acetate	245	-32	0,98 at 20 C	30	3,02 at 25 C	65000	358,11
m-cresol	202	11	1,03 at 22 C		9,8 at 25 C	25000	1328,92
Aniline	184	-6	1,02 at 20 C	42,9	3,77 at 25 C	34000	1345,5
m-toluidine	203	-30	0,99 at 25 C		3,276 at 25 C	15000	1216,13
o-toluidine	200	-16	1,01 at 25 C		3,947 at 25 C	15000	2399,90
Furfural	161,8	-36,5	1,155 at 25 C	41,1	1,49 at 25 C	79000	469,89
Caproic acid	205	-3	0,93 at 20 C		2,826 at 25 C	11000	
Dimetyl sulfate	188	-32	1,33 at 15 C	40,1	1,76 at 25 C	28000	691,38
Valeric acid	186	-35	0,94 at 25 C		1,975 at 25 C	20000	2649,6
Benzyl alcohol	<b>205</b>	<b>-15</b>	<b>1,04 at 25 C</b>	<b>39</b>	<b>6,54 at 25 C</b>	<b>35000</b>	<b>3441,38</b>
Tetrahydrofurfuryl alcohol	178	-80	1,048 at 24 C	37	6,24 at 20 C	infinite	
1-pentanol	137,8	-78,2	0,811 at 25 C	25,6	3,512 at 25 C	22000	1399,04
3-methyl-1-butanol	131,1	-117,2	0,812 at 25 C		3,6876 at 25 C	27000, 28000*	2030,19
2-methyl-1-butanol	<b>128</b>	<b>-70</b>	<b>0,814 at 25 C</b>		<b>4,16 at 25 C</b>	<b>30000</b>	<b>472,31</b>

2,2-dimethyl-1-propanol	113,5	52,5	0,812 at 20 C		0,2262 at 151,67 C	60882,36000*	10519,09
<b>3-pentanol</b>	<b>115,3</b>	<b>-63,68</b>	<b>0,818 at 25 C</b>		<b>4,152 at 25 C</b>	<b>52000,59000*</b>	<b>3029,5</b>
2-pentanol	118	-78,8	0,805 at 25 C		3,3083 at 25 C	45000	974,07
3-methyl-2-butanol	111,5	-99,72	0,814 at 25 C		3,945 at 25 C	56000	4530,7
2-methyl-2-butanol	102	-8,8	0,805 at 25 C		3,726 at 25 C	120000*	960,39
<b>1-hexanol</b>	<b>157,4</b>	<b>-44,6</b>	<b>0,816 at 25 C</b>		<b>4,596 at 25 C</b>	<b>5875</b>	<b>1809,29</b>
2-hexanol	139,89	-50,15	0,81 at 25 C		4,219 at 25 C	14000	23310,86
3-hexanol	135,4	-70,45	0,81441 at 25 C		0,505 at 25 C	14975	18728,54
<b>Cyclohexanol</b>	<b>161,1</b>	<b>25,15</b>	<b>0,9684 at 25 C</b>	<b>33,91</b>	<b>41,07 at 30 C</b>	<b>42000</b>	<b>386,05</b>
2-methyl-2-pentanol	121,41	-102	0,80951 at 25 C		0,396 at 25 C	35663	76146,06
<b>3-methyl-3-pentanol</b>	<b>120,91</b>	<b>-23,6</b>	<b>0,8238 at 25 C</b>		<b>0,61 at 25 C</b>	<b>33476</b>	<b>3383,75</b>
1-heptanol	176	-36	0,82 at 20 C	26,2	5,78 at 25 C	1750	508,08
2-heptanol	159,2	-30,15	0,814 at 25 C		3,321 at 29,85 C	3300	2584,545 455
3-ethyl-2-pentanol	152	-74,18	0,834 at 25 C		0,512 at 25 C	5545,1	3561822, 542
2,4-dimethyl-2-pentanol	133	-56,76	0,808 at 25 C		0,4996 at 25 C	17336	1124801, 98
2-methyl-2-hexanol	142,8	-41,76	0,81 at 25 C		3,016 at 32,85 C	9582,1	80906,17 284

### 9.3 Corrosion of the Couette cell



*Figure 9.1 Corrosion in the Couette cell.*



*Figure 9.2 Stretched rubber due to contact with benzyl alcohol.*